Article:
Chen, S, Zheng, J, Zhang, L et al. (4 more authors) (2021) Synergistic gelling mechanism of RG-I rich citrus pectic polysaccharide at different esterification degree in calcium-induced gelation. Food Chemistry. 129177. ISSN 0308-8146

https://doi.org/10.1016/j.foodchem.2021.129177

Synergistic gelling mechanism of RG-I rich citrus pectins at different esterification degree in calcium-induced gelation

Jiaqi Zheng [a], Laiming Zhang [a], Huan Cheng [a,b,c], Caroline Orfila [d], Xingqian Ye [a,b,c], Shiguo Chen [a,b,c,*]

[a] College of Biosystems Engineering and Food Science, National-Local Joint Engineering Laboratory of Intelligent Food Technology and Equipment, Zhejiang Key Laboratory for Agro-Food Processing, Zhejiang Engineering Laboratory of Food Technology and Equipment, Zhejiang University, Hangzhou 310058, China

[b] Fuli Institute of Food Science, Zhejiang University, Hangzhou 310058, China

[c] Ningbo Research Institute, Zhejiang University, Ningbo 315100, China

[d] School of Food Science and Nutrition, University of Leeds, Leeds LS2 9JT, UK

Abstract

RG-I rich pectin is common in fruit and vegetable and possesses health benefits. However, it is removed during commercial pectin production because of its poor gelling properties. Synergistic gelation can improve rheological properties of RG-I pectin and expand its application in functional food hydrocolloids. In the study, RG-I rich pectins at different degree of esterification was extracted from citrus membrane by sequential mild acidic (0.4% HCl, 28℃) and alkaline (0.6% NaOH, 32℃) treatment. The pectin from acid water (PA) composes of 41% RG-I and 44% HG with DM of 45%, while the pectin from basic water (PB) composed of 63%

RG-I and 19% HG with DM of 15%. PA/PB blend gel under $CaCO_3$-glucono-δ-lactone system showed improved rheological properties compared with pure PA and PB gels. Ca-bridges connected pectin aggregates and promoted the three-dimensional structure of PA/PB blend gels, while neutral sugar side-chains prompted hydrogen bonds and strengthened the gel network.

Keywords

Pectin, rhamnogalacturonan-I, synergistic gelation, hydrogen bonds

1. Introduction

Pectin is a heteropolysaccharide widely existing in plant cell walls, composed of three major domains which include linear homogalacturonan (HG), rhamnogalacturonan-I (RG-I) and rhamnogalacturonan-II (RG-II) (Thakur, & Singh, & Handa, and Rao, 1997). Commercial pectin, dominated with HG, is well known for its gelling properties and widely used in the food, cosmetics and pharmaceutical industry (Willats, & Knox, and Mikkelsen, 2006). In commercial pectin production, RG-I region is removed by hot acid due to its poor gelling capability. However, recently study suggested these RG-I rich pectin from fruits and vegetables (e.g. citrus, okra, potato and sugar beet) having potential health benefits by modulating the gut microbe and promote cell adhesion and migration (Mao, et al., 2019, Wu, et al., 2019).

RG-I region contains a backbone of the repeating disaccharide unit [→2) -α-L-Rha*p*-(1→4)-α-D-Gal*p*A-(1→]$_n$ and neutral sugar side-chains attached to the O-4 and O-3 of rhamnose residues. RG-I backbone is not compatible with the gel formation because the rhamnose inserts on the backbone produce “kinks” thereby limiting cross-linking. But recently, the side-chains of

the RG-I region reportedly possess strong water-binding capacities (Klaassen and Trindade, 2020) and stabilize the gel network structures (Mikshina, et al., 2017; Makshakova, & Faizullin, & Mikshina, & Gorshkova, and Zuev, 2018), providing a new perspective for branched RG-I gelation. However, publish papers in this field report gelling capacity of RG-I rich pectin but rarely focus on the improvement of gel properties and network structures. Thus, further attempts to improve rheological properties and microstructures of RG-I gel based on the novel highly branched structure are needed for the development of functional food hydrocolloids.

Pectin mixtures are widely used in the food industry to obtain products with desired texture and gelling properties. High methoxylated pectin (HMP, DM>50%) and low methoxylated pectin (LMP, DM<50%) are often mixed in order to reduce sucrose content of pectin gels. HMP/LMP blend gels exhibited similar rheological behavior to HMP gels of higher sucrose concentrations, which attributes to the inhomogeneous gel structure (Löfgren and Hermansson, 2007; Lootens, et al., 2003). RG-I rich pectin has a synergistic effect on the gelation of traditional commercial pectins and other polysaccharides (Chen, et al., 2019). RG-I pectin, with long galactan side branches extracted from okra, reduced the sucrose content required for gelation and acted as a synergistic gel for high-methoxyl pectin. Side-chain entanglements create a pliable and continuous network, thus these blended gels show excellent toughness and high fracture strain (Li, et al., 2019). However, few researches extracted RG-I rich citrus pectins at different esterification degree, so the synergistic gelation of RG-I rich pectins of different structures remains unknown. Studying the synergistic gelation mechanism of RG-I rich pectins at different esterification degree gives information for rational selection of RG-I pectin structure when designing or improving food textures, which could provide new perspectives support to

expand the application of RG-I rich pectin as potential food additives and could be helpful in the development of RG-I-based food products.

In our previous work, we have used acid and alkaline extraction conditions at low temperature to extract RG-I rich pectins from citrus peel and segment membrane (Chen, et al., 2017; Zhang, et al., 2017). The flow chart for extraction was shown in figure 1. The structure and rheological properties of branched pectins have been evaluated, the pectin from acid water (PA) mainly composes of GalA with a medium (~45%) DM, while Ara is the main saccharide present in the pectin from basic water (PB) with a low (~15%) DM. PA can form gel under the HMP gelling procedure (pH<3.0, 65 wt% sucrose) and the present of Ca^{2+} increases the gel strength, while PB shows gelling capacity with Ca^{2+} (Chen, et al., 2017). Interestingly, RG-I rich PA/PB blend gels showed improved rheological properties than pure PA and PB gels in $CaCO_3$-glucono-δ-lactone (GDL) system. The aim of this research is to explore the synergistic effect of PA and PB blend gelation with different ratios and gel properties under various conditions. Furthermore, the microstructures of gels were observed by Cryo-SEM. Based on the gel properties and microstructures, we proposed a hypothetical mechanism for the synergistic effect of PA and PB calcium-induced gel.

2. Materials and methods

2.1 Materials

Pectin sample were recovered from acid and basic water discharged from citrus canning factories during the segment membrane removal process described previously (Chen, et al., 2017) with some modifications (see Figure 1). Citrus segments were added into 0.4% HCl

solution (pH=1.0) and stirred at 28℃ for 40 min to loosen the cell wall structure and extract a portion of pectin. Then the mixture was filtered through a 400-mesh filter bag. The first fraction of acid-extracted pectin (PA) was recovered from the acidic filtrate by adjusting pH to 6~7 and precipitation with 95% ethanol in the volume ratio of 1:1 for 2 h. The residue was resuspended in 0.6% NaOH (pH=13.2) and magnetic stirred at 32℃ for 10 min, then a filter bag was used to obtain the liquid and the residue was discarded. The liquid underwent pH-adjustment and precipitation to recover the pectin extracted with base (PB). Finally, precipitates were washed with 0.1% HCl/ethanol for 2 times and ethanol for 2 times to remove salt and oven-dried at 55 ℃ for 24 h. PA was composed of 44.2% HG and 40.6% RG-I (GalA: Rha: Ara: Gal=47.1: 2.87: 23.2:11.6 mol%, DM=45.4%, Mw= 196.6 kDa), while PB was composed of 19.3% HG and 62.7% RG-I (GalA: Rha: Ara: Gal=23.5: 4.19: 43.3:11.1 mol%, DM=15.06%, Mw=282.7 kDa), chemical structure results of PA and PB was shown in supplementary data. All chemicals used were of analytical grade.

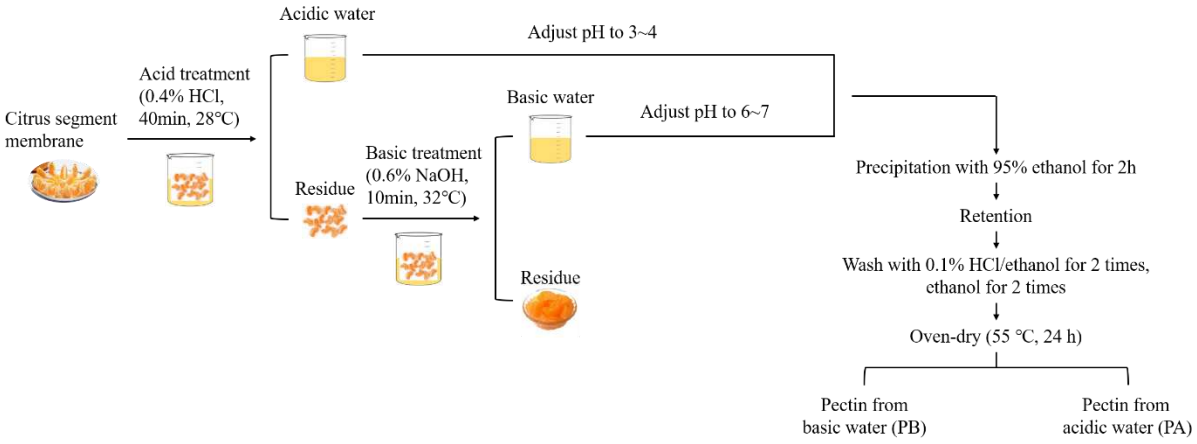

Figure 1. Flow chart for extraction of PA and PB.

2.2 Atomic force microscopy (AFM) observation

The pectin samples (200 μg/mL) were dissolved in ultrapure water with continuous stirring at 80 ℃ for 2 h. The pectin solutions were diluted by sodium dodecyl sulfate (SDS) solution to obtain a mixed solution containing polysaccharides and SDS both 10 μg/mL and then stirred for 48 h. SDS was added for producing stable unaggregated solutions (Wang and Nie, 2019). A 5 μL of mixed solution was filtered through a 0.22 μm filter and dropped onto a freshly cleaved mica substrate and then air-dried overnight. Scanning probe microscopy images were observed by AFM (XE-70, Park Scientific Instruments, Suwon, Korea) using tapping mode in air at room temperature (humidity: 50%-60%). The probe is a classical silicon cantilever (Si_3N_4) with a spring constant of 0.2 N/m and a resonance frequency of approximately 13 kHz (Wei, et al., 2019). NanoScope Analysis 1.8 was used for image manipulation.

2.3 Preparation of pectin gels

PA and PB samples were dissolved in distilled water at content of 0.5, 1.0, 1.5 and 2.0% (w/v)) under magnetic stirring for 3 h at 40℃. The stock PA and PB solutions were mixed under magnetic stirring for 30 min at 40℃ to prepare pectin solutions with different ratio of PA and PB (PA/PB=2:0, 1.5:0.5, 1:1, 0.5:1.0 and 0:2). The pectin solutions were cooled to 25℃ and the pH of each solution was adjusted to 5.0 using 1M NaOH or HCl. The pectin gels were formed using controlled calcium release from the $CaCO_3$-GDL system in order to inhibit pre-gelation. $CaCO_3$ (5, 10, 20 and 40 mM), GDL (0.8, 1.6, 2.0 and 2.8 wt%) and urea (1 M) were added to the pectin solutions under constant stirring for 4 min to obtain mixed gels.

2.4 Rheological measurement

A HAAKE RheoStress 6000 rheometer (Thermo Scientific, USA) with a 60 mm parallel plate was used to analyze the rheological properties of pectins, including steady shear flow

behavior of PA and PB solutions and dynamic-viscoelastic properties of PA and PB synergistic gels. Pectin solutions with different ratio of PA and PB were subjected to steady shearing with the shear rates ranging from 0.01 to 100 s^{-1} at 25℃. Data were fit to a power law model (equation (1)).

$$\eta=k\gamma^{(n-1)} \quad (1)$$

In equation (1), where η is the apparent viscosity (mPa•s), k (mPa•s^n) is the consistency index, γ is the shear rate (s^{-1}) and n (dimensionless) is the flow behavior index.

In order to analyze dynamic-viscoelastic properties of pectin gels with $CaCO_3$ and GDL, the mixed gels were put onto the rheometer and equilibrated for 1 min at 25℃, then analyzed for their rheological behavior. The linear viscoelastic ranges were firstly determined by amplitude sweep from 0.001% to 100% at a constant frequency of 1 Hz. The small deformation oscillatory of time sweep determination was carried out at constant frequency of 1 Hz for 10800 s, under 0.1% deformation (smaller than the maximum value of linear viscoelastic range). The frequency sweep was conducted from 0.1 to 10 Hz at 0.1% deformation to monitor the change in storage modulus (G') and loss modulus (G'') of the mixtures after 10800 s. For pH measurement, mixed gels with $CaCO_3$ and GDL were stirred for 4 min and equilibrated for 1 min, the pH value was measured every 10 min for 3 h.

2.5 Visualization of microstructure of pectin gels (Cryo-SEM)

Cryo-scanning electron microscopy (Cryo-SEM) is used to observe the native microstructure of high water content hydrogels. First, the sample placed in the stub was cryo-vitrified with liquid nitrogen slush at -210 ℃. The vitrified sample was then transferred into the cryo-SEM pre-chamber (PP3010T Cryo-SEM Preparation System, Quorum, UK) for sublimation

147 at -85 ℃ under vacuum conditions for 20-25 min. The sample was sputtered with gold to prevent
148 charging during electron beam targeting. Finally, the sample was transferred on to the SEM stage
149 (Regulus 8100, Hitachi, Japan) at -140 ℃ for observation (Kyomugasho, et al., 2018; Aston, &
150 Sewell, & Klein, & Lawrie, and Grøndahl, 2016).

151 2.6 Statistical analysis

152 Data were expressed as the mean ± standard deviation (SD) with three replicates per
153 sample. Data were analyzed by ANOVA using Duncan's test with SPSS version 21.0 (IBM
154 software, New York, USA). The significance level was set at $P < 0.05$.

155 3. Results and discussion

156 3.1 Morphology properties and steady shear flow behavior of PA and PB solutions

157 The morphology of pectin solutions at 10 μg/mL in the scan area of 2.5 μm×2.5 μm was
158 shown in Figure 2. The PA molecule chains aggregated into a continuous and dense network of
159 2.0 nm height, with gathered pieces ranging from 100 nm to 300 nm of 2.5 nm height (Fig. 2a).
160 The irregular and sparse network structures were observed in PB solution, average vertical height
161 of the main chains was measured to be 3.0 nm. The height of PB was higher than that of PA,
162 which may relate to the high molecular weight and highly branched structure of PB. In addition,
163 PA molecule chains showed more aggregations than PB at the same pectin concentration, which
164 may be relevant to the relatively high GalA content and DM (~45%). Interestingly, in the blend
165 solution containing 5 μg/mL PA and 5 μg/mL PB distributed on mica, the molecules presented
166 an island-like structure of a height of 2.0-3.0 nm, different from the network structure of pure
167 pectin solutions with same polymer concentration. The poor networking and high aggregation
168 degree of mixture of PA and PB could be explained by the structure characteristics. Long side-

chains of PB tend to interact with each other and form aggregates with the backbone located at the periphery (Mikshina, et al., 2015). In addition, the water retaining capacity of arabinan side-chains (Larsen, et al., 2011) promoted the interaction between methoxylated galacturonic acid residues of PA (Fu and Rao, 2001). The intermolecular polymerization in PA/PB blend solution provided the possibility of synergistic mixed gelation.

Steady shear flow behavior of PA and PB solutions (Fig. 2d) suggested that pectin solutions are all typical pseudoplastic fluids. Table 1 showed that the fitting accuracy of data points on the sample curve using the power law model reached 0.98, suggesting the model could be used to analysis pectin samples (Table 1). The consistency coefficient (K) and fluid index (n) were of magnitudes used to express fluid consistency and non-Newtonian fluid behavior in the model. The consistency coefficient of PA was higher than that of PB, which may relate to the abundant HG region with a relatively high DM of PA. PB had the greater shear-thinning property, indicating the orientation of PB molecular chain can be more easily obtained by shearing. This property may be due to the low GalA content and low degree of methoxylation of PB, which resulted in low viscosity and little interactions between molecular chains. The different steady shear flow behavior of pectin solutions was consistent with the chain conformation observed by AFM. Apparent viscosity of PA was higher than that of PB, which could be explained by the continuous and dense network with aggregations observed in PA solution and irregular and sparse network structures of PB. The color of PB solution was clear than PA solution at the same concentration (Fig. S4a and c), supporting that the aggregation of pectin chains in PB solution was less than that of PB solution (Hua, & Yang, & Din, & Chi, and Yang, 2018). In addition, PA/PB blend solution showed medium fluid index and consistency coefficient comparing with PA and PB, consistent with the microstructure of inhomogeneous aggregations. Hydrogen bonds

between polymer chains promoted the aggregation. In order to investigate the contribution of hydrogen bonds in RG-I rich pectin solutions, 1 M urea was added into the solutions. Urea is a hydrogen bond breaking agent can break the intermolecular hydrogen bonding between polysaccharides chains. The influence of 1M urea on the apparent viscosity of PA, PB and PA/PB solutions (PA/PB=1) were showed in Fig. 2e. The fluid index and consistency coefficient of pectin solutions decreased in the present of urea and the influence on PA was most obvious, indicating hydrogen bonds contributed to pectin aggregations and promoted apparent viscosity.

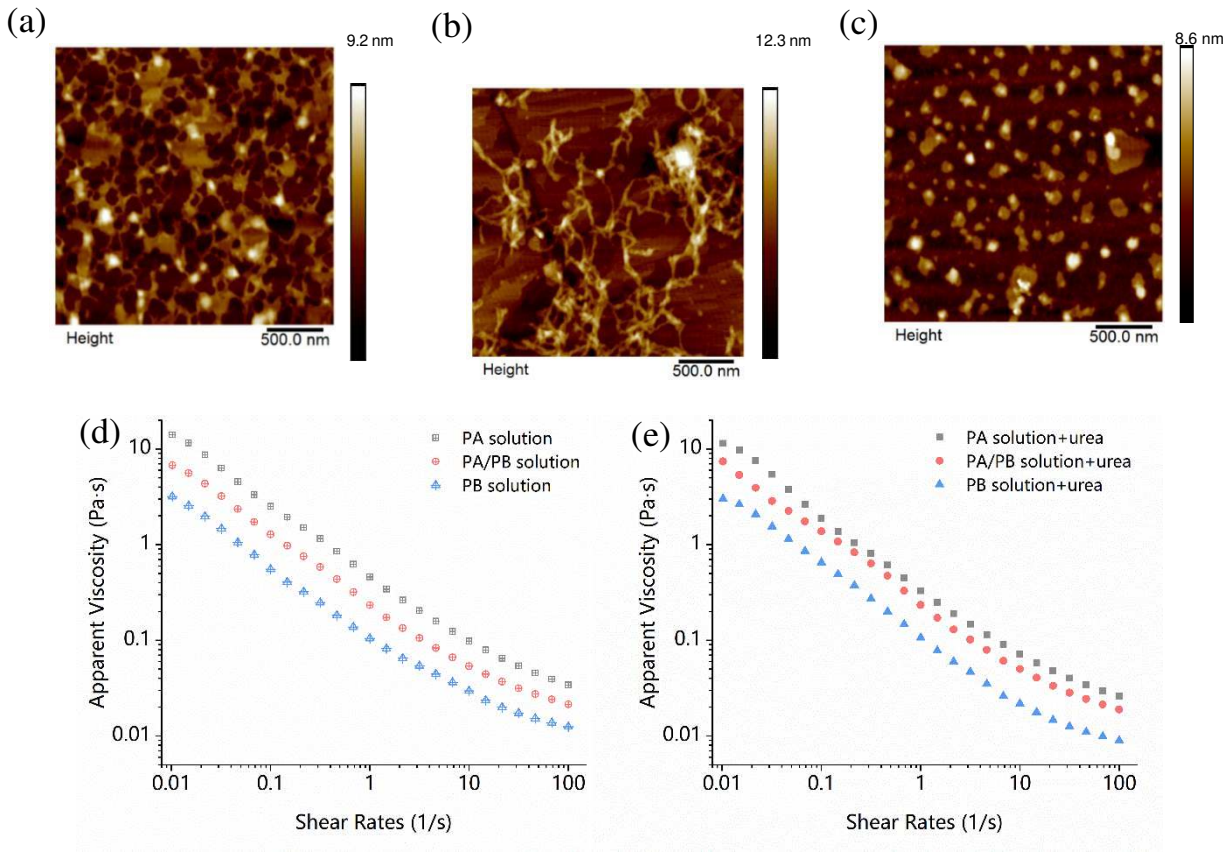

Figure 2. Representative topographical AFM images of (a) PA, (b) PB and (c) mixture of PA/PB; (d) Flow behavior of PA, PB and PA/PB (PA/PB=1) solution at concentration of 1.5%; (e) Flow

203203

behavio r of PA, PB and PA/PB (PA/PB=1) solution at concentration of 1.5% with 1 M urea.

204 **Table 1.** Parameters of flow curves obtained by fitting to power law model.

Index	PA solution	PA/PB solution	PB solution	PA solution+ urea	PA/PB solution+ urea	PB solution+ urea
k	537.9	284.3	137.6	404.7	276.8	126.9
n	0.316	0.339	0.371	0.305	0.323	0.314
R^2	0.9936	0.9901	0.9848	0.9901	0.9922	0.9905

205

206 3.2 Dynamic-viscoelastic properties of PA and PB synergistic gels

207 **Ratio of PA and PB** Fig. 3a showed the modulus and pH evolution of PA/PB blend
208 samples at different ratio with addition of 0.8 wt% GDL and 5 mM $CaCO_3$. Initially, pH was
209 around 5.8 and Ca was present in the form of solid $CaCO_3$. The modulus of PA was the highest
210 among all the samples while that of PB was the lowest, which can be explained by the different
211 structures of PA and PB. PA composed of relatively high content of GalA with DM of 45%, thus
212 the network formation of PA may contribute to calcium-bridge or hydrogen bonds and
213 hydrophobic interactions depending on the distribution of demethylated blocks of HG (Yu, et al.,
214 2017). The presence of abundant rhamnose in PB influenced the conformation of the polymer in
215 solution, disturbing the molecular orientation necessary for junction-zone formation and limiting
216 inter-chain association (Chan, & Choo, & Young, and Loh, 2017). The concentration of Ca ions
217 increased progressively with GDL hydrolysis, which led to an increase modulus of gels. G' and
218 G'' increased mainly due to the "egg box" junction zones formed by binding action between
219 Ca^{2+} and carboxyl groups. Another reason for increasing modulus was the hydrogen bonds and
220 hydrophobic interactions between galacturonic acid backbones (Ngouémazong and Tengweh, et
221 al., 2012) and neutral sugar side-chains prompted by the low pH condition (Ngouémazong, et al.,
222 2012; Sousa, & Nielsen, & Armagan, & Larsen, and Sørensen, 2015). The extremely low DM of
223 PB were beneficial for calcium-bridge formation and abundant side-chains stabilized the network
224 structure through entanglements. As for PA, G' and G'' increased slowly. Blocks of more than

10 non-methoxylated galacturonic acid residues could interact with calcium ions (Chan, et al., 2017). The slow and limited increase could be explained by the occurrence of methyl ester groups in the primary backbone and the RG-I steric hindrance produced on the unesterified HG blocks (Cameron, & Luzio, & Goodner, and Williams, 2008; Luzio and Cameron, 2008). PA system appeared as thick liquid (Fig. S4d), different from the solid appearance of PB or PA/PB blend gel (Fig. S4e and f). But the G' of PA system was always higher than the G'', suggesting it should be considered as a weak gel (Kyomugasho, et al., 2016). Modulus of PA slightly decreased after 5000 s, similar phenomenon has been reported previously (Lootens, et al., 2003). The modulus of pectin with a relatively high DM (~50%) was dependent on the balance of two interactions. Low pH prompted the hydrophobic interactions between methylesterified carboxyl and hydrogen bonds between non-methylesterified carboxyl. It could also convert the carboxyl from dissociated (COO-) to associated (COOH) and reduced affinity for Ca ions. As a result, the modulus of PA gel decreased at pH lower than 4.5 (Fraeye, & Duvetter, & Doungla, & Van Loey, and Hendrickx, 2010). Interestingly, G' and G'' of PA/PB blend samples increased more quickly and were higher than pure PA or PB samples, suggesting the synergistic effect of PA and PB could strengthen the gel network. One possible reason was that the long side-chains of PB decreased the water activity since they contain many hydrophilic groups (Einhorn-Stoll, 2018), thus prompted the interaction of PA chains. Moreover, PA and PB could interact with each other by Ca-bridges with the release of calcium ions. Consequently, mixture of PA and PB prompted the formation of three-dimensional network and increased the moduli of blend gels.

Pectin concentration The modulus and pH of PA/PB blend gels (PA/PB=1) at different pectin concentration (0.5, 1.0, 1.5 and 2% w/v) with addition of 0.8 wt% GDL and 5 mM $CaCO_3$ were shown in Fig. 3b. The effect of pectin concentration on the pH was ignorable for the ratio

GDL to $CaCO_3$ used in the samples. The G' and G'' increased with increasing pectin concentration and the change of G' and G'' at low concentrations (<1.0% w/v) was more apparent than high concentrations (>1.0% w/v). The increased modulus could be attributed to increased number of cross-linking junction zones between pectin chains. With increasing pectin concentration, number of hydrogen bonds and hydrophobic interactions between pectin chains increased, which can be explained by the higher number of binding sites available and the lower water activity of gels. The number of "egg box" junction zones between Ca^{2+} and pectin chains also increased and the probability of ionic bonds formation within the same pectin chain decreased, leading to more junction zones between the separate pectin chains and stronger gels (Kyomugasho, et al., 2016; Fraeye, & Duvetter, & Doungla, & Van Loey, and Hendrickx, 2010). G' and G'' of gels increased with pectin concentration, but the increasing effects was not significant when the concentration reached to a certain level. The high viscosity of pectin solution locked the structure thus hinder the formation of ionic cross-links (Wan, et al., 2019). Interestingly, the modulus increased more quickly at low pectin concentration compared to the high concentration. At constant Ca^{2+} concentration, the lower the pectin concentration was, the higher the ratio of Ca^{2+} to the pectin concentration was, resulting in quick gel formation.

GDL concentration The modulus and pH of PA/PB blend gels (PA/PB=1) with different concentration of GDL (0.8, 1.6, 2.0 and 2.8 wt%) with addition of 5 mM $CaCO_3$ is shown in Fig. 3c. G' and G'' of gels increased rapidly at early stage with Ca ions releasing. The gel formation at GDL concentration of 0.8% was much slower than that at higher GDL concentrations, because GDL can decrease the pH of gels during the hydrolysis and promote the Ca ions release. The differences of gel formation rate at high GDL concentrations (≥1.6%) were not significant, additional GDL had little influence on the rate because the amount of interaction sites was

limited due to the constant pectin concentration. Moduli of the gels reach a plateau within ~3000 s, when most of the Ca ions had been released. G' and G'' of gels after 3h holding period were different at various GDL concentration and the G' and G'' increased with GDL concentration increasing, but the rheological properties of gels at 2.8% GDL was similar with that of 2.0%. Decreased pH promotes formation of hydrogen bonds between protonated carboxyl groups (Fraeye, & Duvetter, & Doungla, & Van Loey, and Hendrickx, 2010) as well as neutral sugar side-chains (Ngouémazong and Kabuye, et al., 2012; Sousa, & Nielsen, & Armagan, & Larsen, and Sørensen, 2015). Meanwhile, the affinity for calcium ions of pectin decreased at low pH condition because of the decreased charge density (Cardoso, & Coimbra, and Lopes Da Silva, 2003). A pH of 5.0 was found to be optimal for Ca^{2+} binding by LM pectin (Celus, & Kyomugasho, & Van Loey, & Grauwet, and Hendrickx, 2018), however, that was 3.0 for PA/PB blend gel with 5 mM Ca ions. The low optimal pH of blend gel suggested that besides ionic cross-links, hydrogen bonds were of great importance to the RG-I rich blend gel formation.

Ca^{2+} concentration The modulus and pH of PA/PB blend gels (PA/PB=1) with different concentration of $CaCO_3$ (5, 10, 20 and 40 mM) with addition of 0.8 wt% GDL were shown in Fig. 3d. The calcium content strongly influenced the kinetic behavior and moduli of the gels. Increased Ca^{2+} concentration of resulted in more rapid gel formation and also a complex behavior in G' and G''. Moduli of gels with high Ca^{2+} concentration increased rapidly and reached a local maximum within ~2000 s, then decreased and reach a plateau within ~6000 s, while that of lower Ca concentration increased continuously. G' of gels with more than 20 mM Ca^{2+} were higher than that of 10 mM Ca^{2+}, but after 3000 s the opposite result was obtained. Pectin chains interacted with cations and formed point-like cross-links at low Ca^{2+} concentration, then dimers occurred and the network of polymer chains formed upon increasing Ca ions

(Kyomugasho, et al., 2016; Huynh, & Lerbret, & Neiers, & Chambin, and Assifaoui, 2016). The increasing $CaCO_3$ concentration contributed to more available Ca ions in gels, which could increase the crosslink density between pectin chains (Wan, et al., 2019). However, the initial structure based on Ca^{2+}-pectin interactions may lock the structure thus diminish the possibilities for further strengthening of gel network by hydrophobic interactions and hydrogen bonds (Löfgren, & Guillotin, & Evenbratt, & Schols, and Hermansson, 2005). Another possible reason was that the structure formation rate of gel at high GDL concentration was fast, which caused incomplete network formation thus reduces the G' of gel (Kastner, & Einhorn-Stoll, and Senge, 2012). Moreover, excess Ca^{2+} caused syneresis of gels with a thin water layer found on the gel surface and decreased the G' (Liu, & Guo, & Li, & Zhu, and Li, 2013). Above pH 4.5 gel properties were relatively independent of pH (Fraeye, & Duvetter, & Doungla, & Van Loey, and Hendrickx, 2010), indicating the various G' and G'' of gels added more than 5 mM Ca ions mainly resulted from the concentration of $CaCO_3$. According to the moduli of gels with different GDL concentration (Fig. 3c), moduli of gels increased with pH decreasing when pH above 3.0, so the G' of gels with 5 mM $CaCO_3$ increased slowly while that of higher Ca^{2+} concentrations keeps constant.

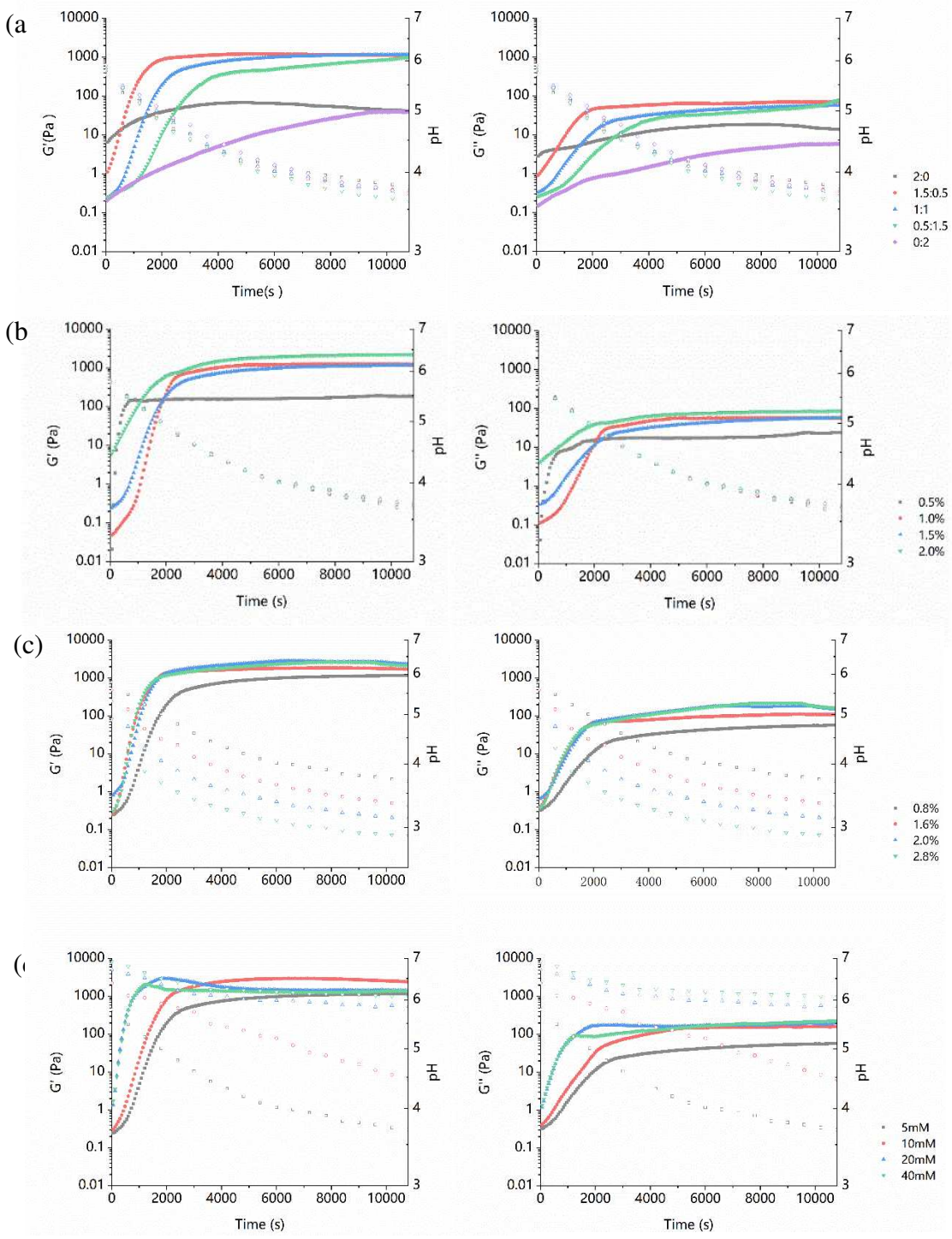

312

313 **Figure 3.** Modulus values (G' and G'') of PA/PB blend gels. (a) PA/PB blend gels (1.5% w/v

314 pectin concentration, 0.8 wt% GDL, 5 mM $CaCO_3$) at PA/PB=2:0, 1.5:0.5, 1:1, 0.5:1.0 and 0:2;

315 (b) PA/PB blend gels (PA/PB=1, 0.8 wt% GDL, 5 mM $CaCO_3$) of pectin concentration of 0.5,

1.0, 1.5 and 2.0% w/v; (c) PA/PB blend gels (PA/PB=1, 1.5% w/v pectin concentration, 5 mM $CaCO_3$) with GDL concentration of 0.8, 1.6, 2.0 and 2.8 wt%; (d) PA/PB blend gels (PA/PB=1, 1.5% w/v pectin concentration, 0.8 wt% GDL) with Ca^{2+} concentration of 5, 10, 20 and 40 mM. Measurement temperature, 25℃; strain, 0.1%; frequency, 1 Hz.

3.3 Effect of urea on dynamic-viscoelastic properties of PA and PB synergistic gels

The synergistic gelation feature of PA/PB blend gels was demonstrated, but a more comprehensive investigation of the association properties of this system is required. For cation-induced RG-I rich pectin gel, junction zones are primarily formed by electrostatic interactions and contributed to hydrogen bond between intra- and intermolecular pectin chains (Liu, & Guo, & Li, & Zhu, and Li, 2013). The contribution of hydrogen bonds in synergistic gel formation was worthy of study, so oscillatory shear measurements of gels are carried out with urea. The influence of 1M urea on the dynamic-viscoelastic properties of PA, PB and PA/PB blend gels (PA/PB=1) were showed in Fig. 4. The decrease of G' and G'' of PA gel was more obvious than that of PB gel in the presence of urea, suggesting that hydrogen bonding contributes to the gel formation of PA. The inhibition of PA gel could be explained by the lack of blocks of more than 10 non-methoxylated galacturonic acid residues, which was consistent with the structure properties of PA. As for PB, the slight decrease of modulus suggested that PB gel mainly composed of the calcium-pectin network, hydrogen bonds could help stabilize the structure. Interestingly, the modulus of PA/PB blend gel was lower than PB gel after addition of urea, in other words, synergistic effect of PA/PB blend gel no longer appeared, indicating the hydrogen bonds were vital for synergistic gelation.

339339 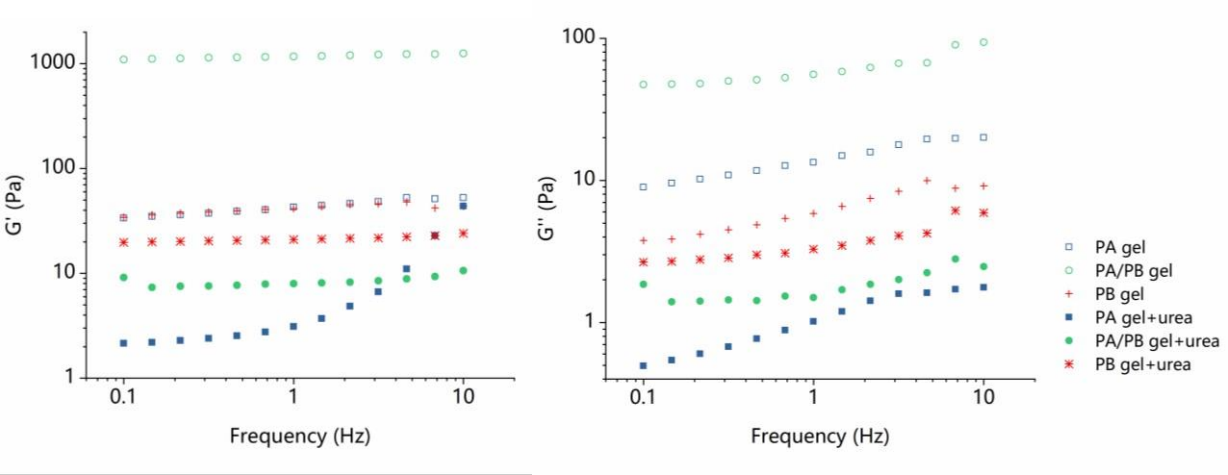

340 **Figure 4.** Modulus values (G' and G'') of PA/PB blend gels. (a) G' of PA, PB and PA/PB blend
341 gels (PA/PB=1) with addition of 0.8 wt% GDL and 5 mM CaCO3; (b) G'' of PA, PB and PA/PB
342 blend gels (PA/PB=1) with addition of 0.8 wt% GDL and 5 mM CaCO3; Measurement
343 temperature, 25℃; strain, 0.1%; frequency, 0.1-10 Hz.

344344

345 3.4 Cryo-SEM analysis

346 Cryo-SEM images of PA, PB and PA/PB blend gels with addition of 5mM $CaCO_3$ were
347 showed in Fig. 5. Formation of intertwined fibrous network and strand-like structure can be
348 promoted by cations (Efthymiou, & Williams, and McGrath, 2017; Kyomugasho, et al., 2016).
349 PA gel mainly composed of strand-like structures but the network was incomplete with open
350 microstructures. PA exhibited higher amounts of GalA with 45% DM, prompting the polymer
351 chain entanglements based on hydrogen bonds. But low amounts of blocks of more than 10 non-
352 methoxylated galacturonic acid residues limited formation of ionic cross-links, resulting the
353 loose and incomplete network and thick liquid appearance (Fig. 5a). PB gel showed intertwined
354 fibrous network, which was similar with the microstructure structures observed in LMP gels

(Kyomugasho, et al., 2018b; Kyomugasho, et al., 2016; Liu, & Guo, & Li, & Zhu, and Li, 2013). Dense cross-links were related to the high number of non-methylated GalA residues, which can form egg-box junction zones with Ca^{2+}. However, open structures could be found in the network, because the "kinks" produced by the rhamnose inserts of backbone limited cross-links (Fraeye, & Duvetter, & Doungla, & Van Loey, and Hendrickx, 2010). Thus, the surface of PB gel showed discontinuous structure in FESEM image (Fig. S3). Furthermore, PB exhibited higher amounts of branch-like structure compared to PA, consisting with the highly branched structure of PB (Santiago, et al., 2018). Cryo-SEM image of PA/PB blend gel showed a clear three-dimensional network composed of strand-like structures (Fig. 5c) and intertwined fibrous structures (Fig. 5d). The entangled strand-like structures converted to cross-linked network, suggesting the blend system promoted the interaction of PA chains. The intertwined fibrous structures interacted with the strand-like structures, indicating Ca^{2+} connected PA and PB polymer chains. The unique microstructure was consistent with the strengthened gel properties of PA/PB blend gel. In addition, the surface of blend gel was more compact than that of pure gels (Fig. S3), representing an improved gelled state (Li, et al., 2019).

3.5 Proposed mechanism of PA/PB synergistic gel formation

Our study showed PA and PB synergistically formed stronger gels with calcium induction. PA and PB consisted mainly of branched RG-I with the ratio of 41% and 63%, respectively, and high content of arabinose and galactose. The methoxylation degree of PA was 45%, but PB was only 15%. The AFM observation illustrated that PA could form dense network structure with gathered pieces, indicating the strong interactions between pectin chains based on hydrogen bonds. PB showed irregular and sparse network structure, based on the interaction of long side-chains of RG-I region. The molecules presented an island-like structure in PA/PB blend solution

at the same polymer concentration, indicating the aggregation trend of PA and PB. RG-I side-chains of PB tended to form aggregates with the backbone located at the periphery (Mikshina, et al., 2015). Meanwhile, neutral sugar side-chains, especially arabinan side chains, could hydrate more readily than the rhamnose-galacturonic acid (Rha-GalA) backbone in RG-I (Larsen, et al., 2011), thus promote aggregations of PA (Mikshina, et al., 2017; Makshakova, & Faizullin, & Mikshina, & Gorshkova, and Zuev, 2018). Different HG/RG-I ratios and DM values of PA and PB induced the separation of their aggregates. The hypothesis of hydration process was consistent with the steady shear flow behavior of pectin solutions (see Section 3.1).

PA and PB could form gels induced by calcium. PA was composed of relatively high content of GalA with DM of 45% and the network formation mainly composed of hydrogen bonds (Yu, et al., 2017), as well as few ionic cross-links. Non-methoxylated galacturonic acid residues can interact with calcium ions but the methyl ester groups limited the extent of such junction zones (Chan, & Choo, & Young, and Loh, 2017). The network of calcium-induced PB gel was mainly composed of the "egg box" junction zones formed by binding action between Ca^{2+} and carboxyl groups. Moreover, abundant side-chains stabilized the network structure through entanglements. For PA/PB blend gels, the synergistic effect of pectins could strengthen the gel network, indicating interactions between PA and PB, including Ca-bridges between carboxyl groups and side-chain entanglements. Moreover, neutral sugar side-chains prompted formation of hydrogen bonds. Calcium-bridges connected PA and PB aggregates with suitable pH, consequently promoted the three-dimensional network formation and improved the rheological properties and microstructure of blend gels (see Fig. 5e).

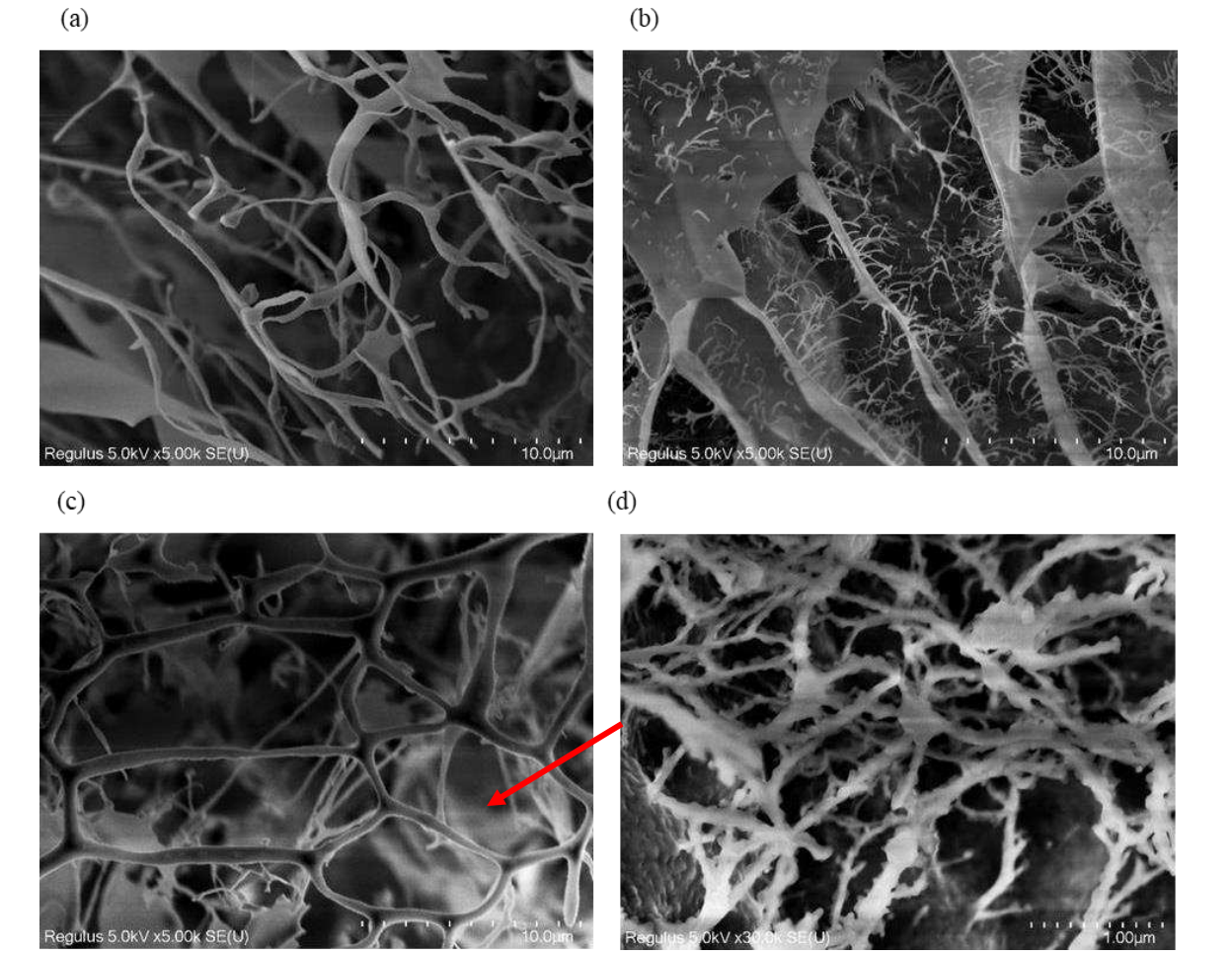
(a)
(b)
Regulus 5.0kV x5.00k SE(U)
10.0μm
Regulus 5.0kV x5.00k SE(U)
10.0μm
(c)
(d)
Regulus 5.0kV x5.00k SE(U)
10.0μm
1.00μm

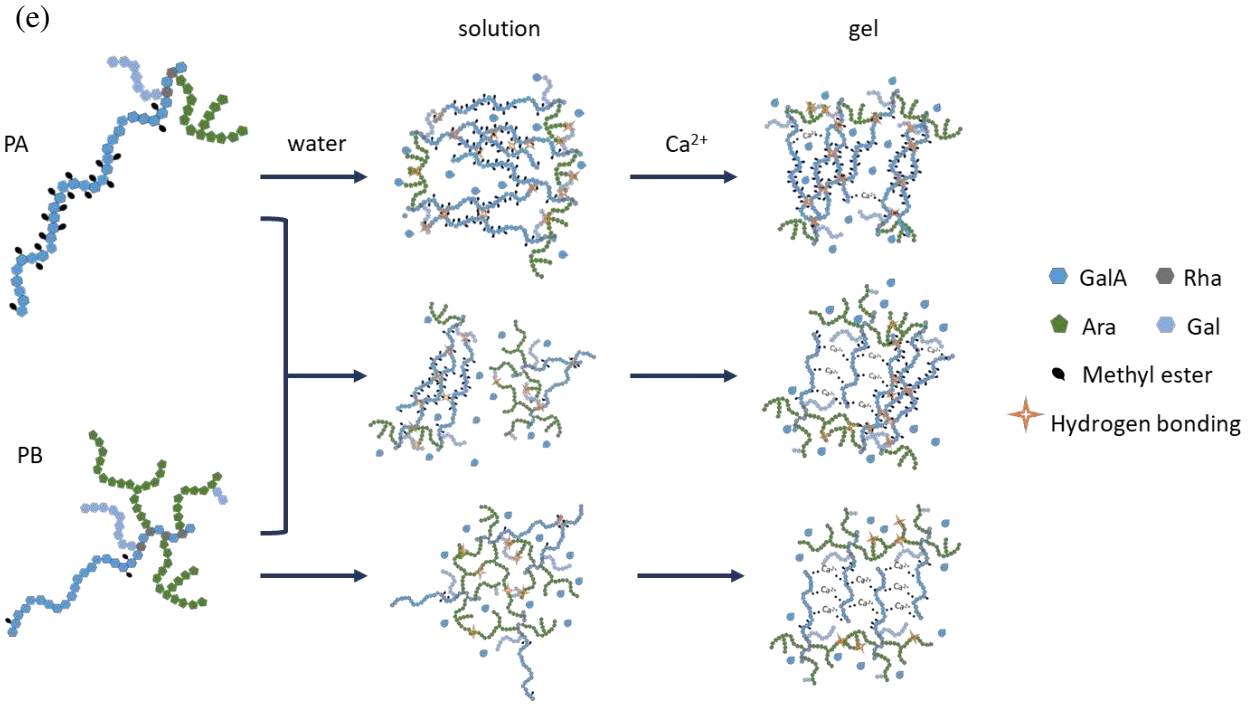
(e)
solution
gel
PA
water
Ca2+
PB
GalA
Rha
Ara
Gal
Methyl ester
Hydrogen bonding

399399

Figure 5. Microstructure of (a) PA, (b) PB, (c) and (d) PA/PB blend gels (1.5% w/v pectin concentration, 0.8 wt% GDL, 5 mM $CaCO_3$). The amplification was 5000 (a), (b), (c) and 30000 (d) times the original size. (e) Schematic diagram of the formation of PA, PB and PA/PB blend gel.

404404

4. Conclusion

Rheological properties, water-holding capacity and microstructure of RG-I rich citrus pectin gels were investigated to elucidate the synergistic gelation mechanism of PA and PB. PA, with higher HG region (~41%) and relatively high DM value (~49%), showed high viscosity and dense network structure in pure solution. PB composed of RG-I region (67%) with long neutral sugar side-chains and HG region (17%) of low DM value (15%), so the network of PB solution was irregular and sparse. Island-like structure was observed by AFM in the PA/PB blend solution, indicating separate aggregation of PA and PB. RG-I rich PA and PB could form gels induced by calcium ions. The network of PA gel was mainly composed of hydrogen bonds between methoxylated galacturonic acid residues. PB gels relied on ionic cross-link junction-zones, stabilized by side-chain entanglements. PA/PB blend gels showed improved rheological properties and microstructure compared with pure PA and PB gels. Ca-bridges connected pectin aggregates and promoted the three-dimensional structure of PA/PB blend gels but excess Ca^{2+} caused syneresis of gels and decreased water-holding capacity. The gel network was stabilized by the hydrogen bonds prompted by neutral sugar side-chains. These findings suggested that synergistic effects can be achieved by mixing PA and PB to produce a strengthened blend gel with calcium induction and provided further development for RG-I rich pectin-based products.

422422

423 Acknowledgements

424 This work was financially supported by National Key R&D Program of China

425 (2017YFE0122300190) and National Natural Science foundation of China (31871815).

426426

4274
2
7
4284
2
8
4294
2
9
4304
3
0
4314
3
1
4324
3
2
4334
3
3
4344
3
4
4354
3
5
4364
3
6
4374
3
7
4384
3
8
4394
3
9
4404
4
0
4414
4
1

442442
443443
444444
445445
446446
447447
448448
449449
450450
451451
452452
453453
454454
455455
456456
457457
458458
459459
460460
461461
462462
463463
464464
465465
466466
467467

References

tion of a model homogalacturonan with a salt-independent pectin methylesterase from citrus: I. Effect of pH on demethylated block size, block number and enzyme mode of action. *Carbohydrate Polymers*, *71*(2), 287-299.

Cardoso, S. M., Coimbra, M. A., & Lopes Da Silva, J. A. (2003). Calcium-mediated gelation of an olive pomace pectic extract. *Carbohydrate Polymers*, *52*(2), 125-133.

Celus, M., Kyomugasho, C., Van Loey, A. M., Grauwet, T., & Hendrickx, M. E. (2018). Influence of Pectin Structural Properties on Interactions with Divalent Cations and Its Associated Functionalities. *Comprehensive Reviews in Food Science and Food Safety*, *17*(6), 1576-1594.

Chan, S. Y., Choo, W. S., Young, D. J., & Loh, X. J. (2017). Pectin as a rheology modifier: Origin, structure, commercial production and rheology. *Carbohydrate Polymers*, *161*, 118-139.

Chen, J., Chen, W., Duan, F., Tang, Q., Li, X., Zeng, L., Zhang, J., Xing, Z., Dong, Y., Jia, L., & Gao, H. (2019). The synergistic gelation of okra polysaccharides with kappa-carrageenan and its influence on gel rheology, texture behaviour and microstructures. *Food Hydrocolloids*, *87*, 425-435.

Chen, J., Cheng, H., Wu, D., Linhardt, R. J., Zhi, Z., Yan, L., Chen, S., & Ye, X. (2017). Green recovery of pectic polysaccharides from citrus canning processing water. *Journal of Cleaner Production*, *144*, 459-469.

Efthymiou, C., Williams, M. A. K., & McGrath, K. M. (2017). Revealing the structure of high-water content biopolymer networks: Diminishing freezing artefacts in cryo-SEM images. *Food Hydrocolloids*, *73*, 203-212.

Einhorn-Stoll, U. (2018). Pectin-water interactions in foods – From powder to gel. *Food Hydrocolloids*, *78*, 109- 119.

Fraeye, I., Duvetter, T., Doungla, E., Van Loey, A., & Hendrickx, M. (2010). Fine-tuning the properties of pectin–calcium gels by control of pectin fine structure, gel composition and environmental conditions. *Trends in Food Science & Technology*, *21*(5), 219-228.

Fu, J., & Rao, M. A. (2001). Rheology and structure development during gelation of low-methoxyl pectin gels: the effect of sucrose. *Food Hydrocolloids*, *15*(1), 93-100.

Hua, X., Yang, H., Din, P., Chi, K., & Yang, R. (2018). Rheological properties of deesterified pectin with different methoxylation degree. *Food Bioscience*, *23*, 91-99.

Huynh, U. T., Lerbret, A., Neiers, F., Chambin, O., & Assifaoui, A. (2016). Binding of Divalent Cations to Polygalacturonate: A Mechanism Driven by the Hydration Water. *Journal of Physical Chemistry B*, *120*(5), 1021-1032.

Kastner, H., Einhorn-Stoll, U., & Senge, B. (2012). Structure formation in sugar containing pectin gels – Influence of Ca2+ on the gelation of low-methoxylated pectin at acidic pH. *Food Hydrocolloids*, *27*(1), 42-49.

Klaassen, M. T., & Trindade, L. M. (2020). RG-I galactan side-chains are involved in the regulation of the water-binding capacity of potato cell walls. *Carbohydrate Polymers*, *227*, 115353.

Kyomugasho, C., Christiaens, S., Van de Walle, D., Van Loey, A. M., Dewettinck, K., & Hendrickx, M. E. (2016). Evaluation of cation-facilitated pectin-gel properties: Cryo-SEM visualisation and rheological properties. *Food Hydrocolloids*, *61*, 172-182.

Kyomugasho, C., Munyensanga, C., Celus, M., Van de Walle, D., Dewettinck, K., Van Loey, A. M., Grauwet, T., & Hendrickx, M. E. (2018a). Molar mass influence on pectin-Ca2+ adsorption capacity, interaction energy and associated functionality: Gel microstructure and stiffness. *Food Hydrocolloids*, *85*, 331-342.

Kyomugasho, C., Munyensanga, C., Celus, M., Van de Walle, D., Dewettinck, K., Van Loey, A. M., Grauwet, T., &

Cameron, R. G., Luzio, G. A., Goodner, K., & Williams, M. A. K. (2008). Demethyla

4684 7
6 488488
8 489489
4694 490490
6 491491
9 492492
4704 493493
7 494494
0 495495
4714 496496
7 497497
1 498498
4724 499499
7 500500
2 501501
4734 502502
7 503503
3 504504
4744 505505
7 506506
4 507507
4754 508508
7 509509
5 510510
4764 511511
7 512512
6 513513
4774 514514
7 515515
7 516516
4784 517517
7 518518
8 519519
4794 520520
7 521521
9 522522
4804
8
0
4814
8
1
4824
8
2
4834
8
3
4844
8
4
4854
8
5
4864
8
6
4874
8

apacity, interaction energy and associated functionality: Gel microstructure and stiffness. *Food Hydrocolloids*, *85*, 331-342.

Larsen, F. H., Byg, I., Damager, I., Diaz, J., Engelsen, S. B., & Ulvskov, P. (2011). Residue Specific Hydration of Primary Cell Wall Potato Pectin Identified by Solid-State 13C Single-Pulse MAS and CP/MAS NMR Spectroscopy. *Biomacromolecules*, *12*(5), 1844-1850.

Li, X., Dong, Y., Guo, Y., Zhang, Z., Jia, L., Gao, H., Xing, Z., & Duan, F. (2019). Okra polysaccharides reduced the gelling-required sucrose content in its synergistic gel with high-methoxyl pectin by microphase separation effect. *Food Hydrocolloids*, *95*, 506-516.

Liu, H., Guo, X., Li, J., Zhu, D., & Li, J. (2013). The effects of MgSO4, d-glucono- δ -lactone (GDL), sucrose, and urea on gelation properties of pectic polysaccharide from soy hull. *Food Hydrocolloids*, *31*(2), 137-145.

Löfgren, C. E. E., Guillotin, S., Evenbratt, H., Schols, H., & Hermansson, A. (2005). Effects of Calcium, pH, and Blockiness on Kinetic Rheological Behavior and Microstructure of HM Pectin Gels. *Biomacromolecules*, *6*(2), 646.

Löfgren, C., & Hermansson, A. (2007). Synergistic rheological behaviour of mixed HM/LM pectin gels. *Food Hydrocolloids*, *21*(3), 480-486.

Lootens, D., Capel, F., Durand, D., Nicolai, T., Boulenguer, P., & Langendorff, V. (2003). Influence of pH, Ca concentration, temperature and amidation on the gelation of low methoxyl pectin. *Food Hydrocolloids*, *17*(3), 237-244.

Luzio, G. A., & Cameron, R. G. (2008). Demethylation of a model homogalacturonan with the salt-independent pectin methylesterase from citrus: Part II. Structure – function analysis. *Carbohydrate Polymers*, *71*(2), 300-309.

Makshakova, O. N., Faizullin, D. A., Mikshina, P. V., Gorshkova, T. A., & Zuev, Y. F. (2018). Spatial structures of rhamnogalacturonan I in gel and colloidal solution identified by 1D and 2D-FTIR spectroscopy. *Carbohydr Polym*, *192*, 231-239.

Mao, G., Wu, D., Wei, C., Tao, W., Ye, X., Linhardt, R. J., Orfila, C., & Chen, S. (2019). Reconsidering conventional and innovative methods for pectin extraction from fruit and vegetable waste: Targeting rhamnogalacturonan I. *Trends in Food Science & Technology*, *94*, 65-78.

Mikshina, P. V., Idiyatullin, B. Z., Petrova, A. A., Shashkov, A. S., Zuev, Y. F., & Gorshkova, T. A. (2015). Physicochemical properties of complex rhamnogalacturonan I from gelatinous cell walls of flax fibers. *Carbohydr Polym*, *117*, 853-861.

Mikshina, P. V., Makshakova, O. N., Petrova, A. A., Gaifullina, I. Z., Idiyatullin, B. Z., Gorshkova, T. A., & Zuev, Y. F. (2017). Gelation of rhamnogalacturonan I is based on galactan side chain interaction and does not involve chemical modifications. *Carbohydrate Polymers*, *171*, 143-151.

Ngouémazong, D. E., Kabuye, G., Fraeye, I., Cardinaels, R., Van Loey, A., Moldenaers, P., & Hendrickx, M. (2012). Effect of debranching on the rheological properties of Ca2+ – pectin gels. *Food Hydrocolloids*, *26*(1), 44-53.

Ngouémazong, D. E., Tengweh, F. F., Fraeye, I., Duvetter, T., Cardinaels, R., Van Loey, A., Moldenaers, P., & Hendrickx, M. (2012). Effect of de-methylesterification on network development and nature of Ca2+-pectin gels: Towards understanding structure – function relations of pectin. *Food Hydrocolloids*, *26*(1), 89-98.

Santiago, J. S. J., Kyomugasho, C., Maheshwari, S., Jamsazzadeh Kermani, Z., Van de Walle, D., Van Loey, A. M., Dewettinck, K., & Hendrickx, M. E. (2018). Unravelling the structure of serum pectin originating from thermally and mechanically processed carrot-based suspensions. *Food Hydrocolloids*, *77*, 482-493.

Sousa, A. G., Nielsen, H. L., Armagan, I., Larsen, J., & Sørensen, S. O. (2015). The impact of rhamnogalacturonan-I side chain monosaccharides on the rheological properties of citrus pectin. *Food Hydrocolloids*, *47*, 130-139.

Thakur, B. R., Singh, R. K., Handa, A. K., & Rao, M. A. (1997). Chemistry and uses of pectin — A review. *C R C Critical Reviews in Food Technology*, *37*(1), 47-73.

Wan, L., Wang, H., Zhu, Y., Pan, S., Cai, R., Liu, F., & Pan, S. (2019). Comparative study on gelling properties of low methoxyl pectin prepared by high hydrostatic pressure-assisted enzymatic, atmospheric enzymatic, and alkaline de-esterification. *Carbohydrate Polymers*, *226*, 115285.

Wang, J., & Nie, S. (2019). Application of atomic force microscopy in microscopic analysis of polysaccharide. *Trends in Food Science & Technology*, *87*, 35-46.

Wei, C., Zhang, Y., He, L., Cheng, J., Li, J., Tao, W., Mao, G., Zhang, H., Linhardt, R. J., Ye, X., & Chen, S. (2019). Structural characterization and anti-proliferative activities of partially degraded polysaccharides from peach gum. *Carbohydrate Polymers*, *203*, 193-202.

Willats, W., Knox, P., & Mikkelsen, J. D. (2006). Pectin: new insights into an old polymer are starting to gel.

Trends in Food Science & Technology, *17*(3), 97-104.
Wu, D., Zheng, J., Mao, G., Hu, W., Ye, X., Linhardt, R. J., & Chen, S. (2019). Rethinking the impact of RG-I mainly from fruits and vegetables on dietary health. *Crit Rev Food Sci Nutr*, 1-23.
Yu, L., Yakubov, G. E., Zeng, W., Xing, X., Stenson, J., Bulone, V., & Stokes, J. R. (2017). Multi-layer mucilage of Plantago ovata seeds: Rheological differences arise from variations in arabinoxylan side chains. *Carbohydr Polym*, *165*, 132-141.
Zhang, H., Chen, J., Li, J., Yan, L., Li, S., Ye, X., Liu, D., Ding, T., Linhardt, R. J., & Orfila, C. (2017). Extraction and characterization of RG-I enriched pectic polysaccharides from mandarin citrus peel. *Food Hydrocolloids*, *79*.

Synergistic gelling mechanism of RG-I rich citrus pectic polysaccharide at different esterification degree in calcium-induced gelation

Shiguo Chen [a,b,c], Jiaqi Zheng [a], Laiming Zhang [a], Huan Cheng [a,b,c], Caroline Orfila [d], Xingqian Ye [a,b,c], Jianle Chen [a,b,c,*]

[a] College of Biosystems Engineering and Food Science, National-Local Joint Engineering Laboratory of Intelligent Food Technology and Equipment, Zhejiang Key Laboratory for Agro-Food Processing, Zhejiang Engineering Laboratory of Food Technology and Equipment, Zhejiang University, Hangzhou 310058, China

[b] Fuli Institute of Food Science, Zhejiang University, Hangzhou 310058, China

[c] Ningbo Research Institute, Zhejiang University, Ningbo 315100, China

[d] School of Food Science and Nutrition, University of Leeds, Leeds LS2 9JT, UK

Abstract

RG-I rich pectic polysaccharide is common in fruit and vegetable and possesses health benefits. However, it is removed during commercial pectin production because of poor gelling properties. Synergistic gelation can improve rheological properties of RG-I pectic polysaccharide and expand its application in functional food hydrocolloids. In the study, RG-I rich pectic polysaccharides at different degree of esterification was extracted from citrus membrane by sequential mild acidic (0.4% HCl, 28℃) and alkaline (0.6% NaOH, 32℃) treatment. The pectic polysaccharide from acid water (PA) composes of 41% RG-I and 44% HG with DM of 45%, while

the pectic polysaccharide from basic water (PB) composed of 63% RG-I and 19% HG with DM of 15%. PA/PB blend gel under $CaCO_3$-glucono-δ-lactone system showed improved rheological properties compared with pure gels. Ca-bridges connected pectin aggregates and promoted the three-dimensional structure of PA/PB blend gels, while neutral sugar side-chains prompted hydrogen bonds and strengthened gel network.

Keywords

Pectic polysaccharide, rhamnogalacturonan-I, synergistic gelation, hydrogen bonds

1. Introduction

Pectin is a heteropolysaccharide widely existing in plant cell walls, composed of three major domains which include linear homogalacturonan (HG), rhamnogalacturonan-I (RG-I) and rhamnogalacturonan-II (RG-II) (Mohnen, 2008; Thakur, Singh, Handa & Rao, 1997). Commercial pectin, dominated with HG, is well known for its gelling properties and widely used in the food, cosmetics and pharmaceutical industry (Willats, Knox & Mikkelsen, 2006). In commercial pectin production, RG-I region is removed by hot acid due to its poor gelling capability. However, recently study suggested these RG-I rich pectic polysaccharide from fruits and vegetables (e.g., citrus, okra, potato and sugar beet) having potential health benefits by modulating the gut microbe and promote cell adhesion and migration (Wu et al., 2019).

RG-I region contains a backbone of the repeating disaccharide unit [→2) -α-L-Rha*p*-(1→4)-α-D-Gal*p*A-(1→]$_n$ and neutral sugar side-chains attached to the O-4 and O-3 of rhamnose residues. RG-I backbone is not compatible with the gel formation because the rhamnose inserts on the

backbone produce “kinks” thereby limiting cross-linking. But recently, the side-chains of the RG-I region reportedly possess strong water-binding capacities (Klaassen & Trindade, 2020) and stabilize the gel network structures (Makshakova, Faizullin, Mikshina, Gorshkova & Zuev, 2018; Mikshina et al., 2017), providing a new perspective for branched RG-I gelation. RG-I rich pectic polysaccharide can form gel under divalent ions, for example Ca^{2+} and Mg^{2+}, and sucrose can strengthen the gel network (Liu, Guo, Li, Zhu & Li, 2013; Wang et al., 2019). Gels made from RG-I rich pectic polysaccharide with high molecular weights will be stronger than gels made with pectic polysaccharide of lower molecular weights. However, publish papers in this field report gelling capacity of RG-I rich pectic polysaccharide but rarely focus on the improvement of gel properties and network structures. Thus, further attempts to improve rheological properties and microstructures of RG-I gel based on the novel highly branched structure are needed for the development of functional food hydrocolloids.

Pectin mixtures are widely used in the food industry to obtain products with desired texture and gelling properties. High methoxylated pectin (HMP, DM>50%) and low methoxylated pectin (LMP, DM<50%) are often mixed in order to reduce sucrose content of pectin gels. HMP/LMP blend gels exhibited similar rheological behavior to HMP gels of higher sucrose concentrations, which attributes to the inhomogeneous gel structure (Löfgren & Hermansson, 2007; Lootens, Capel, Durand, Nicolai, Boulenguer & Langendorff, 2003). RG-I rich pectic polysaccharide has a synergistic effect on the gelation of traditional commercial pectins and other polysaccharides (Chen et al., 2019). RG-I pectic polysaccharide, with long galactan side branches extracted from okra, reduced the sucrose content required for gelation and acted as a synergistic gel for high-methoxyl pectin. Side-chain entanglements create a pliable and continuous network, thus these blended gels show excellent toughness and high fracture strain (Li et al., 2019). However, few

researches extracted RG-I rich citrus pectic polysaccharides at different esterification degree, so the synergistic gelation of RG-I rich pectic polysaccharides of different structures remains unknown. Studying the synergistic gelation mechanism of RG-I rich pectic polysaccharides at different esterification degree gives information for rational selection of RG-I pectic polysaccharide structure when designing or improving food textures, which could provide new perspectives support to expand the application of RG-I rich pectic polysaccharide as potential food additives and could be helpful in the development of RG-I-based food products.

In our previous work, we have used acid and alkaline extraction conditions at low temperature to extract RG-I rich pectic polysaccharides from citrus peel and segment membrane (Chen et al., 2017; Zhang et al., 2017). The flow chart for extraction was shown in figure 1. The structure and rheological properties of branched pectic polysaccharides have been evaluated, the pectic polysaccharide from acid water (PA) mainly composes of GalA with a medium (∼45%) DM, while Ara is the main saccharide present in the pectic polysaccharide from basic water (PB) with a low (~15%) DM. PA can form gel under the HMP gelling procedure (pH<3.0, 65 wt% sucrose) and the present of Ca^{2+} increases the gel strength, while PB shows gelling capacity with Ca^{2+} (Chen et al., 2017). Interestingly, RG-I rich PA/PB blend gels showed improved rheological properties (higher dynamic-viscoelastic modulus) than pure PA and PB gels in $CaCO_3$-glucono-δ-lactone (GDL) system. The aim of this research is to explore the synergistic effect of PA and PB blend gelation with different ratios and gel properties under various conditions. Furthermore, the microstructures of gels were observed by Cryo-SEM. Based on the gel properties and microstructures, we proposed a hypothetical mechanism for the synergistic effect of PA and PB calcium-induced gel.

2. Materials and methods

2.1 Materials

Pectic polysaccharide sample were recovered from acid and basic water discharged from citrus canning factories during the segment membrane removal process described previously (Chen et al., 2017) with some modifications (see Figure 1). The low extraction temperature, applied in canning, limited the hydrolysis of pectin side-chains. The proportion of major side-chain sugars (arabinose and galactose) was much higher than that of commercial citrus pectin, resulting in a lower proportion of galacturonic acid (GalA) (Chen et al., 2021). Citrus segments were added into 0.4% HCl solution (pH=1.0) and stirred at 28℃ for 40 min to loosen the cell wall structure and extract a portion of pectic polysaccharide. Then the mixture was filtered through a 400-mesh filter bag. The first fraction of acid-extracted pectic polysaccharide (PA) was recovered from the acidic filtrate by adjusting pH to 3~4 with 2M NaOH and precipitation with 95% ethanol in the volume ratio of 1:1 for 2 h. The residue was resuspended in 0.6% NaOH (pH=13.2) and magnetic stirred at 32℃ for 10 min, then a filter bag was used to obtain the liquid and the residue was discarded. The liquid underwent pH-adjustment to 6~7 with 2M HCl and precipitation to recover the pectic polysaccharide extracted with base (PB). Finally, precipitates were washed with 0.1% HCl/ethanol for 2 times and ethanol for 2 times to remove salt and oven-dried at 55 ℃ for 24 h. PA was composed of 44.2% HG and 40.6% RG-I (GalA: Rha: Ara: Gal=47.1: 2.87: 23.2:11.6 mol%, DM=45.4%, Mw= 196.6 kDa), while PB was composed of 19.3% HG and 62.7% RG-I (GalA: Rha: Ara: Gal=23.5: 4.19: 43.3:11.1 mol%, DM=15.06%, Mw=282.7 kDa), chemical structure results of PA and PB was shown in supplementary data. All chemicals used were of analytical grade.

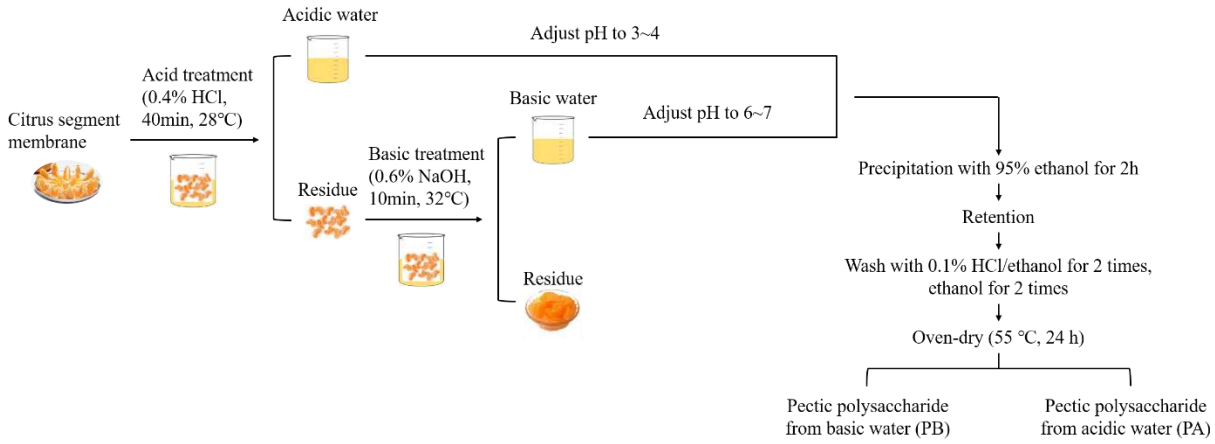

Figure 1. Flow chart for extraction of PA and PB.

2.2 Atomic force microscopy (AFM) observation

The pectic polysaccharide samples (200 μg/mL) were dissolved in ultrapure water with continuous stirring at 80 ℃ for 2 h. The pectic polysaccharide solutions were diluted by sodium dodecyl sulfate (SDS) solution to obtain a mixed solution containing polysaccharides and SDS both 10 μg/mL and then stirred for 48 h. SDS was added for producing stable unaggregated solutions (Wang & Nie, 2019). A 5 μL of mixed solution was filtered through a 0.22 μm filter and dropped onto a freshly cleaved mica substrate and then air-dried overnight. Scanning probe microscopy images were observed by AFM (XE-70, Park Scientific Instruments, Suwon, Korea) using tapping mode in air at room temperature (humidity: 50%-60%). The probe is a classical silicon cantilever (Si_3N_4) with a spring constant of 0.2 N/m and a resonance frequency of approximately 13 kHz (Wei et al., 2019). NanoScope Analysis 1.8 was used for image manipulation.

125 2.3 Preparation of pectic polysaccharide gels

126 PA and PB samples were dissolved in distilled water at content of 0.5, 1.0, 1.5 and 2.0%
127 (w/v)) under magnetic stirring for 3 h at 40℃. The stock PA and PB solutions were mixed under
128 magnetic stirring for 30 min at 40℃to prepare pectic polysaccharide solutions with different ratio
129 of PA and PB (PA/PB=2:0, 1.5:0.5, 1:1, 0.5:1.0 and 0:2). The pectic polysaccharide solutions were
130 cooled to 25℃and the pH of each solution was adjusted to 5.0 using 1M NaOH or HCl. The pectic
131 polysaccharide gels were formed using controlled calcium release from the $CaCO_3$-GDL system
132 in order to inhibit pre-gelation. $CaCO_3$ (5, 10, 20 and 40 mM), GDL (0.8, 1.6, 2.0 and 2.8 wt%)
133 and urea (1 M) were added to the pectic polysaccharide solutions under constant stirring for 4 min
134 to obtain mixed gels and the pH of the gels would be measured every 10 min for 3 h.

135 2.4 Rheological measurement

136 A HAAKE RheoStress 6000 rheometer (Thermo Scientific, USA) with a 60 mm parallel plate
137 was used to analyze the rheological properties of pectic polysaccharides, including steady shear
138 flow behavior of PA and PB solutions (only pectic polysaccharide dissolved in distilled water) and
139 dynamic-viscoelastic properties of PA and PB synergistic gels (pectic polysaccharide dissolved in
140 distilled water with addiction of $CaCO_3$ and GDL). Pectic polysaccharide solutions with different
141 ratio of PA and PB were subjected to steady shearing with the shear rates ranging from 0.01 to 100
142 s^{-1} at 25℃. Data were fit to a power law model (equation (1)).

143 $$\eta=k\gamma^{(n-1)} \qquad (1)$$

144 In equation (1), where η is the apparent viscosity (mPa•s), k (mPa•s^n) is the consistency index,
145 γ is the shear rate (s^{-1}) and n (dimensionless) is the flow behavior index.

146 In order to analyze dynamic-viscoelastic properties of pectic polysaccharide gels with $CaCO_3$
147 and GDL, the mixed gels were put onto the rheometer and equilibrated for 1 min at 25℃, then

analyzed for their rheological behavior. The linear viscoelastic ranges were firstly determined by amplitude sweep from 0.001% to 100% at a constant frequency of 1 Hz. The small deformation oscillatory of time sweep determination was carried out at constant frequency of 1 Hz for 10800 s, under 0.1% deformation (smaller than the maximum value of linear viscoelastic range). The frequency sweep was conducted from 0.1 to 10 Hz at 0.1% deformation to monitor the change in storage modulus (G') and loss modulus (G'') of the mixtures after 10800 s. For pH measurement, mixed gels with $CaCO_3$ and GDL were stirred for 4 min and equilibrated for 1 min, the pH value was measured every 10 min for 3 h.

2.5 Visualization of microstructure of pectic polysaccharide gels (Cryo-SEM)

Cryo-scanning electron microscopy (Cryo-SEM) is used to observe the native microstructure of high water content hydrogels. First, the sample placed in the stub was cryo-vitrified with liquid nitrogen slush at -210 ℃. The vitrified sample was then transferred into the cryo-SEM pre-chamber (PP3010T Cryo-SEM Preparation System, Quorum, UK) for sublimation at -85 ℃ under vacuum conditions for 20-25 min. The sample was sputtered with gold to prevent charging during electron beam targeting. Finally, the sample was transferred on to the SEM stage (Regulus 8100, Hitachi, Japan) at -140 ℃ for observation (Kyomugasho et al., 2018a; Ngouémazong et al., 2012).

2.6 Statistical analysis

Data were expressed as the mean ± standard deviation (SD) with three replicates per sample. Data were analyzed by ANOVA using Duncan's test with SPSS version 21.0 (IBM software, New York, USA). The significance level was set at $P < 0.05$.

3. Results and discussion

3.1 Morphology properties and steady shear flow behavior of PA and PB solutions

The morphology of pectic polysaccharide solutions at 10 μg/mL in the scan area of 2.5 μm×2.5 μm was shown in Figure 2. The PA molecule chains aggregated into a continuous and dense network of 2.0 nm height, with gathered pieces ranging from 100 nm to 300 nm of 2.5 nm height (Fig. 2a). The irregular and sparse network structures were observed in PB solution, average vertical height of the main chains was measured to be 3.0 nm. The height of PB was higher than that of PA, which may relate to the high molecular weight and highly branched structure of PB. In addition, PA molecule chains showed more aggregations than PB at the same pectic polysaccharide concentration, which may be relevant to the relatively high GalA content and DM (~45%). RG-I pectic polysaccharide with higher proportion of GalA showed more aggregates of molecules but not single molecules of complex shape (Petrova et al., 2019). Interestingly, in the blend solution containing 5 μg/mL PA and 5 μg/mL PB distributed on mica, the molecules presented an island-like structure of a height of 2.0-3.0 nm, different from the network structure of pure pectic polysaccharide solutions with same polymer concentration. The poor networking and high aggregation degree of mixture of PA and PB could be explained by the structure characteristics. Long side-chains of PB tend to interact with each other and form aggregates with the backbone located at the periphery (Mikshina, Idiyatullin, Petrova, Shashkov, Zuev & Gorshkova, 2015). In addition, the water retaining capacity of arabinan side-chains (Larsen, Byg, Damager, Diaz, Engelsen & Ulvskov, 2011) promoted the interaction between methoxylated galacturonic acid residues of PA (Fu & Rao, 2001). The intermolecular polymerization in PA/PB blend solution provided the possibility of synergistic mixed gelation.

Steady shear flow behavior of PA and PB solutions (Fig. 2d) suggested that pectic polysaccharide solutions are all typical pseudoplastic fluids. Table 1 showed that the fitting

accuracy of data points on the sample curve using the power law model reached 0.98, suggesting the model could be used to analysis pectic polysaccharide samples (Table 1). The consistency coefficient (K) and fluid index (n) were of magnitudes used to express fluid consistency and non-Newtonian fluid behavior in the model. The consistency coefficient of PA was higher than that of PB, which may relate to the abundant HG region with a relatively high DM of PA. PB had the greater shear-thinning property, indicating the orientation of PB molecular chain can be more easily obtained by shearing. This property may be due to the low GalA content and low degree of methoxylation of PB, which resulted in low viscosity and little interactions between molecular chains. The different steady shear flow behavior of pectic polysaccharide solutions was consistent with the chain conformation observed by AFM. Apparent viscosity of PA was higher than that of PB, which could be explained by the continuous and dense network with aggregations observed in PA solution and irregular and sparse network structures of PB. The color of PB solution was clear than PA solution at the same concentration (Fig. S4a and c), supporting that the aggregation of pectic polysaccharide chains in PB solution was less than that of PB solution (Hua, Yang, Din, Chi & Yang, 2018). In addition, PA/PB blend solution showed medium fluid index and consistency coefficient comparing with PA and PB, consistent with the microstructure of inhomogeneous aggregations. Hydrogen bonds between polymer chains promoted the aggregation. In order to investigate the contribution of hydrogen bonds in RG-I rich pectic polysaccharide solutions, 1 M urea was added into the solutions. Urea is a hydrogen bond breaking agent can break the intermolecular hydrogen bonding between polysaccharides chains. The influence of 1M urea on the apparent viscosity of PA, PB and PA/PB solutions (PA/PB=1) were showed in Fig. 2e. The fluid index and consistency coefficient of pectic polysaccharide solutions decreased in the present of urea and the influence on PA was most

obvious, indicating hydrogen bonds contributed to pectic polysaccharide aggregations and promoted apparent viscosity.

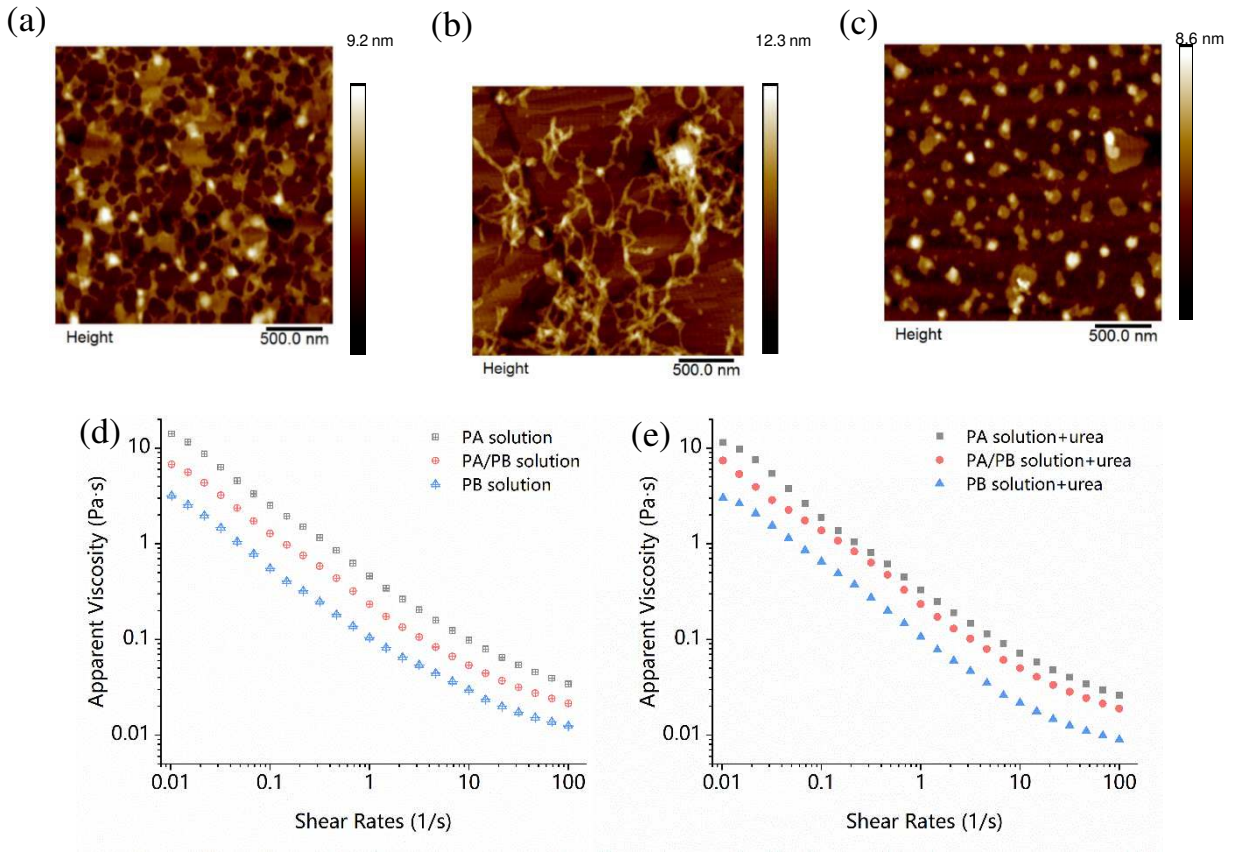

Figure 2. Representative topographical AFM images of (a) PA, (b) PB and (c) mixture of PA/PB; (d) Flow behavior of PA, PB and PA/PB (PA/PB=1) solution at concentration of 1.5%; (e) Flow behavior of PA, PB and PA/PB (PA/PB=1) solution at concentration of 1.5% with 1 M urea.

Table 1. Parameters of flow curves obtained by fitting to power law model.

Index	PA solution	PA/PB solution	PB solution	PA solution+ urea	PA/PB solution+ urea	PB solution+ urea
k	537.9	284.3	137.6	404.7	276.8	126.9
n	0.316	0.339	0.371	0.305	0.323	0.314
R^2	0.9936	0.9901	0.9848	0.9901	0.9922	0.9905

224224

225 3.2 Dynamic-viscoelastic properties of PA and PB synergistic gels

226 **Ratio of PA and PB** Fig. 3a showed the modulus and pH evolution of PA/PB blend
227 samples at different ratio with addition of 0.8 wt% GDL and 5 mM $CaCO_3$. Initially, pH was
228 around 5.8 and Ca was present in the form of solid $CaCO_3$. The modulus of PA was the highest
229 among all the samples while that of PB was the lowest, which can be explained by the different
230 structures of PA and PB. PA composed of relatively high content of GalA with DM of 45%, thus
231 the network formation of PA may contribute to calcium-bridge or hydrogen bonds and
232 hydrophobic interactions depending on the distribution of demethylated blocks of HG (Yu et al.,
233 2017). The presence of abundant rhamnose in PB influenced the conformation of the polymer in
234 solution, disturbing the molecular orientation necessary for junction-zone formation and limiting
235 inter-chain association (Chan, Choo, Young & Loh, 2017). The concentration of Ca ions
236 increased progressively with GDL hydrolysis, which led to an increase modulus of gels. G' and
237 G'' increased mainly due to the "egg box" junction zones formed by binding action between
238 Ca^{2+} and carboxyl groups. Another reason for increasing modulus was the hydrogen bonds and
239 hydrophobic interactions between galacturonic acid backbones (Ngouémazong et al., 2012) and
240 neutral sugar side-chains prompted by the low pH condition (Ngouémazong et al., 2012; Sousa,
241 Nielsen, Armagan, Larsen & Sørensen, 2015). The extremely low DM of PB were beneficial for
242 calcium-bridge formation and abundant side-chains stabilized the network structure through
243 entanglements. As for PA, G' and G'' increased slowly. Blocks of more than 10 non-
244 methoxylated galacturonic acid residues could interact with calcium ions (Chan et al., 2017). The
245 slow and limited increase could be explained by the occurrence of methyl ester groups in the
246 primary backbone and the RG-I steric hindrance produced on the unesterified HG blocks
247 (Cameron, Luzio, Goodner & Williams, 2008; Luzio & Cameron, 2008). PA system appeared as

248 thick liquid (Fig. S4d), different from the solid appearance of PB or PA/PB blend gel (Fig. S4e
249 and f). But the G' of PA system was always higher than the G'', suggesting it should be
250 considered as a weak gel (Kyomugasho, Christiaens, Van de Walle, Van Loey, Dewettinck &
251 Hendrickx, 2016). Modulus of PA slightly decreased after 5000 s, similar phenomenon has been
252 reported previously (Lootens et al., 2003). The modulus of pectic polysaccharide with a
253 relatively high DM (~50%) was dependent on the balance of two interactions. Low pH prompted
254 the hydrophobic interactions between methylesterified carboxyl and hydrogen bonds between
255 non-methylesterified carboxyl. It could also convert the carboxyl from dissociated (COO-) to
256 associated (COOH) and reduced affinity for Ca ions. As a result, the modulus of PA gel
257 decreased at pH lower than 4.5 (Fraeye, Duvetter, Doungla, Van Loey & Hendrickx, 2010).
258 Interestingly, G' and G'' of PA/PB blend samples increased more quickly and were higher than
259 pure PA or PB samples, suggesting the synergistic effect of PA and PB could strengthen the gel
260 network. One possible reason was that the long side-chains of PB decreased the water activity
261 since they contain many hydrophilic groups (Einhorn-Stoll, 2018), thus prompted the interaction
262 of PA chains. Moreover, PA and PB could interact with each other by Ca-bridges with the
263 release of calcium ions. Consequently, mixture of PA and PB prompted the formation of three-
264 dimensional network and increased the moduli of blend gels.

265 **Pectic polysaccharide concentration** The modulus and pH of PA/PB blend gels
266 (PA/PB=1) at different pectic polysaccharide concentration (0.5, 1.0, 1.5 and 2% w/v) with
267 addition of 0.8 wt% GDL and 5 mM $CaCO_3$ were shown in Fig. 3b. The effect of pectic
268 polysaccharide concentration on the pH was ignorable for the ratio GDL to $CaCO_3$ used in the
269 samples. The G' and G'' increased with increasing pectic polysaccharide concentration and the
270 change of G' and G'' at low concentrations (<1.0% w/v) was more apparent than high

concentrations (>1.0% w/v). The increased modulus could be attributed to increased number of cross-linking junction zones between pectic polysaccharide chains. With increasing pectic polysaccharide concentration, number of hydrogen bonds and hydrophobic interactions between pectic polysaccharide chains increased, which can be explained by the higher number of binding sites available and the lower water activity of gels. The number of "egg box" junction zones between Ca^{2+} and pectic polysaccharide chains also increased and the probability of ionic bonds formation within the same pectic polysaccharide chain decreased, leading to more junction zones between the separate pectic polysaccharide chains and stronger gels (Fraeye et al., 2010; Kyomugasho et al., 2016). G' and G'' of gels increased with pectic polysaccharide concentration, but the increasing effects was not significant when the concentration reached to a certain level. The high viscosity of pectic polysaccharide solution locked the structure thus hinder the formation of ionic cross-links (Wan et al., 2019). Interestingly, the modulus increased more quickly at low pectic polysaccharide concentration compared to the high concentration. At constant Ca^{2+} concentration, the lower the pectic polysaccharide concentration was, the higher the ratio of Ca^{2+} to the pectic polysaccharide concentration was, resulting in quick gel formation.

GDL concentration The modulus and pH of PA/PB blend gels (PA/PB=1) with different concentration of GDL (0.8, 1.6, 2.0 and 2.8 wt%) with addition of 5 mM $CaCO_3$ is shown in Fig. 3c. The final Ca^{2+} concentration of gels could be guaranteed to be the same (5 mM), because the pH of gels was lower than 4.0. G' and G'' of gels was lower increased rapidly at early stage with Ca ions releasing. The gel formation at GDL concentration of 0.8% was much slower than that at higher GDL concentrations, because GDL can decrease the pH of gels during the hydrolysis and promote the Ca ions release. The differences of gel formation rate at high GDL concentrations (≥1.6%) were not significant, additional GDL had little influence on the rate because the amount

of interaction sites was limited due to the constant pectic polysaccharide concentration. Moduli of the gels reach a plateau within ~3000 s, when most of the Ca ions had been released. G' and G'' of gels after 3h holding period were different at various GDL concentration and the G' and G'' increased with GDL concentration increasing, but the rheological properties of gels at 2.8% GDL was similar with that of 2.0%. Decreased pH promotes formation of hydrogen bonds between protonated carboxyl groups (Fraeye et al., 2010) as well as neutral sugar side-chains (Ngouémazong et al., 2012; Sousa et al., 2015). Meanwhile, the affinity for calcium ions of pectic polysaccharide decreased at low pH condition because of the decreased charge density (Cardoso, Coimbra & Lopes Da Silva, 2003). A pH of 5.0 was found to be optimal for Ca^{2+} binding by LM pectin (Celus, Kyomugasho, Van Loey, Grauwet & Hendrickx, 2018), however, that was 3.0 for PA/PB blend gel with 5 mM Ca ions. The low optimal pH of blend gel suggested that besides ionic cross-links, hydrogen bonds were of great importance to the RG-I rich blend gel formation.

Ca^{2+} concentration The modulus and pH of PA/PB blend gels (PA/PB=1) with different concentration of $CaCO_3$ (5, 10, 20 and 40 mM) with addition of 0.8 wt% GDL were shown in Fig. 3d. The calcium content strongly influenced the kinetic behavior and moduli of the gels. Increased Ca^{2+} concentration of resulted in more rapid gel formation and also a complex behavior in G' and G''. Moduli of gels with high Ca^{2+} concentration increased rapidly and reached a local maximum within ~2000 s, then decreased and reach a plateau within ~6000 s, while that of lower Ca concentration increased continuously. G' of gels with more than 20 mM Ca^{2+} were higher than that of 10 mM Ca^{2+}, but after 3000 s the opposite result was obtained. Pectic polysaccharide chains interacted with cations and formed point-like cross-links at low Ca^{2+} concentration, then dimers occurred and the network of polymer chains formed upon

317 increasing Ca ions (Huynh, Lerbret, Neiers, Chambin & Assifaoui, 2016; Kyomugasho et al.,
318 2016). The increasing $CaCO_3$ concentration contributed to more available Ca ions in gels, which
319 could increase the crosslink density between pectin chains (Wan et al., 2019). However, the
320 initial structure based on Ca^{2+}-pectin interactions may lock the structure thus diminish the
321 possibilities for further strengthening of gel network by hydrophobic interactions and hydrogen
322 bonds (Löfgren, Guillotin, Evenbratt, Schols & Hermansson, 2005). Another possible reason was
323 that the structure formation rate of gel at high GDL concentration was fast, which caused
324 incomplete network formation thus reduces the G' of gel (Kastner, Einhorn-Stoll & Senge,
325 2012). Moreover, excess Ca^{2+} caused syneresis of gels with a thin water layer found on the gel
326 surface and decreased the G' (Liu et al., 2013). Above pH 4.5 gel properties were relatively
327 independent of pH and the influence of pH can be ignored (Fraeye et al., 2010), indicating the
328 various G' and G'' of gels added more than 5 mM Ca ions mainly resulted from the
329 concentration of $CaCO_3$. According to the moduli of gels with different GDL concentration (Fig.
330 3c), moduli of gels increased with pH decreasing when pH above 3.0, so the G' of gels with 5
331 mM $CaCO_3$ increased slowly while that of higher Ca^{2+} concentrations keeps constant.
332332
333333

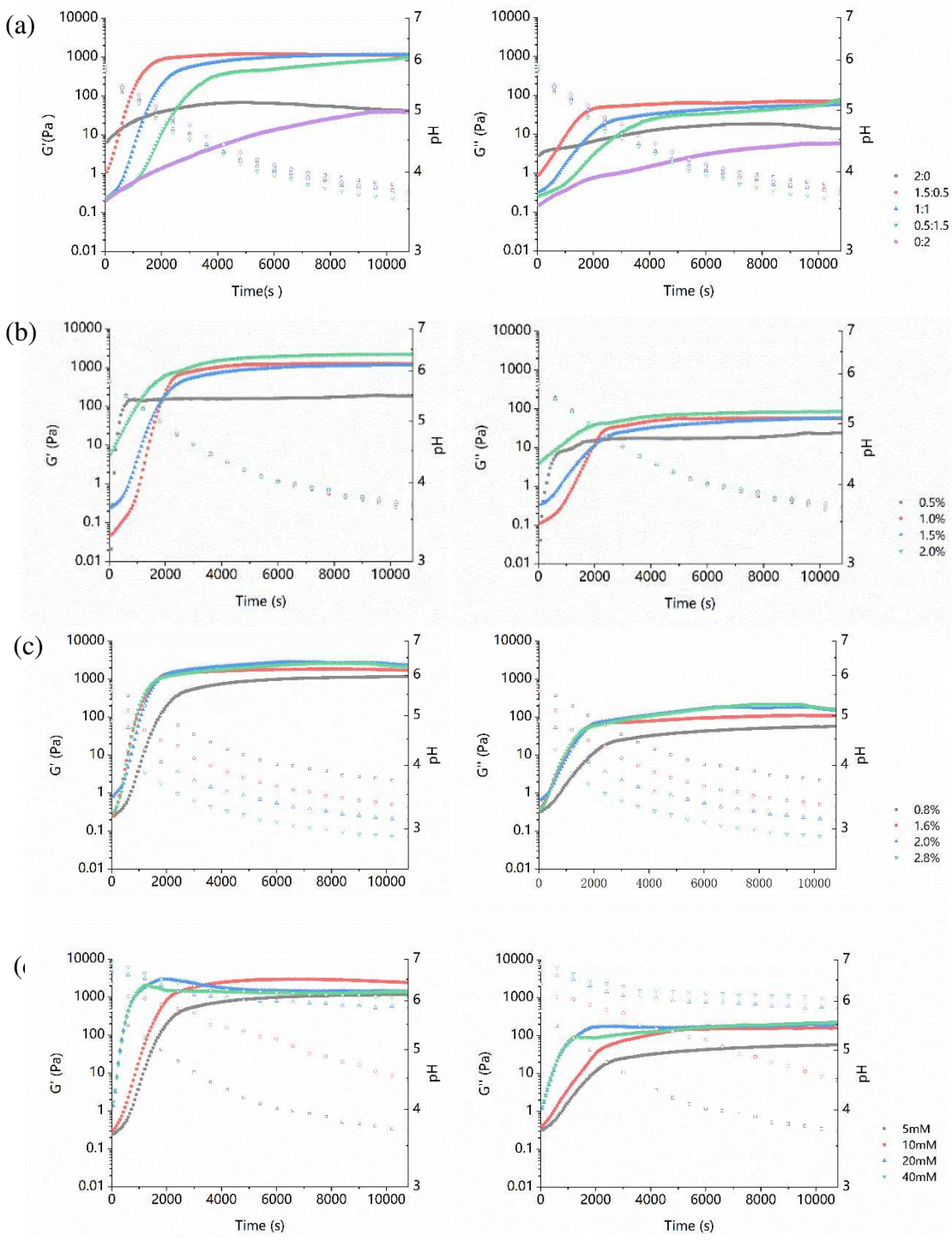

334

335 **Figure 3.** Modulus values (G' and G'') of PA/PB blend gels. (a) PA/PB blend gels (1.5% w/v

336 pectic polysaccharide concentration, 0.8 wt% GDL, 5 mM $CaCO_3$) at PA/PB=2:0, 1.5:0.5, 1:1,

337 0.5:1.0 and 0:2; (b) PA/PB blend gels (PA/PB=1, 0.8 wt% GDL, 5 mM $CaCO_3$) of pectic

polysaccharide concentration of 0.5, 1.0, 1.5 and 2.0% w/v; (c) PA/PB blend gels (PA/PB=1, 1.5% w/v pectic polysaccharide concentration, 5 mM $CaCO_3$) with GDL concentration of 0.8, 1.6, 2.0 and 2.8 wt%; (d) PA/PB blend gels (PA/PB=1, 1.5% w/v pectic polysaccharide concentration, 0.8 wt% GDL) with Ca^{2+} concentration of 5, 10, 20 and 40 mM. Measurement temperature, 25℃; strain, 0.1%; frequency, 1 Hz.

3.3 Effect of urea on dynamic-viscoelastic properties of PA and PB synergistic gels

The synergistic gelation feature of PA/PB blend gels was demonstrated, but a more comprehensive investigation of the association properties of this system is required. For cation-induced RG-I rich pectic polysaccharide gel, junction zones are primarily formed by electrostatic interactions and contributed to hydrogen bond between intra- and intermolecular pectin chains (Liu et al., 2013). The contribution of hydrogen bonds in synergistic gel formation was worthy of study, so oscillatory shear measurements of gels are carried out with urea. The influence of 1M urea on the dynamic-viscoelastic properties of PA, PB and PA/PB blend gels (PA/PB=1) were showed in Fig. 4. The decrease of G' and G'' of PA gel was more obvious than that of PB gel in the presence of urea, suggesting that hydrogen bonding contributes to the gel formation of PA. The inhibition of PA gel could be explained by the lack of blocks of more than 10 non-methoxylated galacturonic acid residues, which was consistent with the structure properties of PA. As for PB, the slight decrease of modulus suggested that PB gel mainly composed of the calcium-pectin network, hydrogen bonds could help stabilize the structure. Interestingly, the modulus of PA/PB blend gel was lower than PB gel after addition of urea, in other words, synergistic effect of PA/PB blend gel no longer appeared, indicating the hydrogen bonds were

360 vital for synergistic gelation.

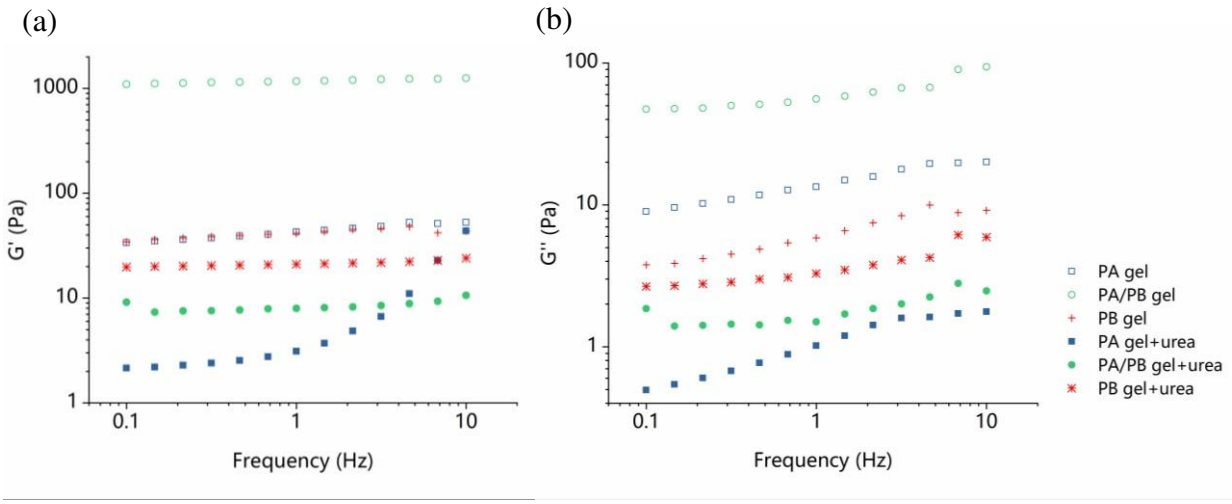

Figure 4. Modulus values (G' and G'') of PA/PB blend gels. (a) G' of PA, PB and PA/PB blend gels (PA/PB=1) with addition of 0.8 wt% GDL and 5 mM CaCO3; (b) G'' of PA, PB and PA/PB blend gels (PA/PB=1) with addition of 0.8 wt% GDL and 5 mM CaCO3; Measurement temperature, 25℃; strain, 0.1%; frequency, 0.1-10 Hz.

3.4 Cryo-SEM analysis

Cryo-SEM images of PA, PB and PA/PB blend gels with addition of 5mM $CaCO_3$ were showed in Fig. 5. Formation of intertwined fibrous network and strand-like structure can be promoted by cations (Efthymiou, Williams & McGrath, 2017; Kyomugasho et al., 2016). PA gel mainly composed of strand-like structures but the network was incomplete with open microstructures. PA exhibited higher amounts of GalA with 45% DM, prompting the polymer chain entanglements based on hydrogen bonds. But low amounts of blocks of more than 10 non-methoxylated galacturonic acid residues limited formation of ionic cross-links, resulting the loose and incomplete network and thick liquid appearance (Fig. 5a). PB gel showed intertwined fibrous network, which was similar with the microstructure structures observed in LMP gels

(Kyomugasho et al., 2016; Kyomugasho et al., 2018b; Liu et al., 2013). Dense cross-links were related to the high number of non-methylated GalA residues, which can form egg-box junction zones with Ca^{2+}. However, open structures could be found in the network, because the "kinks" produced by the rhamnose inserts of backbone limited cross-links (Fraeye et al., 2010). Thus, the surface of PB gel showed discontinuous structure in FESEM image (Fig. S3). Furthermore, PB exhibited higher amounts of branch-like structure compared to PA, consisting with the highly branched structure of PB (Santiago et al., 2018). Cryo-SEM image of PA/PB blend gel showed a clear three-dimensional network composed of strand-like structures (Fig. 5c) and intertwined fibrous structures (Fig. 5d). The entangled strand-like structures converted to cross-linked network, suggesting the blend system promoted the interaction of PA chains. The intertwined fibrous structures interacted with the strand-like structures, indicating Ca^{2+} connected PA and PB polymer chains. The unique microstructure was consistent with the strengthened gel properties of PA/PB blend gel. In addition, the surface of blend gel was more compact than that of pure gels (Fig. S3), representing an improved gelled state (Li et al., 2019).

3.5 Proposed mechanism of PA/PB synergistic gel formation

Our study showed PA and PB synergistically formed stronger gels with calcium induction. PA and PB consisted mainly of branched RG-I with the ratio of 41% and 63%, respectively, and high content of arabinose and galactose. The methoxylation degree of PA was 45%, but PB was only 15%. The AFM observation illustrated that PA could form dense network structure with gathered pieces, indicating the strong interactions between pectin chains based on hydrogen bonds. PB showed irregular and sparse network structure, based on the interaction of long side-chains of RG-I region. The molecules presented an island-like structure in PA/PB blend solution at the same polymer concentration, indicating the aggregation trend of PA and PB. RG-I side-

chains of PB tended to form aggregates with the backbone located at the periphery (Mikshina et al., 2015). Meanwhile, neutral sugar side-chains, especially arabinan side chains, could hydrate more readily than the rhamnose-galacturonic acid (Rha-GalA) backbone in RG-I (Larsen et al., 2011), thus promote aggregations of PA (Makshakova et al., 2018; Mikshina et al., 2017). Different HG/RG-I ratios and DM values of PA and PB induced the separation of their aggregates, similar phenomenon was reported in HM/LM pectin mixed gel, a very inhomogeneous phase-separated was formed and strong synergistic rheological properties were obtained (Löfgren, Walkenström & Hermansson, 2002). The hypothesis of hydration process was consistent with the steady shear flow behavior of pectic polysaccharide solutions (see Section 3.1).

PA and PB could form gels induced by calcium. PA was composed of relatively high content of GalA with DM of 45% and the network formation mainly composed of hydrogen bonds (Yu et al., 2017), as well as few ionic cross-links. Non-methoxylated galacturonic acid residues can interact with calcium ions but the methyl ester groups limited the extent of such junction zones (Chan et al., 2017). The network of calcium-induced PB gel was mainly composed of the “egg box” junction zones formed by binding action between Ca^{2+} and carboxyl groups. Moreover, abundant side-chains stabilized the network structure through entanglements. For PA/PB blend gels, the synergistic effect of pectic polysaccharides could strengthen the gel network, indicating interactions between PA and PB, including Ca-bridges between carboxyl groups and side-chain entanglements. Moreover, neutral sugar side-chains prompted formation of hydrogen bonds. Calcium-bridges connected PA and PB aggregates with suitable pH, consequently promoted the three-dimensional network formation and improved the rheological properties and microstructure of blend gels (see Fig. 5e).

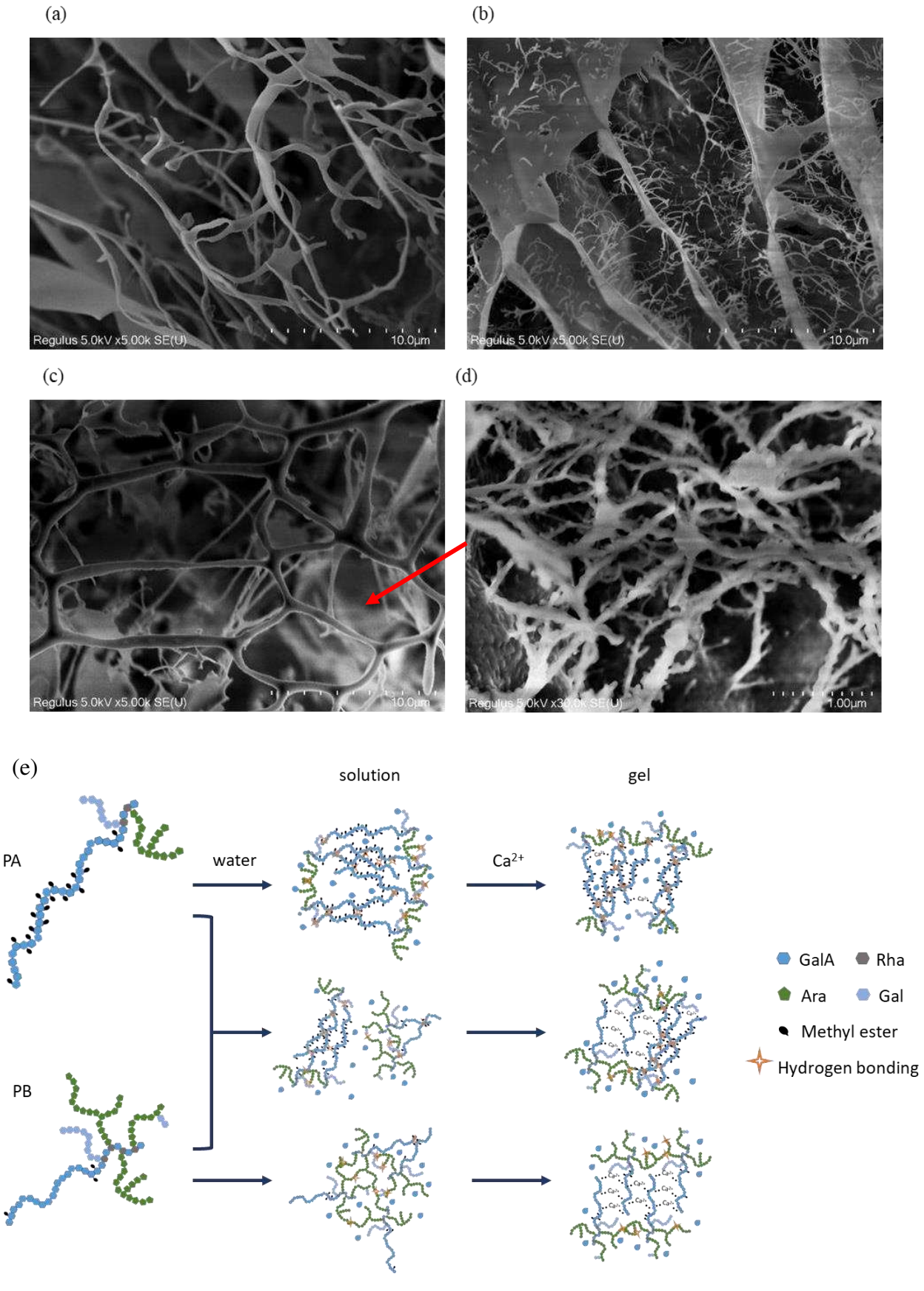
(a)
(b)
Regulus 5.0kV x5.00k SE(U)
10.0μm
Regulus 5.0kV x5.00k SE(U)
10.0μm
(c)
(d)
Regulus 5.0kV x5.00k SE(U)
10.0μm
1.00μm
(e)
solution
gel
PA
water
Ca2+
PB
GalA
Rha
Ara
Gal
Methyl ester
Hydrogen bonding

422422

Figure 5. Microstructure of (a) PA, (b) PB, (c) and (d) PA/PB blend gels (1.5% w/v pectic polysaccharide concentration, 0.8 wt% GDL, 5 mM $CaCO_3$). The amplification was 5000 (a), (b), (c) and 30000 (d) times the original size. (e) Schematic diagram of the formation of PA, PB and PA/PB blend gel.

427427

4. Conclusion

Rheological properties, water-holding capacity and microstructure of RG-I rich citrus pectic polysaccharide gels were investigated to elucidate the synergistic gelation mechanism of PA and PB. PA, with higher HG region (~41%) and relatively high DM value (~49%), showed high viscosity and dense network structure in pure solution. PB composed of RG-I region (67%) with long neutral sugar side-chains and HG region (17%) of low DM value (15%), so the network of PB solution was irregular and sparse. Island-like structure was observed by AFM in the PA/PB blend solution, indicating separate aggregation of PA and PB. RG-I rich PA and PB could form gels induced by calcium ions. The network of PA gel was mainly composed of hydrogen bonds between methoxylated galacturonic acid residues. PB gels relied on ionic cross-link junction-zones, stabilized by side-chain entanglements. PA/PB blend gels showed improved rheological properties and microstructure compared with pure PA and PB gels. Ca-bridges connected pectic polysaccharide aggregates and promoted the three-dimensional structure of PA/PB blend gels but excess Ca^{2+} caused syneresis of gels and decreased water-holding capacity. The gel network was stabilized by the hydrogen bonds prompted by neutral sugar side-chains. These findings suggested that synergistic effects can be achieved by mixing PA and PB to produce a

strengthened blend gel with calcium induction and provided further development for RG-I rich pectic polysaccharide-based products.

Acknowledgements

This work was financially supported by National Key R&D Program of China (2017YFE0122300190), National Natural Science foundation of China (31871815) and the Fundamental Research Funds for the Central Universities (Grant No. 2020FZZX003-02-05).

References

Cameron, R. G., Luzio, G. A., Goodner, K., & Williams, M. A. K. (2008). Demethylation of a model homogalacturonan with a salt-independent pectin methylesterase from citrus: I. Effect of pH on demethylated block size, block number and enzyme mode of action. *CARBOHYDRATE POLYMERS*, *71*(2), 287-299.

Cardoso, S. M., Coimbra, M. A., & Lopes Da Silva, J. A. (2003). Calcium-mediated gelation of an olive pomace pectic extract. *CARBOHYDRATE POLYMERS*, *52*(2), 125-133.

Celus, M., Kyomugasho, C., Van Loey, A. M., Grauwet, T., & Hendrickx, M. E. (2018). Influence of Pectin Structural Properties on Interactions with Divalent Cations and Its Associated Functionalities. *COMPREHENSIVE REVIEWS IN FOOD SCIENCE AND FOOD SAFETY*, *17*(6), 1576-1594.

Chan, S. Y., Choo, W. S., Young, D. J., & Loh, X. J. (2017). Pectin as a rheology modifier: Origin, structure, commercial production and rheology. *CARBOHYDRATE POLYMERS*, *161*, 118-139.

Chen, J., Chen, W., Duan, F., Tang, Q., Li, X., Zeng, L., Zhang, J., Xing, Z., Dong, Y., Jia, L., & Gao, H. (2019). The synergistic gelation of okra polysaccharides with kappa-carrageenan and its influence on gel rheology, texture behaviour and microstructures. *FOOD HYDROCOLLOIDS*, *87*, 425-435.

Chen, J., Cheng, H., Wu, D., Linhardt, R. J., Zhi, Z., Yan, L., Chen, S., & Ye, X. (2017). Green recovery of pectic polysaccharides from citrus canning processing water. *JOURNAL OF CLEANER PRODUCTION*, *144*, 459-469.

Chen, J., Cheng, H., Zhi, Z., Zhang, H., Linhardt, R. J., Zhang, F., Chen, S., & Ye, X. (2021). Extraction temperature is a decisive factor for the properties of pectin. *FOOD HYDROCOLLOIDS*, *112*, 106160.

Efthymiou, C., Williams, M. A. K., & McGrath, K. M. (2017). Revealing the structure of high-water content biopolymer networks: Diminishing freezing artefacts in cryo-SEM images. *FOOD HYDROCOLLOIDS*, *73*, 203-212.

Einhorn-Stoll, U. (2018). Pectin-water interactions in foods – From powder to gel. *FOOD HYDROCOLLOIDS*, *78*, 109-119.

Fraeye, I., Duvetter, T., Doungla, E., Van Loey, A., & Hendrickx, M. (2010). Fine-tuning the properties of pectin–calcium gels by control of pectin fine structure, gel composition and environmental conditions. *TRENDS IN FOOD SCIENCE & TECHNOLOGY*, *21*(5), 219-228.

Fu, J., & Rao, M. A. (2001). Rheology and structure development during gelation of low-methoxyl pectin gels: the effect of sucrose. *FOOD HYDROCOLLOIDS*, *15*(1), 93-100.

Hua, X., Yang, H., Din, P., Chi, K., & Yang, R. (2018). Rheological properties of deesterified pectin with different methoxylation degree. *Food Bioscience*, *23*, 91-99.

Huynh, U. T., Lerbret, A., Neiers, F., Chambin, O., & Assifaoui, A. (2016). Binding of Divalent Cations to Polygalacturonate: A Mechanism Driven by the Hydration Water. *JOURNAL OF PHYSICAL CHEMISTRY B*, *120*(5), 1021-1032.

Kastner, H., Einhorn-Stoll, U., & Senge, B. (2012). Structure formation in sugar containing pectin gels – Influence

485 of Ca2+ on the gelation of low-methoxylated pectin at acidic pH. *FOOD HYDROCOLLOIDS*, *27*(1), 42-49.
486 Klaassen, M. T., & Trindade, L. M. (2020). RG-I galactan side-chains are involved in the regulation of the water-
487 binding capacity of potato cell walls. *CARBOHYDRATE POLYMERS*, *227*, 115353.
488 Kyomugasho, C., Christiaens, S., Van de Walle, D., Van Loey, A. M., Dewettinck, K., & Hendrickx, M. E. (2016).
489 Evaluation of cation-facilitated pectin-gel properties: Cryo-SEM visualisation and rheological properties. *FOOD*
490 *HYDROCOLLOIDS*, *61*, 172-182.
491 Kyomugasho, C., Munyensanga, C., Celus, M., Van de Walle, D., Dewettinck, K., Van Loey, A. M., Grauwet, T., &
492 Hendrickx, M. E. (2018a). Molar mass influence on pectin-Ca2+ adsorption capacity, interaction energy andassociated
493 functionality: Gel microstructure and stiffness. *FOOD HYDROCOLLOIDS*, *85*, 331-342.
494 Kyomugasho, C., Munyensanga, C., Celus, M., Van de Walle, D., Dewettinck, K., Van Loey, A. M., Grauwet, T., &
495 Hendrickx, M. E. (2018b). Molar mass influence on pectin-Ca2+ adsorption capacity, interaction energy and
496 associated functionality: Gel microstructure and stiffness. *FOOD HYDROCOLLOIDS*, *85*, 331-342.
497 Larsen, F. H., Byg, I., Damager, I., Diaz, J., Engelsen, S. B., & Ulvskov, P. (2011). Residue Specific Hydration of
498 Primary Cell Wall Potato Pectin Identified by Solid-State 13C Single-Pulse MAS and CP/MAS NMR Spectroscopy.
499 *BIOMACROMOLECULES*, *12*(5), 1844-1850.
500 Li, X., Dong, Y., Guo, Y., Zhang, Z., Jia, L., Gao, H., Xing, Z., & Duan, F. (2019). Okra polysaccharides reduced the
501 gelling-required sucrose content in its synergistic gel with high-methoxyl pectin by microphase separation effect.
502 *FOOD HYDROCOLLOIDS*, *95*, 506-516.
503 Liu, H., Guo, X., Li, J., Zhu, D., & Li, J. (2013). The effects of MgSO4, d-glucono- δ -lactone (GDL), sucrose, and
504 urea on gelation properties of pectic polysaccharide from soy hull. *FOOD HYDROCOLLOIDS*, *31*(2), 137-145.
505 Löfgren, C. E. E., Guillotin, S., Evenbratt, H., Schols, H., & Hermansson, A. (2005). Effects of Calcium, pH, and
506 Blockiness on Kinetic Rheological Behavior and Microstructure of HM Pectin Gels. *BIOMACROMOLECULES*, *6*(2),
507 646.
508 Löfgren, C., Walkenström, P., & Hermansson, A. (2002). Microstructure and Rheological Behavior of Pure and Mixed
509 Pectin Gels. *BIOMACROMOLECULES*, *3*(6), 1144-1153.
510 Löfgren, C., & Hermansson, A. (2007). Synergistic rheological behaviour of mixed HM/LM pectin gels. *FOOD*
511 *HYDROCOLLOIDS*, *21*(3), 480-486.
512 Lootens, D., Capel, F., Durand, D., Nicolai, T., Boulenguer, P., & Langendorff, V. (2003). Influence of pH, Ca
513 concentration, temperature and amidation on the gelation of low methoxyl pectin. *FOOD HYDROCOLLOIDS*, *17*(3),
514 237-244.
515 Luzio, G. A., & Cameron, R. G. (2008). Demethylation of a model homogalacturonan with the salt-independent pectin
516 methylesterase from citrus: Part II. Structure – function analysis. *CARBOHYDRATE POLYMERS*, *71*(2), 300-309.
517 Makshakova, O. N., Faizullin, D. A., Mikshina, P. V., Gorshkova, T. A., & Zuev, Y. F. (2018). Spatial structures of
518 rhamnogalacturonan I in gel and colloidal solution identified by 1D and 2D-FTIR spectroscopy. *Carbohydr Polym*,
519 *192*, 231-239.
520 Mikshina, P. V., Idiyatullin, B. Z., Petrova, A. A., Shashkov, A. S., Zuev, Y. F., & Gorshkova, T. A. (2015).
521 Physicochemical properties of complex rhamnogalacturonan I from gelatinous cell walls of flax fibers. *Carbohydr*
522 *Polym*, *117*, 853-861.
523 Mikshina, P. V., Makshakova, O. N., Petrova, A. A., Gaifullina, I. Z., Idiyatullin, B. Z., Gorshkova, T. A., & Zuev,
524 Y. F. (2017). Gelation of rhamnogalacturonan I is based on galactan side chain interaction and does not involve
525 chemical modifications. *CARBOHYDRATE POLYMERS*, *171*, 143-151.
526 Mohnen, D. (2008). Pectin structure and biosynthesis. *CURRENT OPINION IN PLANT BIOLOGY*, *11*(3), 266-277.
527 Ngouémazong, D. E., Kabuye, G., Fraeye, I., Cardinaels, R., Van Loey, A., Moldenaers, P., & Hendrickx, M. (2012).
528 Effect of debranching on the rheological properties of Ca2+ – pectin gels. *FOOD HYDROCOLLOIDS*, *26*(1), 44-53.
529 Ngouémazong, D. E., Tengweh, F. F., Fraeye, I., Duvetter, T., Cardinaels, R., Van Loey, A., Moldenaers, P., &
530 Hendrickx, M. (2012). Effect of de-methylesterification on network development and nature of Ca2+-pectin gels:
531 Towards understanding structure – function relations of pectin. *FOOD HYDROCOLLOIDS*, *26*(1), 89-98.
532 Petrova, A. A., Kozlova, L. V., Gaifullina, I. Z., Ananchenko, B. A., Martinson, E. A., Mikshina, P. V., & Gorshkova,
533 T. A. (2019). AFM analysis reveals polymorphism of purified flax rhamnogalacturonans I of distinct functional types.
534 *CARBOHYDRATE POLYMERS*, *216*, 238-246.
535 Santiago, J. S. J., Kyomugasho, C., Maheshwari, S., Jamsazzadeh Kermani, Z., Van de Walle, D., Van Loey, A. M.,
536 Dewettinck, K., & Hendrickx, M. E. (2018). Unravelling the structure of serum pectin originating from thermally and
537 mechanically processed carrot-based suspensions. *FOOD HYDROCOLLOIDS*, *77*, 482-493.
538 Sousa, A. G., Nielsen, H. L., Armagan, I., Larsen, J., & Sørensen, S. O. (2015). The impact of rhamnogalacturonan-I
539 side chain monosaccharides on the rheological properties of citrus pectin. *FOOD HYDROCOLLOIDS*, *47*, 130-139.

Thakur, B. R., Singh, R. K., Handa, A. K., & Rao, M. A. (1997). Chemistry and uses of pectin — A review. *C R C Critical Reviews in Food Technology*, *37*(1), 47-73.
Wan, L., Wang, H., Zhu, Y., Pan, S., Cai, R., Liu, F., & Pan, S. (2019). Comparative study on gelling properties of low methoxyl pectin prepared by high hydrostatic pressure-assisted enzymatic, atmospheric enzymatic, and alkaline de-esterification. *CARBOHYDRATE POLYMERS*, *226*, 115285.
Wang, J., & Nie, S. (2019). Application of atomic force microscopy in microscopic analysis of polysaccharide. *TRENDS IN FOOD SCIENCE & TECHNOLOGY*, *87*, 35-46.
Wang, S., Zhao, L., Li, Q., Liu, C., Han, J., Zhu, L., Zhu, D., He, Y., & Liu, H. (2019). Rheological properties and chain conformation of soy hull water-soluble polysaccharide fractions obtained by gradient alcohol precipitation. *FOOD HYDROCOLLOIDS*, *91*, 34-39.
Wei, C., Zhang, Y., He, L., Cheng, J., Li, J., Tao, W., Mao, G., Zhang, H., Linhardt, R. J., Ye, X., & Chen, S. (2019). Structural characterization and anti-proliferative activities of partially degraded polysaccharides from peach gum. *CARBOHYDRATE POLYMERS*, *203*, 193-202.
Willats, W., Knox, P., & Mikkelsen, J. D. (2006). Pectin: new insights into an old polymer are starting to gel. *TRENDS IN FOOD SCIENCE & TECHNOLOGY*, *17*(3), 97-104.
Wu, D., Zheng, J., Mao, G., Hu, W., Ye, X., Linhardt, R. J., & Chen, S. (2019). Rethinking the impact of RG-I mainly from fruits and vegetables on dietary health. *Crit Rev Food Sci Nutr*, 1-23.
Yu, L., Yakubov, G. E., Zeng, W., Xing, X., Stenson, J., Bulone, V., & Stokes, J. R. (2017). Multi-layer mucilage of Plantago ovata seeds: Rheological differences arise from variations in arabinoxylan side chains. *Carbohydr Polym*, *165*, 132-141.
Zhang, H., Chen, J., Li, J., Yan, L., Li, S., Ye, X., Liu, D., Ding, T., Linhardt, R. J., & Orfila, C. (2017). Extraction and characterization of RG-I enriched pectic polysaccharides from mandarin citrus peel. *FOOD HYDROCOLLOIDS*, *79*.

Synergistic gelling mechanism of RG-I rich citrus pectic polysaccharide at different esterification degree in calcium-induced gelation

Shiguo Chen [a,b,c], Jiaqi Zheng [a], Laiming Zhang [a], Huan Cheng [a,b,c], Caroline Orfila [d], Xingqian Ye [a,b,c], Jianle Chen [a,b,c,*]

[a] College of Biosystems Engineering and Food Science, National-Local Joint Engineering Laboratory of Intelligent Food Technology and Equipment, Zhejiang Key Laboratory for Agro-Food Processing, Zhejiang Engineering Laboratory of Food Technology and Equipment, Zhejiang University, Hangzhou 310058, China

[b] Fuli Institute of Food Science, Zhejiang University, Hangzhou 310058, China

[c] Ningbo Research Institute, Zhejiang University, Ningbo 315100, China

[d] School of Food Science and Nutrition, University of Leeds, Leeds LS2 9JT, UK

Abstract

RG-I rich pectic polysaccharide is common in fruit and vegetable and possesses health benefits. However, it is removed during commercial pectin production because of poor gelling properties. Synergistic gelation can improve rheological properties of RG-I pectic polysaccharide and expand its application in functional food hydrocolloids. In the study, RG-I rich pectic polysaccharides at different degree of esterification was extracted from citrus membrane by sequential mild acidic (0.4% HCl, 28℃) and alkaline (0.6% NaOH, 32℃) treatment. The pectic polysaccharide from acid water (PA) composes of 41% RG-I and 44% HG with DM of 45%, while

the pectic polysaccharide from basic water (PB) composed of 63% RG-I and 19% HG with DM of 15%. PA/PB blend gel under $CaCO_3$-glucono-δ-lactone system showed improved rheological properties compared with pure gels. Ca-bridges connected pectin aggregates and promoted the three-dimensional structure of PA/PB blend gels, while neutral sugar side-chains prompted hydrogen bonds and strengthened gel network.

Keywords

Pectic polysaccharide, rhamnogalacturonan-I, synergistic gelation, hydrogen bonds

1. Introduction

Pectin is a heteropolysaccharide widely existing in plant cell walls, composed of three major domains which include linear homogalacturonan (HG), rhamnogalacturonan-I (RG-I) and rhamnogalacturonan-II (RG-II) (Mohnen, 2008; Thakur, Singh, Handa & Rao, 1997). Commercial pectin, dominated with HG, is well known for its gelling properties and widely used in the food, cosmetics and pharmaceutical industry (Willats, Knox & Mikkelsen, 2006). In commercial pectin production, RG-I region is removed by hot acid due to its poor gelling capability. However, recently study suggested these RG-I rich pectic polysaccharide from fruits and vegetables (e.g., citrus, okra, potato and sugar beet) having potential health benefits by modulating the gut microbe and promote cell adhesion and migration (Wu et al., 2019).

RG-I region contains a backbone of the repeating disaccharide unit [→2) -α-L-Rha*p*-(1→4)-α-D-Gal*p*A-(1→]$_n$ and neutral sugar side-chains attached to the O-4 and O-3 of rhamnose residues. RG-I backbone is not compatible with the gel formation because the rhamnose inserts on the

backbone produce “kinks” thereby limiting cross-linking. But recently, the side-chains of the RG-I region reportedly possess strong water-binding capacities (Klaassen & Trindade, 2020) and stabilize the gel network structures (Makshakova, Faizullin, Mikshina, Gorshkova & Zuev, 2018; Mikshina et al., 2017), providing a new perspective for branched RG-I gelation. RG-I rich pectic polysaccharide can form gel under divalent ions, for example Ca^{2+} and Mg^{2+}, and sucrose can strengthen the gel network (Liu, Guo, Li, Zhu & Li, 2013; Wang et al., 2019). Gels made from RG-I rich pectic polysaccharide with high molecular weights will be stronger than gels made with pectic polysaccharide of lower molecular weights. However, publish papers in this field report gelling capacity of RG-I rich pectic polysaccharide but rarely focus on the improvement of gel properties and network structures. Thus, further attempts to improve rheological properties and microstructures of RG-I gel based on the novel highly branched structure are needed for the development of functional food hydrocolloids.

Pectin mixtures are widely used in the food industry to obtain products with desired texture and gelling properties. High methoxylated pectin (HMP, DM>50%) and low methoxylated pectin (LMP, DM<50%) are often mixed in order to reduce sucrose content of pectin gels. HMP/LMP blend gels exhibited similar rheological behavior to HMP gels of higher sucrose concentrations, which attributes to the inhomogeneous gel structure (Löfgren & Hermansson, 2007; Lootens, Capel, Durand, Nicolai, Boulenguer & Langendorff, 2003). RG-I rich pectic polysaccharide has a synergistic effect on the gelation of traditional commercial pectins and other polysaccharides (Chen et al., 2019). RG-I pectic polysaccharide, with long galactan side branches extracted from okra, reduced the sucrose content required for gelation and acted as a synergistic gel for high-methoxyl pectin. Side-chain entanglements create a pliable and continuous network, thus these blended gels show excellent toughness and high fracture strain (Li et al., 2019). However, few

researches extracted RG-I rich citrus pectic polysaccharides at different esterification degree, so the synergistic gelation of RG-I rich pectic polysaccharides of different structures remains unknown. Studying the synergistic gelation mechanism of RG-I rich pectic polysaccharides at different esterification degree gives information for rational selection of RG-I pectic polysaccharide structure when designing or improving food textures, which could provide new perspectives support to expand the application of RG-I rich pectic polysaccharide as potential food additives and could be helpful in the development of RG-I-based food products.

In our previous work, we have used acid and alkaline extraction conditions at low temperature to extract RG-I rich pectic polysaccharides from citrus peel and segment membrane (Chen et al., 2017; Zhang et al., 2017). The flow chart for extraction was shown in figure 1. The structure and rheological properties of branched pectic polysaccharides have been evaluated, the pectic polysaccharide from acid water (PA) mainly composes of GalA with a medium (~45%) DM, while Ara is the main saccharide present in the pectic polysaccharide from basic water (PB) with a low (~15%) DM. PA can form gel under the HMP gelling procedure (pH<3.0, 65 wt% sucrose) and the present of Ca^{2+} increases the gel strength, while PB shows gelling capacity with Ca^{2+} (Chen et al., 2017). Interestingly, RG-I rich PA/PB blend gels showed improved rheological properties (higher dynamic-viscoelastic modulus) than pure PA and PB gels in $CaCO_3$-glucono-δ-lactone (GDL) system. The aim of this research is to explore the synergistic effect of PA and PB blend gelation with different ratios and gel properties under various conditions. Furthermore, the microstructures of gels were observed by Cryo-SEM. Based on the gel properties and microstructures, we proposed a hypothetical mechanism for the synergistic effect of PA and PB calcium-induced gel.

2. Materials and methods

2.1 Materials

Pectic polysaccharide sample were recovered from acid and basic water discharged from citrus canning factories during the segment membrane removal process described previously (Chen et al., 2017) with some modifications (see Figure 1). The low extraction temperature, applied in canning, limited the hydrolysis of pectin side-chains. The proportion of major side-chain sugars (arabinose and galactose) was much higher than that of commercial citrus pectin, resulting in a lower proportion of galacturonic acid (GalA) (Chen et al., 2021). Citrus segments were added into 0.4% HCl solution (pH=1.0) and stirred at 28℃ for 40 min to loosen the cell wall structure and extract a portion of pectic polysaccharide. Then the mixture was filtered through a 400-mesh filter bag. The first fraction of acid-extracted pectic polysaccharide (PA) was recovered from the acidic filtrate by adjusting pH to 3~4 with 2M NaOH and precipitation with 95% ethanol in the volume ratio of 1:1 for 2 h. The residue was resuspended in 0.6% NaOH (pH=13.2) and magnetic stirred at 32℃ for 10 min, then a filter bag was used to obtain the liquid and the residue was discarded. The liquid underwent pH-adjustment to 6~7 with 2M HCl and precipitation to recover the pectic polysaccharide extracted with base (PB). Finally, precipitates were washed with 0.1% HCl/ethanol for 2 times and ethanol for 2 times to remove salt and oven-dried at 55 ℃ for 24 h. PA was composed of 44.2% HG and 40.6% RG-I (GalA: Rha: Ara: Gal=47.1: 2.87: 23.2:11.6 mol%, DM=45.4%, Mw= 196.6 kDa), while PB was composed of 19.3% HG and 62.7% RG-I (GalA: Rha: Ara: Gal=23.5: 4.19: 43.3:11.1 mol%, DM=15.06%, Mw=282.7 kDa), chemical structure results of PA and PB was shown in supplementary data. All chemicals used were of analytical grade.

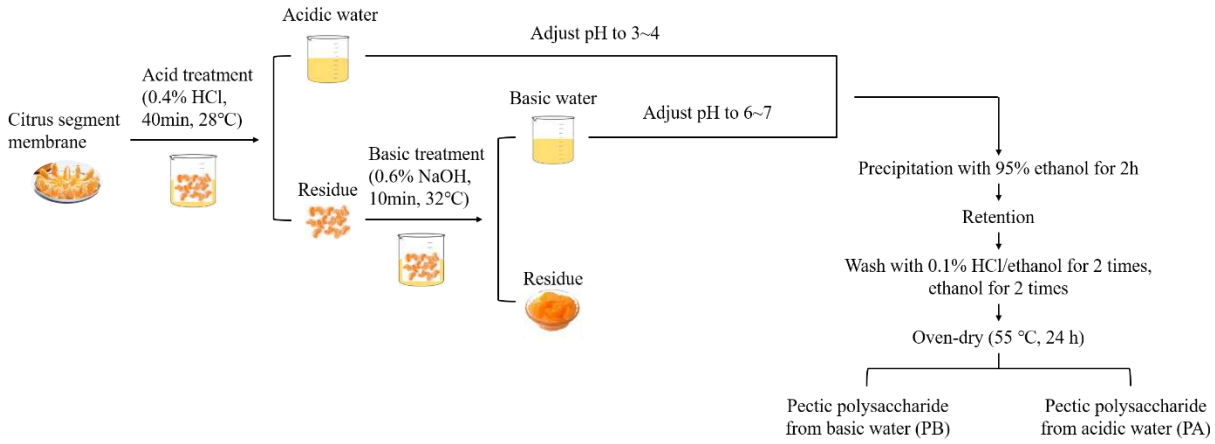

Figure 1. Flow chart for extraction of PA and PB.

2.2 Atomic force microscopy (AFM) observation

The pectic polysaccharide samples (200 μg/mL) were dissolved in ultrapure water with continuous stirring at 80 ℃ for 2 h. The pectic polysaccharide solutions were diluted by sodium dodecyl sulfate (SDS) solution to obtain a mixed solution containing polysaccharides and SDS both 10 μg/mL and then stirred for 48 h. SDS was added for producing stable unaggregated solutions (Wang & Nie, 2019). A 5 μL of mixed solution was filtered through a 0.22 μm filter and dropped onto a freshly cleaved mica substrate and then air-dried overnight. Scanning probe microscopy images were observed by AFM (XE-70, Park Scientific Instruments, Suwon, Korea) using tapping mode in air at room temperature (humidity: 50%-60%). The probe is a classical silicon cantilever (Si_3N_4) with a spring constant of 0.2 N/m and a resonance frequency of approximately 13 kHz (Wei et al., 2019). NanoScope Analysis 1.8 was used for image manipulation.

125 2.3 Preparation of pectic polysaccharide gels

PA and PB samples were dissolved in distilled water at content of 0.5, 1.0, 1.5 and 2.0% (w/v)) under magnetic stirring for 3 h at 40℃. The stock PA and PB solutions were mixed under magnetic stirring for 30 min at 40℃to prepare pectic polysaccharide solutions with different ratio of PA and PB (PA/PB=2:0, 1.5:0.5, 1:1, 0.5:1.0 and 0:2). The pectic polysaccharide solutions were cooled to 25℃and the pH of each solution was adjusted to 5.0 using 1M NaOH or HCl. The pectic polysaccharide gels were formed using controlled calcium release from the $CaCO_3$-GDL system in order to inhibit pre-gelation. $CaCO_3$ (5, 10, 20 and 40 mM), GDL (0.8, 1.6, 2.0 and 2.8 wt%) and urea (1 M) were added to the pectic polysaccharide solutions under constant stirring for 4 min to obtain mixed gels and the pH of the gels would be measured every 10 min for 3 h.

2.4 Rheological measurement

A HAAKE RheoStress 6000 rheometer (Thermo Scientific, USA) with a 60 mm parallel plate was used to analyze the rheological properties of pectic polysaccharides, including steady shear flow behavior of PA and PB solutions (only pectic polysaccharide dissolved in distilled water) and dynamic-viscoelastic properties of PA and PB synergistic gels (pectic polysaccharide dissolved in distilled water with addiction of $CaCO_3$ and GDL). Pectic polysaccharide solutions with different ratio of PA and PB were subjected to steady shearing with the shear rates ranging from 0.01 to 100 s^{-1} at 25℃. Data were fit to a power law model (equation (1)).

$$\eta=k\gamma^{(n-1)} \qquad (1)$$

In equation (1), where η is the apparent viscosity (mPa•s), k (mPa•s^n) is the consistency index, γ is the shear rate (s^{-1}) and n (dimensionless) is the flow behavior index.

In order to analyze dynamic-viscoelastic properties of pectic polysaccharide gels with $CaCO_3$ and GDL, the mixed gels were put onto the rheometer and equilibrated for 1 min at 25℃, then

analyzed for their rheological behavior. The linear viscoelastic ranges were firstly determined by amplitude sweep from 0.001% to 100% at a constant frequency of 1 Hz. The small deformation oscillatory of time sweep determination was carried out at constant frequency of 1 Hz for 10800 s, under 0.1% deformation (smaller than the maximum value of linear viscoelastic range). The frequency sweep was conducted from 0.1 to 10 Hz at 0.1% deformation to monitor the change in storage modulus (G') and loss modulus (G'') of the mixtures after 10800 s. For pH measurement, mixed gels with $CaCO_3$ and GDL were stirred for 4 min and equilibrated for 1 min, the pH value was measured every 10 min for 3 h.

2.5 Visualization of microstructure of pectic polysaccharide gels (Cryo-SEM)

Cryo-scanning electron microscopy (Cryo-SEM) is used to observe the native microstructure of high water content hydrogels. First, the sample placed in the stub was cryo-vitrified with liquid nitrogen slush at -210 ℃. The vitrified sample was then transferred into the cryo-SEM pre-chamber (PP3010T Cryo-SEM Preparation System, Quorum, UK) for sublimation at -85 ℃ under vacuum conditions for 20-25 min. The sample was sputtered with gold to prevent charging during electron beam targeting. Finally, the sample was transferred on to the SEM stage (Regulus 8100, Hitachi, Japan) at -140 ℃ for observation (Kyomugasho et al., 2018a; Ngouémazong et al., 2012).

2.6 Statistical analysis

Data were expressed as the mean ± standard deviation (SD) with three replicates per sample. Data were analyzed by ANOVA using Duncan's test with SPSS version 21.0 (IBM software, New York, USA). The significance level was set at $P < 0.05$.

3. Results and discussion

3.1 Morphology properties and steady shear flow behavior of PA and PB solutions

The morphology of pectic polysaccharide solutions at 10 μg/mL in the scan area of 2.5 μm×2.5 μm was shown in Figure 2. The PA molecule chains aggregated into a continuous and dense network of 2.0 nm height, with gathered pieces ranging from 100 nm to 300 nm of 2.5 nm height (Fig. 2a). The irregular and sparse network structures were observed in PB solution, average vertical height of the main chains was measured to be 3.0 nm. The height of PB was higher than that of PA, which may relate to the high molecular weight and highly branched structure of PB. In addition, PA molecule chains showed more aggregations than PB at the same pectic polysaccharide concentration, which may be relevant to the relatively high GalA content and DM (~45%). RG-I pectic polysaccharide with higher proportion of GalA showed more aggregates of molecules but not single molecules of complex shape (Petrova et al., 2019). Interestingly, in the blend solution containing 5 μg/mL PA and 5 μg/mL PB distributed on mica, the molecules presented an island-like structure of a height of 2.0-3.0 nm, different from the network structure of pure pectic polysaccharide solutions with same polymer concentration. The poor networking and high aggregation degree of mixture of PA and PB could be explained by the structure characteristics. Long side-chains of PB tend to interact with each other and form aggregates with the backbone located at the periphery (Mikshina, Idiyatullin, Petrova, Shashkov, Zuev & Gorshkova, 2015). In addition, the water retaining capacity of arabinan side-chains (Larsen, Byg, Damager, Diaz, Engelsen & Ulvskov, 2011) promoted the interaction between methoxylated galacturonic acid residues of PA (Fu & Rao, 2001). The intermolecular polymerization in PA/PB blend solution provided the possibility of synergistic mixed gelation.

Steady shear flow behavior of PA and PB solutions (Fig. 2d) suggested that pectic polysaccharide solutions are all typical pseudoplastic fluids. Table 1 showed that the fitting

accuracy of data points on the sample curve using the power law model reached 0.98, suggesting the model could be used to analysis pectic polysaccharide samples (Table 1). The consistency coefficient (K) and fluid index (n) were of magnitudes used to express fluid consistency and non-Newtonian fluid behavior in the model. The consistency coefficient of PA was higher than that of PB, which may relate to the abundant HG region with a relatively high DM of PA. PB had the greater shear-thinning property, indicating the orientation of PB molecular chain can be more easily obtained by shearing. This property may be due to the low GalA content and low degree of methoxylation of PB, which resulted in low viscosity and little interactions between molecular chains. The different steady shear flow behavior of pectic polysaccharide solutions was consistent with the chain conformation observed by AFM. Apparent viscosity of PA was higher than that of PB, which could be explained by the continuous and dense network with aggregations observed in PA solution and irregular and sparse network structures of PB. The color of PB solution was clear than PA solution at the same concentration (Fig. S4a and c), supporting that the aggregation of pectic polysaccharide chains in PB solution was less than that of PB solution (Hua, Yang, Din, Chi & Yang, 2018). In addition, PA/PB blend solution showed medium fluid index and consistency coefficient comparing with PA and PB, consistent with the microstructure of inhomogeneous aggregations. Hydrogen bonds between polymer chains promoted the aggregation. In order to investigate the contribution of hydrogen bonds in RG-I rich pectic polysaccharide solutions, 1 M urea was added into the solutions. Urea is a hydrogen bond breaking agent can break the intermolecular hydrogen bonding between polysaccharides chains. The influence of 1M urea on the apparent viscosity of PA, PB and PA/PB solutions (PA/PB=1) were showed in Fig. 2e. The fluid index and consistency coefficient of pectic polysaccharide solutions decreased in the present of urea and the influence on PA was most

obvious, indicating hydrogen bonds contributed to pectic polysaccharide aggregations and promoted apparent viscosity.

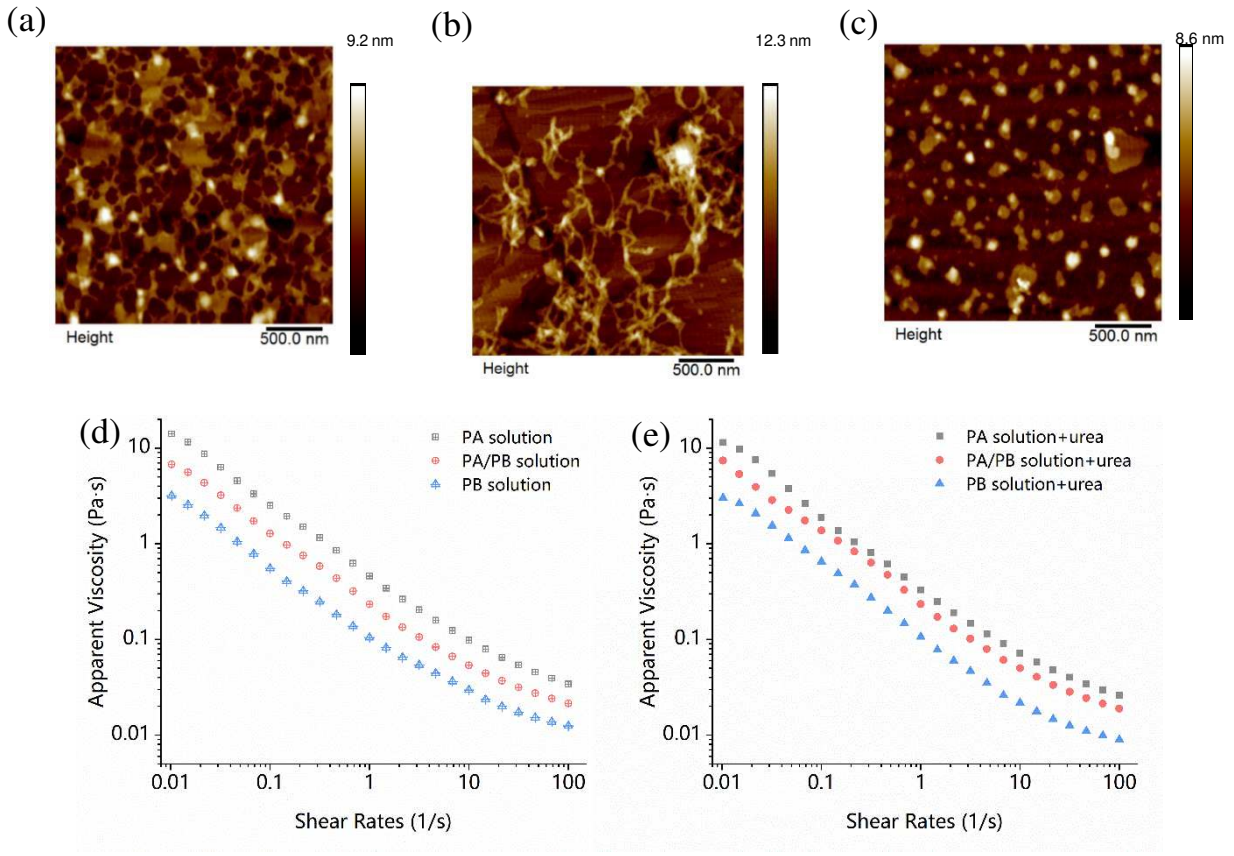

Figure 2. Representative topographical AFM images of (a) PA, (b) PB and (c) mixture of PA/PB; (d) Flow behavior of PA, PB and PA/PB (PA/PB=1) solution at concentration of 1.5%; (e) Flow behavior of PA, PB and PA/PB (PA/PB=1) solution at concentration of 1.5% with 1 M urea.

Table 1. Parameters of flow curves obtained by fitting to power law model.

Index	PA solution	PA/PB solution	PB solution	PA solution+ urea	PA/PB solution+ urea	PB solution+ urea
k	537.9	284.3	137.6	404.7	276.8	126.9
n	0.316	0.339	0.371	0.305	0.323	0.314
R^2	0.9936	0.9901	0.9848	0.9901	0.9922	0.9905

224224

225 3.2 Dynamic-viscoelastic properties of PA and PB synergistic gels

226 **Ratio of PA and PB** Fig. 3a showed the modulus and pH evolution of PA/PB blend
227 samples at different ratio with addition of 0.8 wt% GDL and 5 mM $CaCO_3$. Initially, pH was
228 around 5.8 and Ca was present in the form of solid $CaCO_3$. The modulus of PA was the highest
229 among all the samples while that of PB was the lowest, which can be explained by the different
230 structures of PA and PB. PA composed of relatively high content of GalA with DM of 45%, thus
231 the network formation of PA may contribute to calcium-bridge or hydrogen bonds and
232 hydrophobic interactions depending on the distribution of demethylated blocks of HG (Yu et al.,
233 2017). The presence of abundant rhamnose in PB influenced the conformation of the polymer in
234 solution, disturbing the molecular orientation necessary for junction-zone formation and limiting
235 inter-chain association (Chan, Choo, Young & Loh, 2017). The concentration of Ca ions
236 increased progressively with GDL hydrolysis, which led to an increase modulus of gels. G' and
237 G'' increased mainly due to the "egg box" junction zones formed by binding action between
238 Ca^{2+} and carboxyl groups. Another reason for increasing modulus was the hydrogen bonds and
239 hydrophobic interactions between galacturonic acid backbones (Ngouémazong et al., 2012) and
240 neutral sugar side-chains prompted by the low pH condition (Ngouémazong et al., 2012; Sousa,
241 Nielsen, Armagan, Larsen & Sørensen, 2015). The extremely low DM of PB were beneficial for
242 calcium-bridge formation and abundant side-chains stabilized the network structure through
243 entanglements. As for PA, G' and G'' increased slowly. Blocks of more than 10 non-
244 methoxylated galacturonic acid residues could interact with calcium ions (Chan et al., 2017). The
245 slow and limited increase could be explained by the occurrence of methyl ester groups in the
246 primary backbone and the RG-I steric hindrance produced on the unesterified HG blocks
247 (Cameron, Luzio, Goodner & Williams, 2008; Luzio & Cameron, 2008). PA system appeared as

248 thick liquid (Fig. S4d), different from the solid appearance of PB or PA/PB blend gel (Fig. S4e
249 and f). But the G' of PA system was always higher than the G'', suggesting it should be
250 considered as a weak gel (Kyomugasho, Christiaens, Van de Walle, Van Loey, Dewettinck &
251 Hendrickx, 2016). Modulus of PA slightly decreased after 5000 s, similar phenomenon has been
252 reported previously (Lootens et al., 2003). The modulus of pectic polysaccharide with a
253 relatively high DM (~50%) was dependent on the balance of two interactions. Low pH prompted
254 the hydrophobic interactions between methylesterified carboxyl and hydrogen bonds between
255 non-methylesterified carboxyl. It could also convert the carboxyl from dissociated (COO-) to
256 associated (COOH) and reduced affinity for Ca ions. As a result, the modulus of PA gel
257 decreased at pH lower than 4.5 (Fraeye, Duvetter, Doungla, Van Loey & Hendrickx, 2010).
258 Interestingly, G' and G'' of PA/PB blend samples increased more quickly and were higher than
259 pure PA or PB samples, suggesting the synergistic effect of PA and PB could strengthen the gel
260 network. One possible reason was that the long side-chains of PB decreased the water activity
261 since they contain many hydrophilic groups (Einhorn-Stoll, 2018), thus prompted the interaction
262 of PA chains. Moreover, PA and PB could interact with each other by Ca-bridges with the
263 release of calcium ions. Consequently, mixture of PA and PB prompted the formation of three-
264 dimensional network and increased the moduli of blend gels.

265 **Pectic polysaccharide concentration** The modulus and pH of PA/PB blend gels
266 (PA/PB=1) at different pectic polysaccharide concentration (0.5, 1.0, 1.5 and 2% w/v) with
267 addition of 0.8 wt% GDL and 5 mM $CaCO_3$ were shown in Fig. 3b. The effect of pectic
268 polysaccharide concentration on the pH was ignorable for the ratio GDL to $CaCO_3$ used in the
269 samples. The G' and G'' increased with increasing pectic polysaccharide concentration and the
270 change of G' and G'' at low concentrations (<1.0% w/v) was more apparent than high

concentrations (>1.0% w/v). The increased modulus could be attributed to increased number of cross-linking junction zones between pectic polysaccharide chains. With increasing pectic polysaccharide concentration, number of hydrogen bonds and hydrophobic interactions between pectic polysaccharide chains increased, which can be explained by the higher number of binding sites available and the lower water activity of gels. The number of "egg box" junction zones between Ca^{2+} and pectic polysaccharide chains also increased and the probability of ionic bonds formation within the same pectic polysaccharide chain decreased, leading to more junction zones between the separate pectic polysaccharide chains and stronger gels (Fraeye et al., 2010; Kyomugasho et al., 2016). G' and G'' of gels increased with pectic polysaccharide concentration, but the increasing effects was not significant when the concentration reached to a certain level. The high viscosity of pectic polysaccharide solution locked the structure thus hinder the formation of ionic cross-links (Wan et al., 2019). Interestingly, the modulus increased more quickly at low pectic polysaccharide concentration compared to the high concentration. At constant Ca^{2+} concentration, the lower the pectic polysaccharide concentration was, the higher the ratio of Ca^{2+} to the pectic polysaccharide concentration was, resulting in quick gel formation.

GDL concentration The modulus and pH of PA/PB blend gels (PA/PB=1) with different concentration of GDL (0.8, 1.6, 2.0 and 2.8 wt%) with addition of 5 mM $CaCO_3$ is shown in Fig. 3c. The final Ca^{2+} concentration of gels could be guaranteed to be the same (5 mM), because the pH of gels was lower than 4.0. G' and G'' of gels was lower increased rapidly at early stage with Ca ions releasing. The gel formation at GDL concentration of 0.8% was much slower than that at higher GDL concentrations, because GDL can decrease the pH of gels during the hydrolysis and promote the Ca ions release. The differences of gel formation rate at high GDL concentrations (≥1.6%) were not significant, additional GDL had little influence on the rate because the amount

of interaction sites was limited due to the constant pectic polysaccharide concentration. Moduli of the gels reach a plateau within ~3000 s, when most of the Ca ions had been released. G' and G'' of gels after 3h holding period were different at various GDL concentration and the G' and G'' increased with GDL concentration increasing, but the rheological properties of gels at 2.8% GDL was similar with that of 2.0%. Decreased pH promotes formation of hydrogen bonds between protonated carboxyl groups (Fraeye et al., 2010) as well as neutral sugar side-chains (Ngouémazong et al., 2012; Sousa et al., 2015). Meanwhile, the affinity for calcium ions of pectic polysaccharide decreased at low pH condition because of the decreased charge density (Cardoso, Coimbra & Lopes Da Silva, 2003). A pH of 5.0 was found to be optimal for Ca^{2+} binding by LM pectin (Celus, Kyomugasho, Van Loey, Grauwet & Hendrickx, 2018), however, that was 3.0 for PA/PB blend gel with 5 mM Ca ions. The low optimal pH of blend gel suggested that besides ionic cross-links, hydrogen bonds were of great importance to the RG-I rich blend gel formation.

Ca^{2+} concentration The modulus and pH of PA/PB blend gels (PA/PB=1) with different concentration of $CaCO_3$ (5, 10, 20 and 40 mM) with addition of 0.8 wt% GDL were shown in Fig. 3d. The calcium content strongly influenced the kinetic behavior and moduli of the gels. Increased Ca^{2+} concentration of resulted in more rapid gel formation and also a complex behavior in G' and G''. Moduli of gels with high Ca^{2+} concentration increased rapidly and reached a local maximum within ~2000 s, then decreased and reach a plateau within ~6000 s, while that of lower Ca concentration increased continuously. G' of gels with more than 20 mM Ca^{2+} were higher than that of 10 mM Ca^{2+}, but after 3000 s the opposite result was obtained. Pectic polysaccharide chains interacted with cations and formed point-like cross-links at low Ca^{2+} concentration, then dimers occurred and the network of polymer chains formed upon

317 increasing Ca ions (Huynh, Lerbret, Neiers, Chambin & Assifaoui, 2016; Kyomugasho et al.,
318 2016). The increasing $CaCO_3$ concentration contributed to more available Ca ions in gels, which
319 could increase the crosslink density between pectin chains (Wan et al., 2019). However, the
320 initial structure based on Ca^{2+}-pectin interactions may lock the structure thus diminish the
321 possibilities for further strengthening of gel network by hydrophobic interactions and hydrogen
322 bonds (Löfgren, Guillotin, Evenbratt, Schols & Hermansson, 2005). Another possible reason was
323 that the structure formation rate of gel at high GDL concentration was fast, which caused
324 incomplete network formation thus reduces the G' of gel (Kastner, Einhorn-Stoll & Senge,
325 2012). Moreover, excess Ca^{2+} caused syneresis of gels with a thin water layer found on the gel
326 surface and decreased the G' (Liu et al., 2013). Above pH 4.5 gel properties were relatively
327 independent of pH and the influence of pH can be ignored (Fraeye et al., 2010), indicating the
328 various G' and G'' of gels added more than 5 mM Ca ions mainly resulted from the
329 concentration of $CaCO_3$. According to the moduli of gels with different GDL concentration (Fig.
330 3c), moduli of gels increased with pH decreasing when pH above 3.0, so the G' of gels with 5
331 mM $CaCO_3$ increased slowly while that of higher Ca^{2+} concentrations keeps constant.
332332
333333

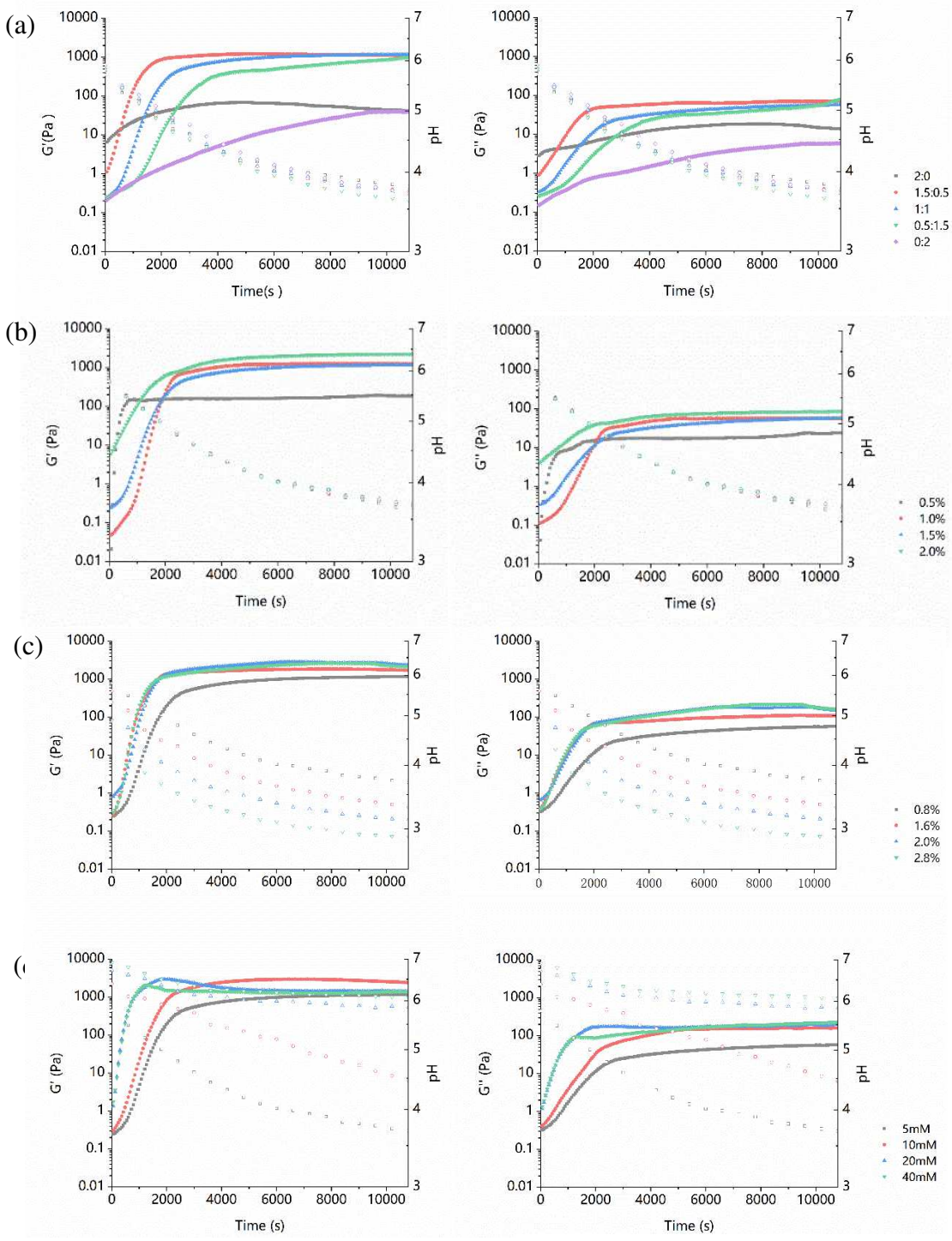

334

335 **Figure 3.** Modulus values (G' and G'') of PA/PB blend gels. (a) PA/PB blend gels (1.5% w/v

336 pectic polysaccharide concentration, 0.8 wt% GDL, 5 mM $CaCO_3$) at PA/PB=2:0, 1.5:0.5, 1:1,

337 0.5:1.0 and 0:2; (b) PA/PB blend gels (PA/PB=1, 0.8 wt% GDL, 5 mM $CaCO_3$) of pectic

polysaccharide concentration of 0.5, 1.0, 1.5 and 2.0% w/v; (c) PA/PB blend gels (PA/PB=1, 1.5% w/v pectic polysaccharide concentration, 5 mM $CaCO_3$) with GDL concentration of 0.8, 1.6, 2.0 and 2.8 wt%; (d) PA/PB blend gels (PA/PB=1, 1.5% w/v pectic polysaccharide concentration, 0.8 wt% GDL) with Ca^{2+} concentration of 5, 10, 20 and 40 mM. Measurement temperature, 25℃; strain, 0.1%; frequency, 1 Hz.

3.3 Effect of urea on dynamic-viscoelastic properties of PA and PB synergistic gels

The synergistic gelation feature of PA/PB blend gels was demonstrated, but a more comprehensive investigation of the association properties of this system is required. For cation-induced RG-I rich pectic polysaccharide gel, junction zones are primarily formed by electrostatic interactions and contributed to hydrogen bond between intra- and intermolecular pectin chains (Liu et al., 2013). The contribution of hydrogen bonds in synergistic gel formation was worthy of study, so oscillatory shear measurements of gels are carried out with urea. The influence of 1M urea on the dynamic-viscoelastic properties of PA, PB and PA/PB blend gels (PA/PB=1) were showed in Fig. 4. The decrease of G' and G'' of PA gel was more obvious than that of PB gel in the presence of urea, suggesting that hydrogen bonding contributes to the gel formation of PA. The inhibition of PA gel could be explained by the lack of blocks of more than 10 non-methoxylated galacturonic acid residues, which was consistent with the structure properties of PA. As for PB, the slight decrease of modulus suggested that PB gel mainly composed of the calcium-pectin network, hydrogen bonds could help stabilize the structure. Interestingly, the modulus of PA/PB blend gel was lower than PB gel after addition of urea, in other words, synergistic effect of PA/PB blend gel no longer appeared, indicating the hydrogen bonds were

360 vital for synergistic gelation.

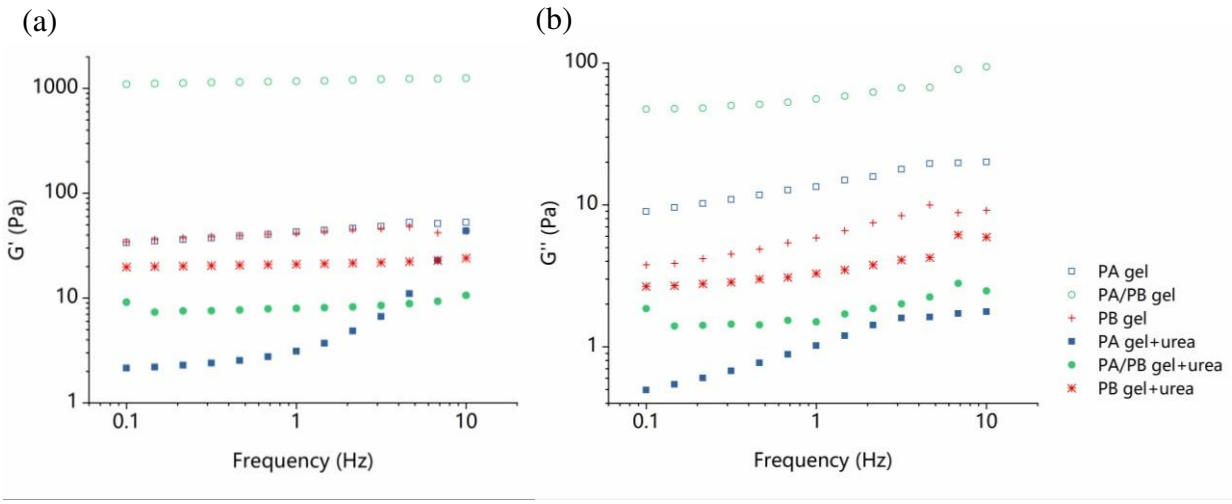

Figure 4. Modulus values (G' and G'') of PA/PB blend gels. (a) G' of PA, PB and PA/PB blend gels (PA/PB=1) with addition of 0.8 wt% GDL and 5 mM CaCO3; (b) G'' of PA, PB and PA/PB blend gels (PA/PB=1) with addition of 0.8 wt% GDL and 5 mM CaCO3; Measurement temperature, 25℃; strain, 0.1%; frequency, 0.1-10 Hz.

3.4 Cryo-SEM analysis

Cryo-SEM images of PA, PB and PA/PB blend gels with addition of 5mM $CaCO_3$ were showed in Fig. 5. Formation of intertwined fibrous network and strand-like structure can be promoted by cations (Efthymiou, Williams & McGrath, 2017; Kyomugasho et al., 2016). PA gel mainly composed of strand-like structures but the network was incomplete with open microstructures. PA exhibited higher amounts of GalA with 45% DM, prompting the polymer chain entanglements based on hydrogen bonds. But low amounts of blocks of more than 10 non-methoxylated galacturonic acid residues limited formation of ionic cross-links, resulting the loose and incomplete network and thick liquid appearance (Fig. 5a). PB gel showed intertwined fibrous network, which was similar with the microstructure structures observed in LMP gels

(Kyomugasho et al., 2016; Kyomugasho et al., 2018b; Liu et al., 2013). Dense cross-links were related to the high number of non-methylated GalA residues, which can form egg-box junction zones with Ca^{2+}. However, open structures could be found in the network, because the "kinks" produced by the rhamnose inserts of backbone limited cross-links (Fraeye et al., 2010). Thus, the surface of PB gel showed discontinuous structure in FESEM image (Fig. S3). Furthermore, PB exhibited higher amounts of branch-like structure compared to PA, consisting with the highly branched structure of PB (Santiago et al., 2018). Cryo-SEM image of PA/PB blend gel showed a clear three-dimensional network composed of strand-like structures (Fig. 5c) and intertwined fibrous structures (Fig. 5d). The entangled strand-like structures converted to cross-linked network, suggesting the blend system promoted the interaction of PA chains. The intertwined fibrous structures interacted with the strand-like structures, indicating Ca^{2+} connected PA and PB polymer chains. The unique microstructure was consistent with the strengthened gel properties of PA/PB blend gel. In addition, the surface of blend gel was more compact than that of pure gels (Fig. S3), representing an improved gelled state (Li et al., 2019).

3.5 Proposed mechanism of PA/PB synergistic gel formation

Our study showed PA and PB synergistically formed stronger gels with calcium induction. PA and PB consisted mainly of branched RG-I with the ratio of 41% and 63%, respectively, and high content of arabinose and galactose. The methoxylation degree of PA was 45%, but PB was only 15%. The AFM observation illustrated that PA could form dense network structure with gathered pieces, indicating the strong interactions between pectin chains based on hydrogen bonds. PB showed irregular and sparse network structure, based on the interaction of long side-chains of RG-I region. The molecules presented an island-like structure in PA/PB blend solution at the same polymer concentration, indicating the aggregation trend of PA and PB. RG-I side-

chains of PB tended to form aggregates with the backbone located at the periphery (Mikshina et al., 2015). Meanwhile, neutral sugar side-chains, especially arabinan side chains, could hydrate more readily than the rhamnose-galacturonic acid (Rha-GalA) backbone in RG-I (Larsen et al., 2011), thus promote aggregations of PA (Makshakova et al., 2018; Mikshina et al., 2017). Different HG/RG-I ratios and DM values of PA and PB induced the separation of their aggregates, similar phenomenon was reported in HM/LM pectin mixed gel, a very inhomogeneous phase-separated was formed and strong synergistic rheological properties were obtained (Löfgren, Walkenström & Hermansson, 2002). The hypothesis of hydration process was consistent with the steady shear flow behavior of pectic polysaccharide solutions (see Section 3.1).

PA and PB could form gels induced by calcium. PA was composed of relatively high content of GalA with DM of 45% and the network formation mainly composed of hydrogen bonds (Yu et al., 2017), as well as few ionic cross-links. Non-methoxylated galacturonic acid residues can interact with calcium ions but the methyl ester groups limited the extent of such junction zones (Chan et al., 2017). The network of calcium-induced PB gel was mainly composed of the "egg box" junction zones formed by binding action between Ca^{2+} and carboxyl groups. Moreover, abundant side-chains stabilized the network structure through entanglements. For PA/PB blend gels, the synergistic effect of pectic polysaccharides could strengthen the gel network, indicating interactions between PA and PB, including Ca-bridges between carboxyl groups and side-chain entanglements. Moreover, neutral sugar side-chains prompted formation of hydrogen bonds. Calcium-bridges connected PA and PB aggregates with suitable pH, consequently promoted the three-dimensional network formation and improved the rheological properties and microstructure of blend gels (see Fig. 5e).

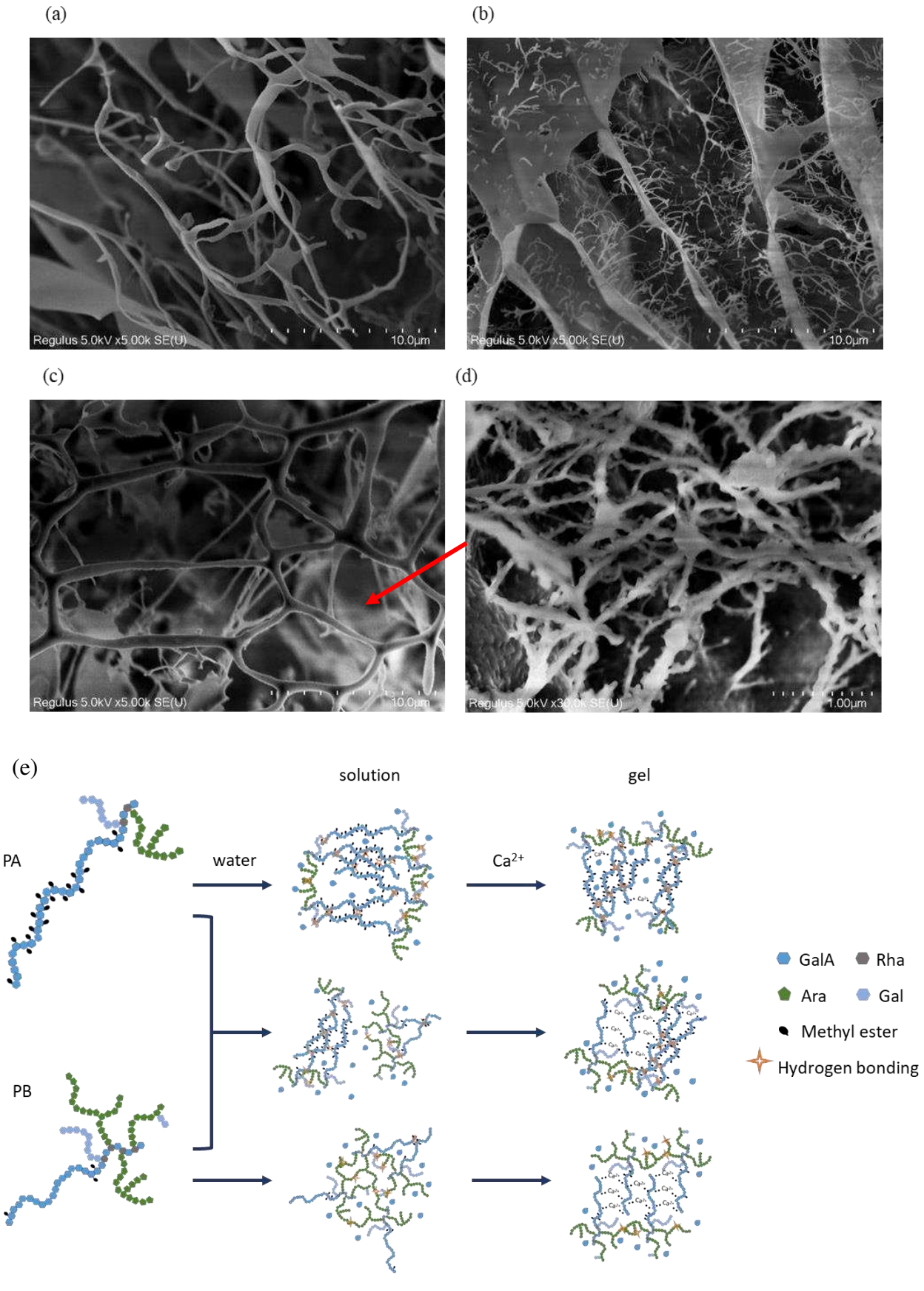
(a)
(b)
Regulus 5.0kV x5.00k SE(U)
10.0μm
Regulus 5.0kV x5.00k SE(U)
10.0μm
(c)
(d)
Regulus 5.0kV x5.00k SE(U)
10.0μm
1.00μm
(e)
solution
gel
PA
water
Ca2+
PB
GalA
Rha
Ara
Gal
Methyl ester
Hydrogen bonding

422422

Figure 5. Microstructure of (a) PA, (b) PB, (c) and (d) PA/PB blend gels (1.5% w/v pectic polysaccharide concentration, 0.8 wt% GDL, 5 mM $CaCO_3$). The amplification was 5000 (a), (b), (c) and 30000 (d) times the original size. (e) Schematic diagram of the formation of PA, PB and PA/PB blend gel.

427427

4. Conclusion

Rheological properties, water-holding capacity and microstructure of RG-I rich citrus pectic polysaccharide gels were investigated to elucidate the synergistic gelation mechanism of PA and PB. PA, with higher HG region (~41%) and relatively high DM value (~49%), showed high viscosity and dense network structure in pure solution. PB composed of RG-I region (67%) with long neutral sugar side-chains and HG region (17%) of low DM value (15%), so the network of PB solution was irregular and sparse. Island-like structure was observed by AFM in the PA/PB blend solution, indicating separate aggregation of PA and PB. RG-I rich PA and PB could form gels induced by calcium ions. The network of PA gel was mainly composed of hydrogen bonds between methoxylated galacturonic acid residues. PB gels relied on ionic cross-link junction-zones, stabilized by side-chain entanglements. PA/PB blend gels showed improved rheological properties and microstructure compared with pure PA and PB gels. Ca-bridges connected pectic polysaccharide aggregates and promoted the three-dimensional structure of PA/PB blend gels but excess Ca^{2+} caused syneresis of gels and decreased water-holding capacity. The gel network was stabilized by the hydrogen bonds prompted by neutral sugar side-chains. These findings suggested that synergistic effects can be achieved by mixing PA and PB to produce a

strengthened blend gel with calcium induction and provided further development for RG-I rich pectic polysaccharide-based products.

Acknowledgements

This work was financially supported by National Key R&D Program of China (2017YFE0122300190), National Natural Science foundation of China (31871815) and the Fundamental Research Funds for the Central Universities (Grant No. 2020FZZX003-02-05).

References

Cameron, R. G., Luzio, G. A., Goodner, K., & Williams, M. A. K. (2008). Demethylation of a model homogalacturonan with a salt-independent pectin methylesterase from citrus: I. Effect of pH on demethylated block size, block number and enzyme mode of action. *CARBOHYDRATE POLYMERS*, *71*(2), 287-299.

Cardoso, S. M., Coimbra, M. A., & Lopes Da Silva, J. A. (2003). Calcium-mediated gelation of an olive pomace pectic extract. *CARBOHYDRATE POLYMERS*, *52*(2), 125-133.

Celus, M., Kyomugasho, C., Van Loey, A. M., Grauwet, T., & Hendrickx, M. E. (2018). Influence of Pectin Structural Properties on Interactions with Divalent Cations and Its Associated Functionalities. *COMPREHENSIVE REVIEWS IN FOOD SCIENCE AND FOOD SAFETY*, *17*(6), 1576-1594.

Chan, S. Y., Choo, W. S., Young, D. J., & Loh, X. J. (2017). Pectin as a rheology modifier: Origin, structure, commercial production and rheology. *CARBOHYDRATE POLYMERS*, *161*, 118-139.

Chen, J., Chen, W., Duan, F., Tang, Q., Li, X., Zeng, L., Zhang, J., Xing, Z., Dong, Y., Jia, L., & Gao, H. (2019). The synergistic gelation of okra polysaccharides with kappa-carrageenan and its influence on gel rheology, texture behaviour and microstructures. *FOOD HYDROCOLLOIDS*, *87*, 425-435.

Chen, J., Cheng, H., Wu, D., Linhardt, R. J., Zhi, Z., Yan, L., Chen, S., & Ye, X. (2017). Green recovery of pectic polysaccharides from citrus canning processing water. *JOURNAL OF CLEANER PRODUCTION*, *144*, 459-469.

Chen, J., Cheng, H., Zhi, Z., Zhang, H., Linhardt, R. J., Zhang, F., Chen, S., & Ye, X. (2021). Extraction temperature is a decisive factor for the properties of pectin. *FOOD HYDROCOLLOIDS*, *112*, 106160.

Efthymiou, C., Williams, M. A. K., & McGrath, K. M. (2017). Revealing the structure of high-water content biopolymer networks: Diminishing freezing artefacts in cryo-SEM images. *FOOD HYDROCOLLOIDS*, *73*, 203-212.

Einhorn-Stoll, U. (2018). Pectin-water interactions in foods – From powder to gel. *FOOD HYDROCOLLOIDS*, *78*, 109-119.

Fraeye, I., Duvetter, T., Doungla, E., Van Loey, A., & Hendrickx, M. (2010). Fine-tuning the properties of pectin–calcium gels by control of pectin fine structure, gel composition and environmental conditions. *TRENDS IN FOOD SCIENCE & TECHNOLOGY*, *21*(5), 219-228.

Fu, J., & Rao, M. A. (2001). Rheology and structure development during gelation of low-methoxyl pectin gels: the effect of sucrose. *FOOD HYDROCOLLOIDS*, *15*(1), 93-100.

Hua, X., Yang, H., Din, P., Chi, K., & Yang, R. (2018). Rheological properties of deesterified pectin with different methoxylation degree. *Food Bioscience*, *23*, 91-99.

Huynh, U. T., Lerbret, A., Neiers, F., Chambin, O., & Assifaoui, A. (2016). Binding of Divalent Cations to Polygalacturonate: A Mechanism Driven by the Hydration Water. *JOURNAL OF PHYSICAL CHEMISTRY B*, *120*(5), 1021-1032.

Kastner, H., Einhorn-Stoll, U., & Senge, B. (2012). Structure formation in sugar containing pectin gels – Influence

485 of Ca2+ on the gelation of low-methoxylated pectin at acidic pH. *FOOD HYDROCOLLOIDS*, *27*(1), 42-49.
486 Klaassen, M. T., & Trindade, L. M. (2020). RG-I galactan side-chains are involved in the regulation of the water-
487 binding capacity of potato cell walls. *CARBOHYDRATE POLYMERS*, *227*, 115353.
488 Kyomugasho, C., Christiaens, S., Van de Walle, D., Van Loey, A. M., Dewettinck, K., & Hendrickx, M. E. (2016).
489 Evaluation of cation-facilitated pectin-gel properties: Cryo-SEM visualisation and rheological properties. *FOOD*
490 *HYDROCOLLOIDS*, *61*, 172-182.
491 Kyomugasho, C., Munyensanga, C., Celus, M., Van de Walle, D., Dewettinck, K., Van Loey, A. M., Grauwet, T., &
492 Hendrickx, M. E. (2018a). Molar mass influence on pectin-Ca2+ adsorption capacity, interaction energy and
493 associated functionality: Gel microstructure and stiffness. *FOOD HYDROCOLLOIDS*, *85*, 331-342.
494 Kyomugasho, C., Munyensanga, C., Celus, M., Van de Walle, D., Dewettinck, K., Van Loey, A. M., Grauwet, T., &
495 Hendrickx, M. E. (2018b). Molar mass influence on pectin-Ca2+ adsorption capacity, interaction energy and
496 associated functionality: Gel microstructure and stiffness. *FOOD HYDROCOLLOIDS*, *85*, 331-342.
497 Larsen, F. H., Byg, I., Damager, I., Diaz, J., Engelsen, S. B., & Ulvskov, P. (2011). Residue Specific Hydration of
498 Primary Cell Wall Potato Pectin Identified by Solid-State 13C Single-Pulse MAS and CP/MAS NMR Spectroscopy.
499 *BIOMACROMOLECULES*, *12*(5), 1844-1850.
500 Li, X., Dong, Y., Guo, Y., Zhang, Z., Jia, L., Gao, H., Xing, Z., & Duan, F. (2019). Okra polysaccharides reduced the
501 gelling-required sucrose content in its synergistic gel with high-methoxyl pectin by microphase separation effect.
502 *FOOD HYDROCOLLOIDS*, *95*, 506-516.
503 Liu, H., Guo, X., Li, J., Zhu, D., & Li, J. (2013). The effects of MgSO4, d-glucono- δ -lactone (GDL), sucrose, and
504 urea on gelation properties of pectic polysaccharide from soy hull. *FOOD HYDROCOLLOIDS*, *31*(2), 137-145.
505 Löfgren, C. E. E., Guillotin, S., Evenbratt, H., Schols, H., & Hermansson, A. (2005). Effects of Calcium, pH, and
506 Blockiness on Kinetic Rheological Behavior and Microstructure of HM Pectin Gels. *BIOMACROMOLECULES*, *6*(2),
507 646.
508 Löfgren, C., Walkenström, P., & Hermansson, A. (2002). Microstructure and Rheological Behavior of Pure and Mixed
509 Pectin Gels. *BIOMACROMOLECULES*, *3*(6), 1144-1153.
510 Löfgren, C., & Hermansson, A. (2007). Synergistic rheological behaviour of mixed HM/LM pectin gels. *FOOD*
511 *HYDROCOLLOIDS*, *21*(3), 480-486.
512 Lootens, D., Capel, F., Durand, D., Nicolai, T., Boulenguer, P., & Langendorff, V. (2003). Influence of pH, Ca
513 concentration, temperature and amidation on the gelation of low methoxyl pectin. *FOOD HYDROCOLLOIDS*, *17*(3),
514 237-244.
515 Luzio, G. A., & Cameron, R. G. (2008). Demethylation of a model homogalacturonan with the salt-independent pectin
516 methylesterase from citrus: Part II. Structure – function analysis. *CARBOHYDRATE POLYMERS*, *71*(2), 300-309.
517 Makshakova, O. N., Faizullin, D. A., Mikshina, P. V., Gorshkova, T. A., & Zuev, Y. F. (2018). Spatial structures of
518 rhamnogalacturonan I in gel and colloidal solution identified by 1D and 2D-FTIR spectroscopy. *Carbohydr Polym*,
519 *192*, 231-239.
520 Mikshina, P. V., Idiyatullin, B. Z., Petrova, A. A., Shashkov, A. S., Zuev, Y. F., & Gorshkova, T. A. (2015).
521 Physicochemical properties of complex rhamnogalacturonan I from gelatinous cell walls of flax fibers. *Carbohydr*
522 *Polym*, *117*, 853-861.
523 Mikshina, P. V., Makshakova, O. N., Petrova, A. A., Gaifullina, I. Z., Idiyatullin, B. Z., Gorshkova, T. A., & Zuev,
524 Y. F. (2017). Gelation of rhamnogalacturonan I is based on galactan side chain interaction and does not involve
525 chemical modifications. *CARBOHYDRATE POLYMERS*, *171*, 143-151.
526 Mohnen, D. (2008). Pectin structure and biosynthesis. *CURRENT OPINION IN PLANT BIOLOGY*, *11*(3), 266-277.
527 Ngouémazong, D. E., Kabuye, G., Fraeye, I., Cardinaels, R., Van Loey, A., Moldenaers, P., & Hendrickx, M. (2012).
528 Effect of debranching on the rheological properties of Ca2+ – pectin gels. *FOOD HYDROCOLLOIDS*, *26*(1), 44-53.
529 Ngouémazong, D. E., Tengweh, F. F., Fraeye, I., Duvetter, T., Cardinaels, R., Van Loey, A., Moldenaers, P., &
530 Hendrickx, M. (2012). Effect of de-methylesterification on network development and nature of Ca2+-pectin gels:
531 Towards understanding structure – function relations of pectin. *FOOD HYDROCOLLOIDS*, *26*(1), 89-98.
532 Petrova, A. A., Kozlova, L. V., Gaifullina, I. Z., Ananchenko, B. A., Martinson, E. A., Mikshina, P. V., & Gorshkova,
533 T. A. (2019). AFM analysis reveals polymorphism of purified flax rhamnogalacturonans I of distinct functional types.
534 *CARBOHYDRATE POLYMERS*, *216*, 238-246.
535 Santiago, J. S. J., Kyomugasho, C., Maheshwari, S., Jamsazzadeh Kermani, Z., Van de Walle, D., Van Loey, A. M.,
536 Dewettinck, K., & Hendrickx, M. E. (2018). Unravelling the structure of serum pectin originating from thermally and
537 mechanically processed carrot-based suspensions. *FOOD HYDROCOLLOIDS*, *77*, 482-493.
538 Sousa, A. G., Nielsen, H. L., Armagan, I., Larsen, J., & Sørensen, S. O. (2015). The impact of rhamnogalacturonan-I
539 side chain monosaccharides on the rheological properties of citrus pectin. *FOOD HYDROCOLLOIDS*, *47*, 130-139.

Thakur, B. R., Singh, R. K., Handa, A. K., & Rao, M. A. (1997). Chemistry and uses of pectin — A review. *C R C Critical Reviews in Food Technology*, *37*(1), 47-73.
Wan, L., Wang, H., Zhu, Y., Pan, S., Cai, R., Liu, F., & Pan, S. (2019). Comparative study on gelling properties of low methoxyl pectin prepared by high hydrostatic pressure-assisted enzymatic, atmospheric enzymatic, and alkaline de-esterification. *CARBOHYDRATE POLYMERS*, *226*, 115285.
Wang, J., & Nie, S. (2019). Application of atomic force microscopy in microscopic analysis of polysaccharide. *TRENDS IN FOOD SCIENCE & TECHNOLOGY*, *87*, 35-46.
Wang, S., Zhao, L., Li, Q., Liu, C., Han, J., Zhu, L., Zhu, D., He, Y., & Liu, H. (2019). Rheological properties and chain conformation of soy hull water-soluble polysaccharide fractions obtained by gradient alcohol precipitation. *FOOD HYDROCOLLOIDS*, *91*, 34-39.
Wei, C., Zhang, Y., He, L., Cheng, J., Li, J., Tao, W., Mao, G., Zhang, H., Linhardt, R. J., Ye, X., & Chen, S. (2019). Structural characterization and anti-proliferative activities of partially degraded polysaccharides from peach gum. *CARBOHYDRATE POLYMERS*, *203*, 193-202.
Willats, W., Knox, P., & Mikkelsen, J. D. (2006). Pectin: new insights into an old polymer are starting to gel. *TRENDS IN FOOD SCIENCE & TECHNOLOGY*, *17*(3), 97-104.
Wu, D., Zheng, J., Mao, G., Hu, W., Ye, X., Linhardt, R. J., & Chen, S. (2019). Rethinking the impact of RG-I mainly from fruits and vegetables on dietary health. *Crit Rev Food Sci Nutr*, 1-23.
Yu, L., Yakubov, G. E., Zeng, W., Xing, X., Stenson, J., Bulone, V., & Stokes, J. R. (2017). Multi-layer mucilage of Plantago ovata seeds: Rheological differences arise from variations in arabinoxylan side chains. *Carbohydr Polym*, *165*, 132-141.
Zhang, H., Chen, J., Li, J., Yan, L., Li, S., Ye, X., Liu, D., Ding, T., Linhardt, R. J., & Orfila, C. (2017). Extraction and characterization of RG-I enriched pectic polysaccharides from mandarin citrus peel. *FOOD HYDROCOLLOIDS*, *79*.

Declaration of interests

The authors declare that they have no known competing financial interests or personal relationships that could have appeared to influence the work reported in this paper.

Credit Author Statement

Shiguo Chen conceived the study; **Jiaqi Zheng** designed the experiments, performed the experiments and statistical analysis and wrote the manuscript; **Laiming Zhang** helped to perform the experiments; **Huan Cheng**, **Caroline Orfila** and **Xingqian Ye** interpreted the data; **Jianle Chen** critically revised the manuscript. All authors read and approved the final manuscript.

Figure1

Click here to access/download;Figure(s);Figure 1.png

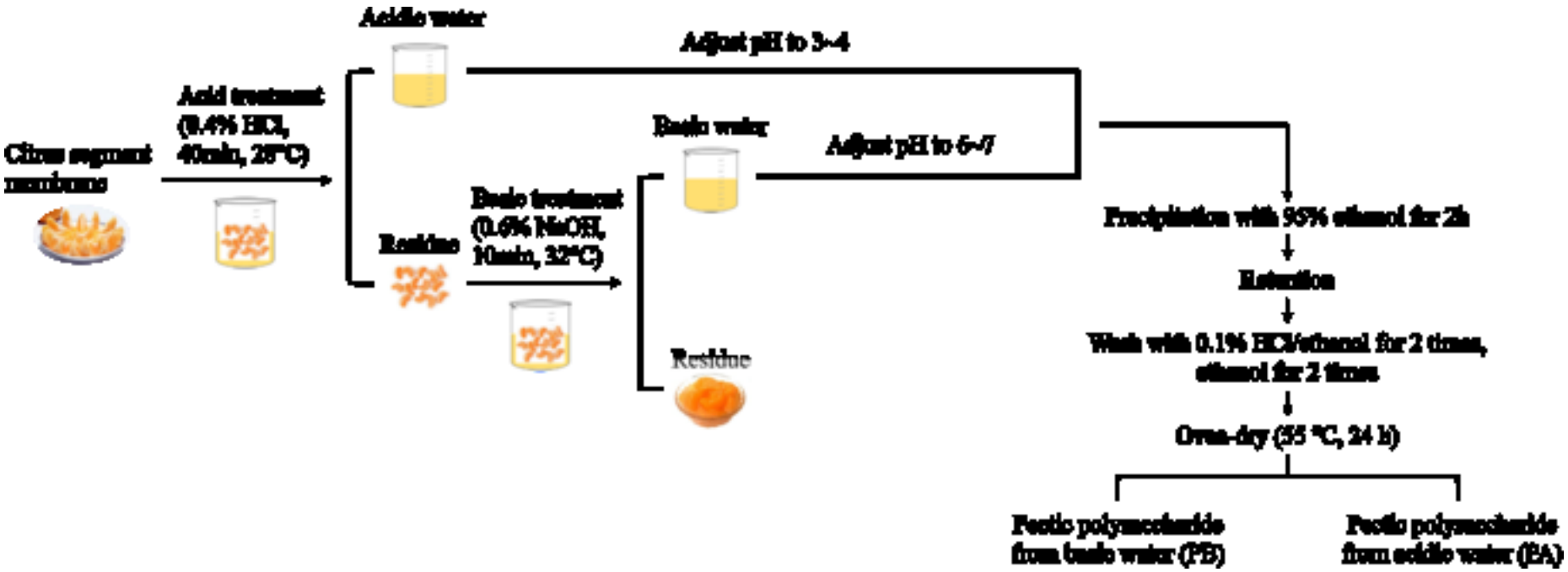

Figure2-1

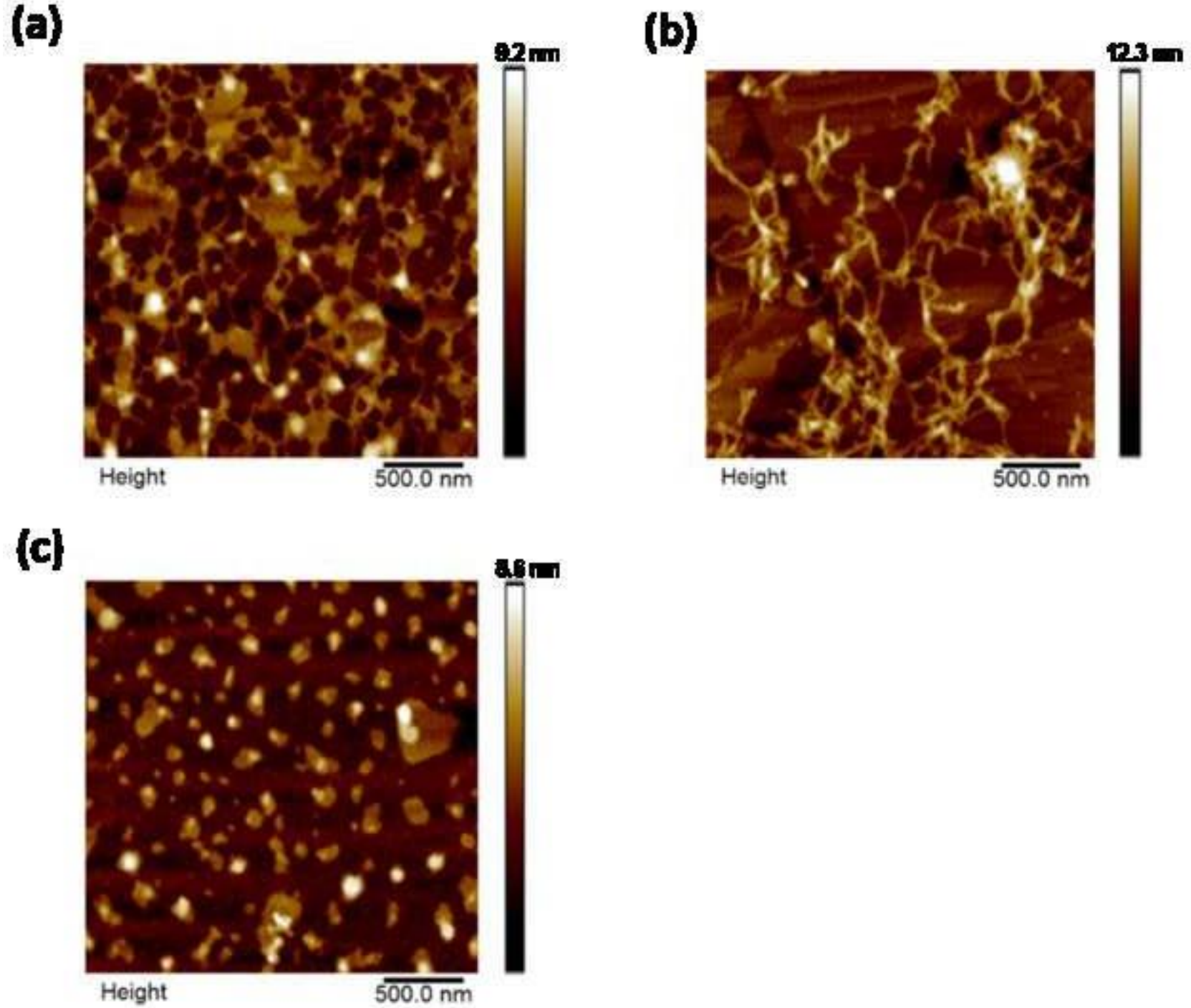

Figure2-2

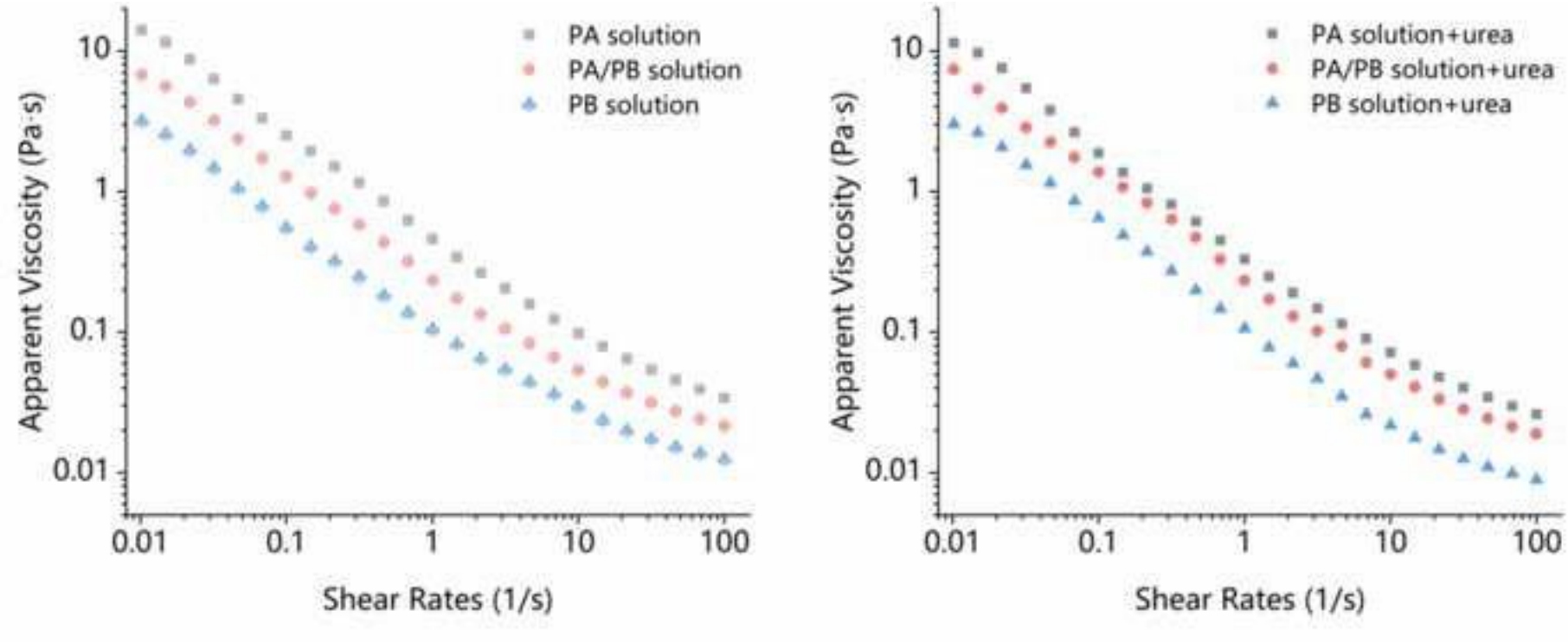

Figure3

Click here to access/download;Figure(s);Figure 3.tif

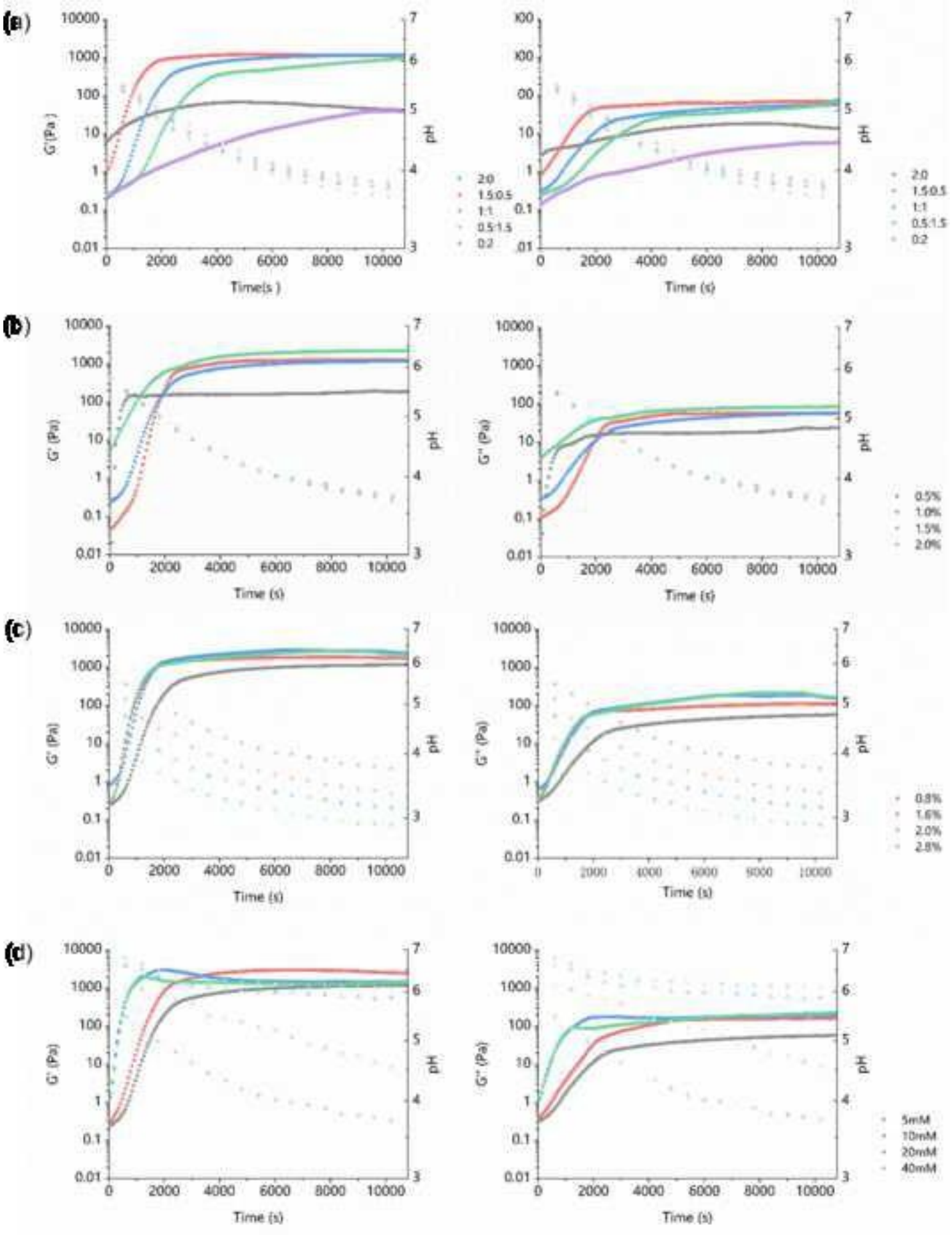

Figure4

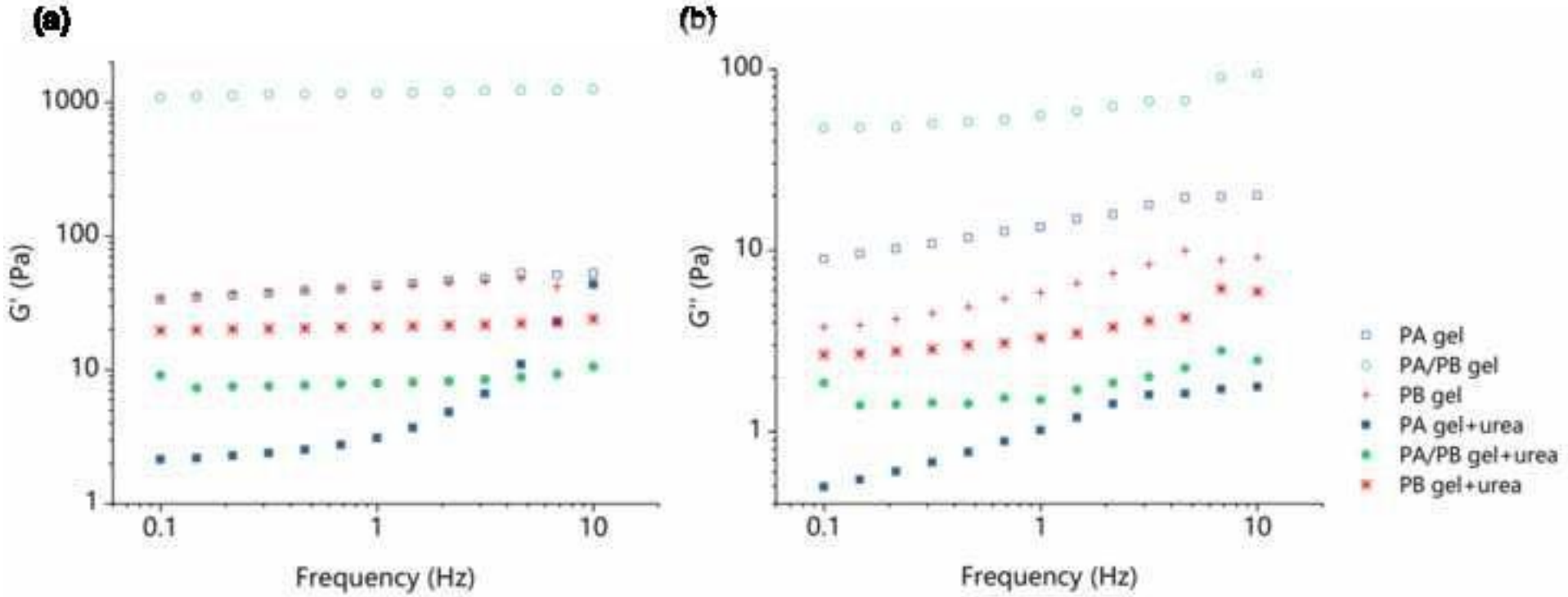

Supplementary data

Synergistic gelling mechanism of RG-I rich citrus pectic polysaccharide at different esterification degree in calcium-induced gelation

Shiguo Chen [a,b,c],Jiaqi Zheng [a], Laiming Zhang [a], Huan Cheng [a,b,c], Caroline Orfila [d], Xingqian Ye [a,b,c], Jianle Chen [a,b,c,*]

[a] College of Biosystems Engineering and Food Science, National-Local Joint Engineering Laboratory of Intelligent Food Technology and Equipment, Zhejiang Key Laboratory for Agro-Food Processing, Zhejiang Engineering Laboratory of Food Technology and Equipment, Zhejiang University, Hangzhou 310058, China

[b] Fuli Institute of Food Science, Zhejiang University, Hangzhou 310058, China

[c] Ningbo Research Institute, Zhejiang University, Ningbo 315100, China

[d] School of Food Science and Nutrition, University of Leeds, Leeds LS2 9JT, UK

1. Chemical composition of pectins

Monosaccharide composition was analyzed by a modified 1-phenyl-3-methyl-5-pyrazolone (PMP)-high performance liquid chromatography (HPLC) method (Strydom, 1994). First, pectic polysaccharides samples (typically 2-3 mg) were hydrolyzed with 2 M trifluoroacetic acid at 110℃ for 8 h in an ampoule. Then, the samples were dried using a stream of nitrogen and neutralized with 0.1 M sodium hydroxide. The hydrolyzates dissolved in 450 mL of 0.3 M sodium hydroxide

were derivatized with 450 mL PMP solution (0.5 M, in methanol) at 70℃ for 30 min. Finally, the reaction was stopped by neutralization with 0.3 M hydrochloric acid, and excess reagent was extracted using 3 × 1 mL of chloroform. The upper (aqueous) phase was filtered through a 0.22 mm membrane and 1 mL of the resulting solution was injected for analysis. Waters e2695 (Waters, US) with a Zorbax Eclipse XDB-C18 column (250 mm 4.6 mm, 5 mm, Agilent, USA) was used to perform HPLC analysis at 25℃. The mobile phases were: solvent A, 15% acetonitrile with potassium phosphate buffer (0.05 M, pH 6.9), solvent B, 40% acetonitrile with the same buffer. The flow rate was 1 mL/min, relying on a gradient of B from 0% to 15% in the initial 10 min, then from 15% to 25% in the next 20 min. Detection was with a 2489 UV/Vis Detector (Waters, US) at 250 nm.

The degree of methylation (DM) was analyzed by the m-phenylphenol method calculated from methanol and acetic acid content with the GalA%. Pectins after saponification were used to determine methanol and acetic acid content by HPLC (Waters 1525, US) with a C18 column (SinoChrom ODS-BP 250 mm × 4.6 mm, 5 mm, Elite, China) with refractive index (RI) detection (Waters 2414, US) using isopropanol as internal standard and the mobile phase was 4 mM sulfuric acid (Levigne, & Thomas, & Ralet, & Quemener, and Thibault, 2002).

The monosaccharide composition of pectin recovered from acidic water (PA) and basic water (PB) revealed that sequential mild acid and alkaline extraction generates RG-I rich pectin, different from HG dominated commercial pectins (Table S1). PA was composed of 44.2% HG (mole % (GalA-Rha)) and 40.6% RG-I (mole % (2Rha+Ara+Gal)) (Kazemi, & Khodaiyan, & Labbafi, & Saeid Hosseini, and Hojjati, 2019), while PB was composed of 19.3% HG and 62.7% RG-I. Rha and GalA are the main structural units of the RG-I region, while Gal and Ara are monosaccharides belonging to the side chains of RG-I. The ratio of Rha/GalA indicated both PA and PB were RG-

I rich pectin, especially PB. The high ratio of (Ara+Gal)/Rha suggested the RG-I portion of PA and PB has abundant Ara and Gal side-chains. DM value confirmed PA was relatively high-methoxylated pectin and PB was low-methoxylated pectin regarding the number of methyl-ester groups in HG region.

Table S1. Chemical composition of pectin.

	Monosaccharides (mol%)								Rha/ GalA	RG-I%[A]	(Ara+Gal)/ Rha[B]	DM%[C]	DAc%[D]
	Man	Rha	GalA	Glc	Gal	Xyl	Ara	Fuc					
PA	1.82± 0.08^{b}	2.87± 0.03^{b}	47.08 ±0.33^{a}	0.14± 0.02^{b}	11.62 ±0.23^{a}	9.41± 0.14^{b}	23.20 ±0.69^{b}	3.88± 0.20^{a}	0.06± 0.00^{b}	40.56 ±0.51^{b}	12.13±0.03^{a}	45.40 ±0.91^{a}	1.03± 0.12^{a}
PB	3.20± 0.11^{a}	4.19± 0.09^{a}	23.47 ±0.20^{b}	0.35± 0.01^{a}	11.05 ±0.04^{a}	12.82 ±0.11^{a}	43.27 ±0.26^{a}	1.28± 0.27^{b}	0.18± 0.00^{a}	62.70 ±0.04^{a}	12.96±0.33^{a}	15.06 ±0.16^{b}	0.83± 0.09^{a}

[A] RG-I% = 2Rha% + Ara% + Gal%;
[B] (Ara+Gal)/Rha: average length of RG-I side chains.
[C] DM: degree of methylation.
[D] DAc: degree of acetylation.
Values represent means ± standard derivatives of three replicates; values with different small case superscript letters in the same column indicate significant difference ($p < 0.05$), with the same letters indicate insignificant differences ($p > 0.05$).

2. Molecular weight of pectins

Size exclusion columns including a OHpak SB-G guard column, SB-806 HQ and SB-804 HQ column (Shodex, Japan), equipped with a multi-angle laser light scattering detector (DAWN HELEOS II, Wyatt Technology, USA) and refractive index detector (SEC-MALLS-RI) were applied to provide molecular weight information on the pectins. The molar mass was calculated using specific refractive index increment at 0.1355 and 0.0880 mL/g for PA and PB, respectively. Pectins were dissolved in H2O (3 mg/mL) and filtered through 0.22 mm membranes. Mobile phase was 0.2 M NaCl contained 0.02% NaN3 (pH 7.0), at a flow rate of 0.5 mL/min (Chen, et al., 2017).

SEC-MALLS-RI system gave accurate information for molecular size of a pectin sample. The Mw of PB was larger than PA (Table S2), but the difference of Rz was not significant

comparing with Mw, indicating the "tighter" molecular structure of PB than Pa, and this "tight" structure is due to abundant neutral sugar side-chains in PB.

Table S2. Molecular weight of pectin.

	Mn[A] (kDa)	Mw[B] (kDa)	Polydispersity (Mw/Mn)	Rz[C] (mm)
PA	114.1 (±1.5%)[b]	196.6 (±1.5%)[b]	1.722 (±2.1%)[b]	35.0 (±4.8%)[a]
PB	188.6 (±4.3%)[a]	282.7 (±2.5%)[a]	1.499 (±4.9%)[a]	36.6 (±6.7%)[a]

[A] Mn: number-average of molar mass.
[B] Mw: weight-average of molar mass.
[C] Rz: z-average of root mean square radius of gyration.
Values represent means ± standard derivatives of three replicates; values with different small case superscript letters in the same column indicate significant difference ($p < 0.05$), with the same letters indicate insignificant differences ($p > 0.05$).

3. Dynamic-viscoelastic properties of PA and PB synergistic gels

In order to analyze dynamic-viscoelastic properties of pectin gels with $CaCO_3$ and GDL, the mixed gels were put onto the rheometer and equilibrated for 1 min at 25℃, then analyzed for their rheological behavior. The linear viscoelastic ranges were firstly determined by amplitude sweep from 0.001% to 100% at a constant frequency of 1 Hz. The frequency sweep was conducted from 0.1 to 10 Hz at 0.1% deformation to monitor the change in storage modulus (G') and loss modulus (G'') of the mixtures after 10800 s.

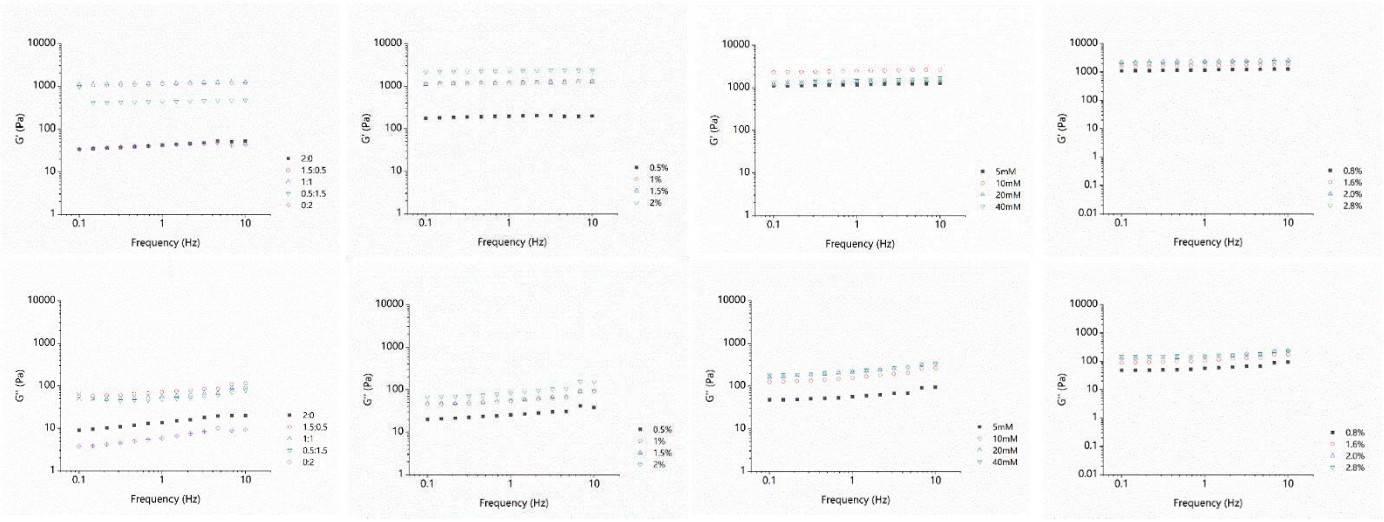

Figure S1. Modulus values (G' and G'') of PA/PB blend gels. (a) PA/PB blend gels (1.5% w/v pectin concentration, 0.8 wt% GDL, 5 mM $CaCO_3$) at PA/PB= 2:0, 1.5:0.5, 1:1, 0.5:1.0 and 0:2; (b) PA/PB blend gels (PA/PB=1, 0.8 wt% GDL, 5 mM $CaCO_3$) of pectin concentration of 0.5, 1.0, 1.5 and 2.0% w/v; (c) PA/PB blend gels (PA/PB=1, 1.5% w/v pectin concentration, 5 mM $CaCO_3$) with GDL concentration of 0.8, 1.6, 2.0 and 2.8 wt%; (d) PA/PB blend gels (PA/PB=1, 1.5% w/v pectin concentration, 0.8 wt% GDL) with Ca^{2+} concentration of 5, 10, 20 and 40 mM. Measurement temperature, 25℃; strain, 0.1%; frequency, 0.1-10 Hz.

4. Water holding capacity (WHC) of PA and PB synergistic gels

Mixed gels (7 mL) in the centrifuge tubes were stored under 4℃ for 24 h and then used to measure water holding capacity. The mixed gel was centrifuged at 8000 rpm for 10 min at 25 °C. The released water was drained with filter paper (Wan, et al., 2019). Record the weight of the mixed gel before (W_1) and after (W_2) centrifugation. Water holding capacity is expressed as the percentage of gel weight after centrifugation relative to the weight of the initial gel (equation (1)).

$$\boldsymbol{WHC} = \frac{\boldsymbol{W(g)}}{\boldsymbol{W_1(g)}} \times \mathbf{100\%} \qquad (1)$$

Ratio of PA and PB WHC of PA/PB blend gels at different PA/PB ratio with addition of 0.8 wt% GDL and 5 mM $CaCO_3$ was presented in Fig. 5a. WHC among samples with different PA/PB ratio was approximately 98%, indicating excellent water holding capacity of both PA and PB calcium-induced gels. Low DM of PB led to high charge densities, which provided opportunities to form ion junction zones. In addition, long neutral sugar side-chains of PB

increased the water holding capacity, involving in the molecular entanglements in gels (Klaassen and Trindade, 2020). Compared with PB, PA had less neutral sugar side-chains as well as higher

content of GalA with relatively high DM (~50%), relating to more hydrogen bonds and hydrophobic interactions for network junction zones, which can hold water in pectin gels. No significant differences can be found among mixed gels and PA or PB gels, which was inconsistent with the differences on gel moduli. The possible reason was that thin network structure in pure pectin gels was dominant in setting the WHC and the three-dimensional network of blend gels can increased the gel moduli, but useless on water holding capacity.

Pectin concentration WHC of PA/PB blend gels (PA/PB=1) at different pectin concentration (0.5, 1.0, 1.5 and 2% w/v) with addition of 0.8 wt% GDL and 5 mM $CaCO_3$with different concentration was showed in Fig. 5b. The WHC increased with pectin concentration increasing, because low pectin concentration resulted in sparse gel network, easily damaged by centrifugal force. Moreover, the high Ca^{2+}/pectin ratio decreased the WHC (Einhorn-Stoll, 2018). However, it seemed to attain a saturated value at a certain concentration and the tendency was consistent with gel strength. The rheological properties of different pectin concentration gels (Fig. 4b) suggested that high pectin concentration can hinder the network formation, consequently, difficult to improve the WHC further. Moreover, big voids in the gel contributed to water holding ability and higher pectin concentration may not change the range of big voids and can't increase the WHC (Wan, et al., 2019).

GDL concentration WHC of PA/PB blend gels (PA/PB=1) with different concentration of GDL (0.8, 1.6, 2.0 and 2.8 wt%) with addition of 5 mM $CaCO_3$ was comparable (Fig. 5c). The WHC was less dependent on pH comparing to the moduli, because water holding ability contributes to big voids in the gel. With pH decreasing, the number of hydrogen bonds increased but the affinity for calcium ions of pectin decreased. The balance between two interactions changed the gel moduli but not the big voids of the gel. In addition, both PA and PB were RG-I

rich pectin with abundant neutral sugar side-chains, which helped to maintain high WHC because of the strong water binding capacity (Einhorn-Stoll, 2018).

Ca^{2+} concentration Fig. 5d showed the WHC of PA/PB blend gels (PA/PB=1) with different concentration of $CaCO_3$ (5, 10, 20 and 40 mM) with addition of 0.8 wt% GDL. The WHC decreased with the $CaCO_3$ concentration increasing, suggesting excess Ca ions induce syneresis of pectin gel. A certain amount of Ca ions was essential for cation-induced pectin gelation, but additional ions could decreased the water holding capacity. Big voids in the gel were necessary for water holding capacity. High Ca^{2+} concentration promoted formation of dense network, thus increasing the gel strength but decreasing the WHC, even causing pectate precipitation above a critical concentration (Einhorn-Stoll, 2018). Another reason was that the network formation rate of low Ca ions concentration was slower than that of high concentration, inducing a more complete network during the overnight store (Liu, & Guo, & Li, & Zhu, and Li, 2013).

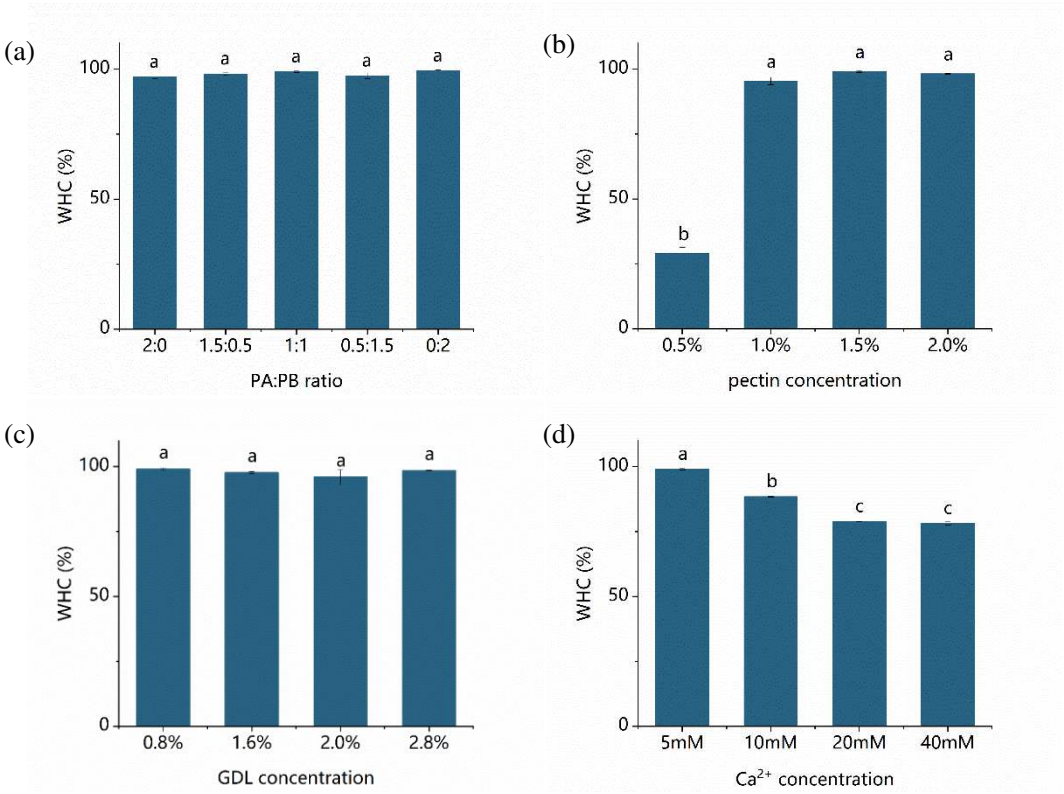

Figure S2. Water holding capacity (WHC) of PA/PB blend gels. (a) PA/PB blend gels (1.5% w/v pectin concentration, 0.8 wt% GDL, 5 mM $CaCO_3$) at PA/PB= 2:0, 1.5:0.5, 1:1, 0.5:1.0 and 0:2; (b) PA/PB blend gels (PA/PB=1, 0.8 wt% GDL, 5 mM $CaCO_3$) of pectin concentration of 0.5, 1.0, 1.5 and 2.0% w/v; (c) PA/PB blend gels (PA/PB=1, 1.5% w/v pectin concentration, 5 mM $CaCO_3$) with GDL concentration of 0.8, 1.6, 2.0 and 2.8 wt%; (d) PA/PB blend gels (PA/PB=1, 1.5% w/v pectin concentration, 0.8 wt% GDL) with Ca^{2+} concentration of 5, 10, 20 and 40 mM.

5. Scanning electron microscopy (SEM) observation

The microstructures of the gel surface were observed by scanning electron microscopy. The

samples were photographed using a SU8010 cold field-emission scanning electron microscope

(Hitachi Ltd., Tokyo, Japan) with an accelerating voltage of 3 kV. Each sample was cut into small pieces, freeze-dried for 48 h and covered with a thin gold layer prior to analysis. The porosity of the network structure captured by the SEM images (5000×) was analysed using ImageJ 1.51 software. PB gel showed a discontinuous structure in the SEM observation (Fig. S1), suggesting a weak gel network structure. The surface of PA/PB blend gel was smooth and compact comparing with the pure pectin gels, indicating the strengthened network consistent with the improved gel properties (Li, et al., 2019).

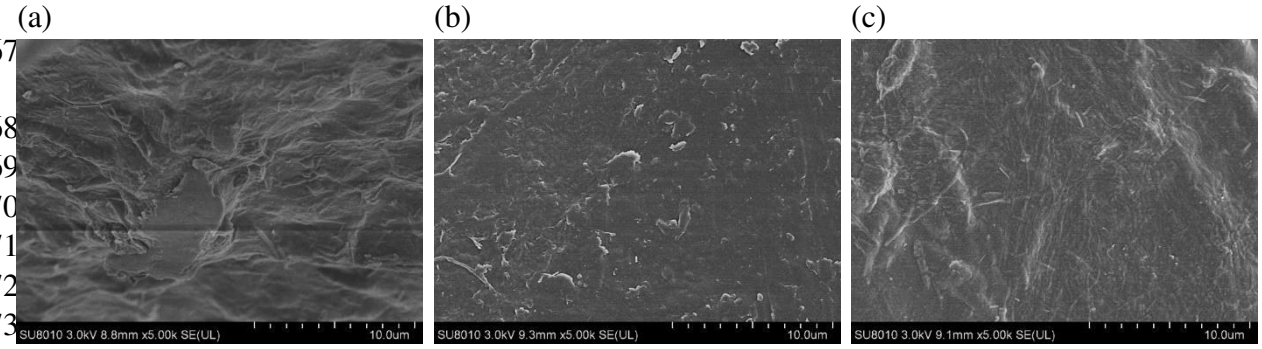

Figure S3. Microstructure of (a) PA, (b) PB and (c) PA/PB blend gels.

6. appearance of PA and PB synergistic gels

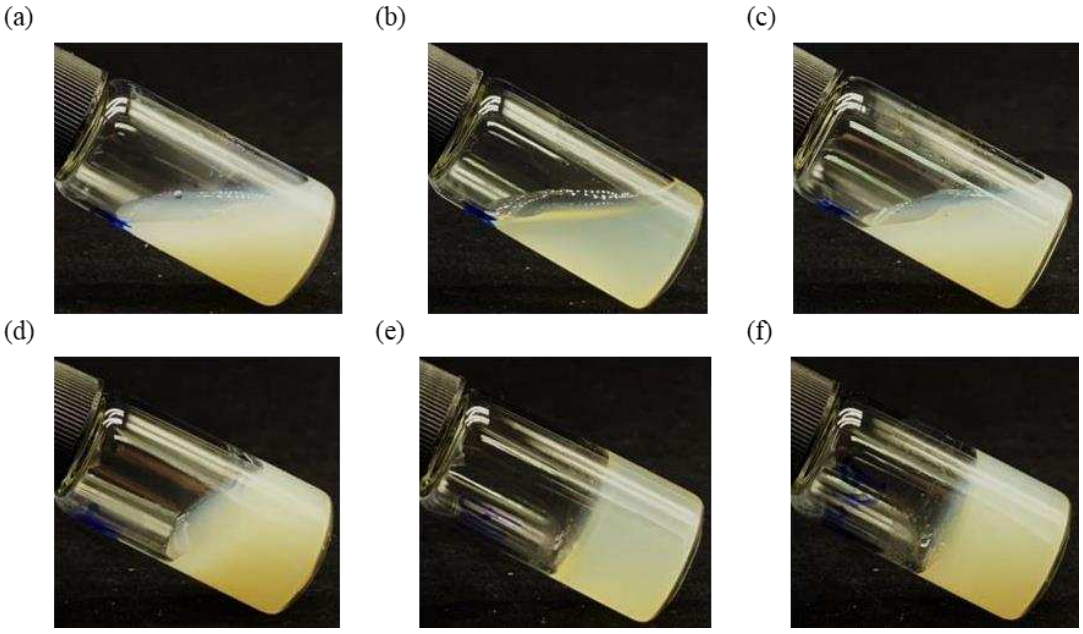

Figure S4. pictures of (a) PA, (b) PB and (c) PA/PB blend solutions (1.5% w/v pectin concentration); (d) PA, (e) PB and (f) PA/PB blend gels (1.5% w/v pectin concentration, 0.8 wt% GDL, 5 mM $CaCO_3$).